FS/RV SONNE

FAHRTBERICHT SO162
CRUISE REPORT SO162

INGGAS TEST

INTEGRATED GEOPHYSICAL CHARACTERISATION AND QUANTIFICATION OF GAS HYDRATES
- INSTRUMENTATION TEST CRUISE -

VALPARAISO - BALBOA
FEBRUARY 21 - MARCH 12, 2002

Edited by
Timothy John Reston and Jörg Bialas
with contributions of cruise participants

GEOTECHNOLOGIEN

GEOMAR
Forschungszentrum
für marine Geowissenschaften
der Christian-Albrechts-Universität
zu Kiel

KIEL 2002

GEOMAR REPORT 103

GEOMAR
Research Center
for Marine Geosciences
Christian Albrechts University
in Kiel

Redaktion dieses Reports:
Timothy John Reston und Jörg Bialas

Umschlag und Titelei: Gerhard Haass

GEOMAR REPORT
ISSN 0936 - 5788

GEOMAR
Forschungszentrum
für marine Geowissenschaften
Wischhofstr. 1-3
D - 24148 Kiel
Tel. (0431) 600-2555, 600-2505

Editors of this issue:
Timothy John Reston und Jörg Bialas

Cover and prelims: Gerhard Haass

GEOMAR REPORT
ISSN 0936 - 5788

GEOMAR
Research Center
for Marine Geosciences
Wischhofstr. 1-3
D - 24148 Kiel
Tel. (49) 431 / 600-2555, 600-2505

Table of Contents

Summary

The cruise SO162 INGGAS-Test set out to test equipment developed in three Subprojects of the BMBF-funded INGGAS project (**In**tegrated **G**eophysical Characterisation and Quantification of **Gas** Hydrates) , part of the "Geotechnologie Gashydraten Initiative". These Sub-projects, and the equipment to be tested are:

1. **INGGAS-HISS. (Hamburg Integrated Seismic System).** This subproject designed and constructed ocean bottom sources capable of generating the shear waves needed to determine (in conjunction with P-waves) the physical properties of the hydrated and the free gas zone, were designed and built . This information can reveal the amount and distribution of both gas hydrates and free gas within the sediment, and will allow assessment of the influence of gas hydrate and the underlying gas zone on slope stability. These ocean bottom sources were tested during the SO-162 INGGAS-Test cruise.
2. **INGGAS-OBS (Ocean Bottom Seismometers).** This Subproject constructed the 3-component ocean bottom seismometers needed for multi-component ocean floor seismology, and in particular the recording of S-waves. In conjunction with more traditional P-waves, these allow the physical properties of the subsurface to be fully characterised, revealing the amount and distribution of gas hydrates within the sediments in the interwell gap. The OBS developed during this project were deployed during the SO162 INGGAS-Test cruise, both to test their own function and also that of the ocean-floor seismic sources developed in INGGAS-HISS.
3. **INGGAS-DEEP TOW:** This Subproject has developed a deep-towed multi-channel streamer system rated for ocean depths. Lowering the streamer to the seafloor reduces the size of the Fresnel Zone and hence increases the spatial resolution. Previous studies have shown the benefit of such systems for imaging small-scale structures such as faults that are likely to be important fluid conduits, and for revealing the fine structure of the BSR.

   Incorporated within the deep tow system is a navigation system rated for ocean depths, to allow accurate location of the streamer. This navigation system is also used for the side-scan sonar acquired within the OMEGA project, and which together with the deep-tow streamer forms a single, integrated deep-tow system. All of the deep-tow streamer, the deep-tow side-scan sonar and the positioning system were tested successfully during SO-162 INGGAS-Test.

The equipment tested thus consisted of

- BeatGun weight drop seismic source, developed by the University of Hamburg as part of SP1 - INGGAS-HISS;
- SeeBoSeis glass sphere imploders, modified by the University of Hamburg as part of the SP1 - INGGAS-HISS;
- Ocean Bottom Seismometers (OBS), developed by GEOMAR as part of SP2 - INGGAS-OBS;
- Deep tow Streamer, acquired by GEOMAR as part of SP3 - INGGAS-Deep Tow;
- Posidonia positioning system, acquired by GEOMAR as part of SP3 - INGGAS-Deep Tow;
- Deep-tow side-scan sonar, acquired within OMEGA, another project within the Gas Hydrate Initiative, and closely integrated with the Deep Tow Streamer system.

These new equpment were successfully tested during the SO162 cruise, operating mainly in the Yaquina Basin region off Peru in water depths between 800 and 4000 m. Invaluable experience was gained in the handling, deployment and use of the different tools, in particular the deep tow system. Various improvements were made during the cruise: others were identified for incorporation after the cruise.

Zusammenfassung

Die Reise SO162 INGGAS-Test diente dem Test von Gerätschaften, die im Rahmen von drei Teilprojekten des INGGAS Projektes (**Int**egrated **G**eophysical Characterisation and Quantification of **Gas** Hydrates) entwickelt wurden. INGGAS wird durch das BMBF als Teil der Gashydrat Intiative innerhalb der Geotechnologien gefördert.

Die teilprojekte sind:

1. **INGGAS-HISS (Hamburg Integrated Seismic System).**
   In diesem Teilprojekt werden Ozean-Boden-Quellen entworfen und gebaut, die es ermöglichen Scherwellen zu erzeugen. Zusammen mit P-Wellen sind diese notwendig um die physikalischen Eigenschaften der mit Hydrat oder freiem Gas durchsetzten Zone zu bestimmen. Mit dieser Information kann die Menge und Verteilung von Hydrat und freiem Gas im Sediment bestimmt werden. Sie liefert ebenso den Zugang zu einer Abschätzung des Einfluß von Gashydraten und der darunte liegenden Gaszone auf Hangstabilitäten.

2. **INGGAS-OBS (Ozean Boden Seismometer, OBS)**
   Dieses Projekt stellt die 3-Komponenten Ozean-Boden-Seismometer bereit, die in der mehrkomponenten Seismologie des Ozeanbodens und insbesondere für die Aufnahme von S-Wellen notwendig sind. In Verbindung mit den konventionellen P-Wellen erlauben diese Messungen die volle Beschreibung der physikalischen Parameter des Untergrundes und der Bestimmung von Volumen und Verteilung der Gashydrate im Sediment (interwell gap???). Die hier eingesetzten OBS wurden zum eigenen Funktionstest und zur Kontrolle der neu entwickelten Quellen eingesetzt.

3. **INGGAS-DEEP TOW**
   In diesem Projekt wurde ein tiefgeschleppter mehrkanaliger Streamer entwickelt, der für die Tiefsee geeignet ist (bis 6000 m Wassertiefe eingesetzt werden kann). Durch Annäherung des Streamer an den Meeresboden wird die Fresnelzone verringert und somit die räumliche Auflösung erhöht. Frühere Studien haben den Nutzen solcher Systeme bei der Erkennung von kleinskaligen Störungen, die wichtige mögliche Transportwege für Wässer darstellen, ebenso gezeigt, wie bei der Auflösung der Feinstruktur des BSR.

   Verbunden mit dem tiefgeschleppten Streamer ist ein tiefseetaugliches Navigationssystem, das ein genaue Lokalisierung des Systems ermöglicht. Dieses Navigationssystem wird ebenfalls für das SideScan Sonar verwendet, welches im Projekt OMEGA beschafft wurde. Beide Geräte zusammen bilden ein einheitliches tiefgeschlepptes Meßgerät. Alle Komponenten wurden während der Reise erfolgreich getestet.

Der gesamte getestete Gerätebestand setzte sich zusammen aus:

- BEATGUN: ein Fallgewicht als seismische Quelle; entwickelt von der Universität Hamburg im Teilprojekt SP1- INGGAS-HISS
- SEEBOSEIS: Glaskugeln als Implosionsquelle, weiternetwickelt von der Universität Hamburg im Teilprojekt SP1- INGGAS-HISS
- Ozean Boden Seismometer (OBS): entwickelt von GEOMAR im Teilprojekt SP2- INGGAS-OBS
- Tiefgeschleppter Streamer: entwickelt von GEOMAR im Teilprojekt SP3- INGGAS-DeepTow
- POSIDONIA: Navigationssystem, angeschafft von GEOMAR im T eilprojekt SP3- INGGAS-DeepTow
- Tiefgeschlepptes SideScan Sonar: angeschafft im Projekt OMEGA im Rahmen der Gashydratinitiative; eng verbunden mit dem tiefgeschleppten Streamer

Diese Geräte wurden erfolgreich während der Reise SO162 im Yaquina Becken vor Peru getestet. Die Einsatztiefe lag zwischen 800 m und 4000 m Wassertiefe. Wertvolle Erfahrungen wurden in der Handhabung, Ausbringung und Einsatz der verschiedenen Geräte gewonnen, insbesondere bei dem tiefgeschleppten System. Verschiedentliche Verbesserungen wurden bereits während der Reise vorgenommen, andere konnten erst im Anschluß umgesetzt werden.

Resumen

La campaña SO162 INGGAS-Test fue diseñada para probar el equipo desarrollado en tres subproyectos del proyecto INGGAS (Integrated Geophysical Characterisation and Quantification of Gas Hydrates), financiado por el BMBF, que es parte de la iniciativa „Geotechnologie Gashydraten Initiative". Los subproyectos y el equipamiento que se probaron son los siguientes:

1. INGGAS-HISS (Hamburg Integrated Seismic System). Este proyecto diseñó y construyó las fuentes sísmicas de fondo marino para general las ondas de cizalla (ondas S) necesarias (en conjunción con ondas P) para determinar las propiedades físicas de los hidratos y de la zona de gas libre. Esta información puede revelar tanto la cantidad como la distribución de hidratos de gas y de gas libre en los sedimentos. Asimismo permitirá una estimación de la influencia de los hidratos de gas y del gas libre en la estabilidad de taludes.

2. INGGAS-OBS (Ocean Bottom Seismometers). En este subproyecto se contruyerón los sísmometros de fondo marino de tres componentes que son necesarios para sismología de multicomponentes de fondo oceánico y particularmente para registrar ondas S. In conjunción con los estudios más tradicionales de ondas P, se obtienen las propiedades físicas del subsuelo, revelando la cantidad y distribución de hidratos de gas en los sedimentos. Los OBSs desarrollados en este subproyecto fueron usados durante la campaña SO162 INGGAS-Test, tanto para probar su funcionamiento como para probar la fuentes sísmicas desarrolladas en el subproyecto INGGAS-HISS.

3. INGGAS-DEEP TOW. Este subproyecto ha desarrollado un sistema de cable multicanal de arrastre profundo para profundidades oceánicas. Bajando el cable cerca del fondo oceánico se reduce el tamaño de la zona de Fresnel y por lo tanto se aumenta la resolución espacial. Estudios anteriores han mostrado el beneficio de este tipo de sístemas para obtener imagenes de estructuras de tamaño pequeño, tal como fallas que podrían ser conductos de flujo de fluidos, ademas de revelar la estructura fina de los BSRs.

Se ha incorporado al sistema de arrastre profundo un sístema de navegación de gran profundidad, para obtener una detallada localización del cable multicanal. Este sístema de navegación también se usa para el „side-scan sonar" del proyecto OMEGA, el cual junto con el cable multicanal forma un solo sistema integrado de arrastre profundo. Tanto el cable multicanal de arrastre profundo, como el „side-scan sonar" y el sístema de posicionamiento, fueron probados con exito durante la campaña SO162 INGGAS-Test.

El equipo que se probo consiste de:

- Fuente sísmica „BeatGun weight drop", desarrollada por la Universidad de Hamburg como parte del subproyecto SP1 – INGGAS-HISS.
- Esferas de vidrio de implosión „SeeBoSeis", modificadas por la Universidad de Hamburg como parte del SP1 – INGASS-HISS.
- Sismómetros de fondo oceánico (Ocean Bottom Seismometers, OBS), desarrollados por GEOMAR como parte del SP 2 – INGGAS-OBS.
- Cable de arrastre profundo, adquirido por GEOMAR como parte del SP3 – INGGAS-Deep Tow.
- El sístema de posicionamiento Posidonia, adquirido por GEOMAR como parte del SP3 – INGGAS – DeepTow.
- Side-scan sonar de arrastre profundo, adquirido en OMEGA, que es otro proyecto dentro de la „Gas Hydrate Initiative" e integrado con el sístema de cable de arrastre profundo.

Los nuevos equipos fueron probados con exito durante la campaña SO162, utilizandolos principalmente en la cuenca de Yaquina del Peru en profundidades de agua entre 800 y 4000 m. Se obtuvo una importante experiencia tanto en el manejo, como ls disposición y uso de los diferentes equipos, en particular del sístema de arrastre profundo. Se hicieron varias mejoras durante la campaña y se identificarón otras que han de ser incorporadas al sístema despues de la campaña.

1. Background to the cruise

1.1 Introduction to the INGGAS Project.

At the pressures and temperatures characteristic of the top several hundred metres of the subsurface of continental margins, methane and water combine to form a stable clathrate (methane or gas hydrate). This clathrate is an ice-like substance in which methane molecules are physically trapped within a cage of water molecules. The base of the hydrate stability zone (HSZ) is controlled by temperature and pressure: a drop in pressure or an increase in temperature will lead to an upward shift of the base of the hydrate stability zone and the dissociation of gas hydrate at the base of that zone into free gas and water.

1.1.1 Importance of Gas Hydrates: Potential Resource and Hazard.

Over half of the world's organic carbon is to be found as methane locked up in such hydrates (Kvenholden, 1988), making them a potentially important resource (Kvenholden, 1993), if one currently difficult to exploit. However, methane is also a major greenhouse gas. If as little as one part per thousand of the methane in gas hydrates were to be released into the atmosphere, the effect would be equivalent to a doubling of the atmospheric CO_2, and lead to catastrophic global warming (e.g., Paull et al., 1991). Knowledge of the processes of hydrate formation and dissociation, and quantification of hydrate volumes world-wide are thus essential to improve our understanding of the potential influence of hydrates on climate.

Gas hydrates may increase the shear strength of the sediments immediately below the seafloor (Henriet and Mienert, 1998) and thus might play an important role in stabilising the continental slope (thus reducing the methane flux). However, the presence of hydrate in pores may hinder porosity loss and sediment compaction (Booth et al., 1998). Destabilisation and dissociation of the hydrate consequently results in the development of a zone of high porosity and low shear strength at the base of the hydrate zone. This is particularly the case if high gas pressures arise beneath a low permeability hydrate layer (e.g., Booth et al., 1984) or if hydrate dissociation leads to salinity reduction (Henriet and Mienert, 1998). This weak zone (Figure 1.1) may play an important role in the formation of tsunamogenic landslides, such as that off New Guinea in 1998 (Monastersky, 1998; Tappin et al., 1999) and the Storegga slide off Norway (Mienert et al., 1998). Thus quantification of the amount of hydrate present, its distribution within the sedimentary sequence (i.e., its effect on physical properties), the amount of free gas and the porosity of the sediments has important implications for understanding the effect of gas hydra tes on the stability of continental slopes.

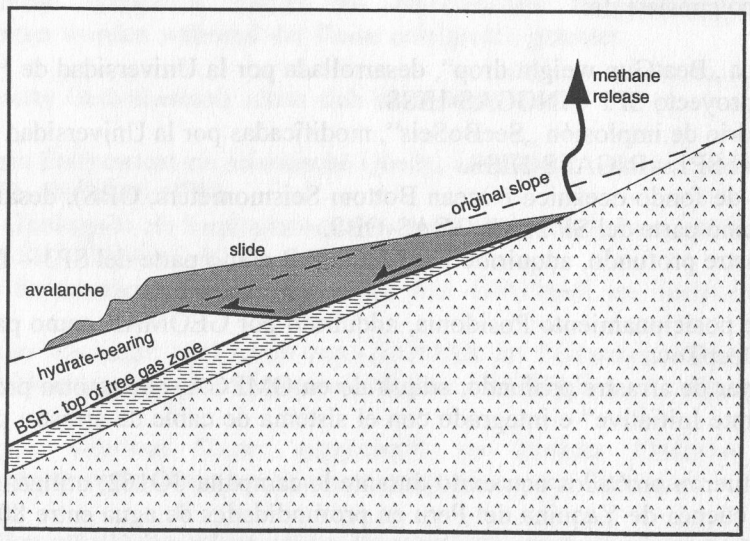

Figure 1.1: A weak zone (containing free gas) at the base of gas hydrates may result in submarine slope failure. Determining the physical properties within and beneath the hydrate-bearing zone may help predict such slides.

The stability of gas hydrate filled sediments also has implications for deep water engineering (e.g., Henriet and Mienert, 1998). Finally, the stability field of gas hydrates is controlled by, among other things, temperature and pressure. Thus the base of the gas hydrates, believed to correspond to the BSR (but see below), can be used to investigate the dynamic processes occurring beneath the seafloor and in particular the flow of heat and fluids out of deforming sediment piles at continental margins.

1.1.2 Physical properties of sediments containing gas hydrates

Pure gas hydrate is thought to have physical properties comparable to those of ice (**Table 1**). As a result, the presence of hydrate in the top few hundred metres of the subsurface leads to an increase in p-wave velocity, probably depending on the proportion of pore and other space occupied by hydrate and the distribution of hydrate within the sediment (see below). What is far less clear is the effect that hydrates have on the shear wave velocity. This is likely to depend not only on the amount of hydrate present but also on the distribution of that hydrate within the sedimentary section (Ecker, 1998; Sakai, 1999).

	gas	water	ice	gas hydrate
Bulk modulus at 272K [GPa]	0.1	2.5	8.8	5.6
Shear modulus at 272K [GPa]	-	-	3.9	2.4
Poisson's ratio	-	-	0.33	0.33
Vp/Vs at 272K	-	-	1.88	1.95
density [g/cm^3]	0.235	1.032	0.95	0.9

Table 1: Comparison of physical properties of hydrate with those of ice, water and gas under conditions appropriate for the BSR beneath Blake Ridge. After Sloan, 1998 and Ecker, 1998.

Effect of hydrate distribution within sediment. From samples obtained by coring and dredging, we know that methane hydrate occurs both as nodules/lenses within the sedimentary strata and at least partially replacing water to infill porespace (e.g., Uchida et al., 1999). Three different models (Figure 1.2) exist for the distribution of the solid clathrate within the porespace (Ecker, 1998). First, the hydrate may be suspended in water, thus affecting only the bulk modulus of the pore fluid. Note that this should not therefore affect the s-wave velocity. Second, the hydrate may be loosely connected to the sediment grains, reducing other porosity and increasing the shear modulus slightly. Third, the hydrate may act as a cement between the grains, significantly increasing rock stiffness (shear modulus), and hence leading to an increase in S-wave velocity. Furthermore, once hydrate formation has started, new hydrate may preferentially nucleate on existing hydrate, leading to the development of nodules and lenses of hydrate between sediment. This may be particularly true for fine-grained sediment (Clennell et al., 1995; Booth et al., 1998) at shallow depths beneath the seafloor (Figure 1.3). Although as yet this sort of structure has not been modelled, it is likely that its seismic properties, and in particular their shear wave velocity, will depend on the connectivity of the nodules and lenses into a semi-rigid framework within the weaker sediment.

It has proved difficult to distinguish between these models with P–wave data alone (Ecker, 1998) as the different models can all explain the observed P-wave characteristics by assuming quite different amounts of hydrate present. The determination of the shear wave velocity should help, but as yet little work has been done. One multicomponent VSP study of the Mallik 2L-38 well (Sakia, 1999) indicates that the cement model does not appear appropriate: instead the effect of hydrate on the physical properteis of the sediment appears more akin to a loss of porosity through compaction (Walia et al., 1999), implying that the hydrate does not bind the sediment together into a rigid framework. The different models also have implications for the shear strength of the sediment: if the hydrate cements the grains together, the shear strength will be greatly increased, and methane hydrates may help stabilise the continental slope. Thus the determination of the shear modulus (e.g., through Scholte wave dispersion – see below) will also strongly constrain hydrate distribution in sediments and thus allow more accurate quantification of hydrate volumes.

The distribution of hydrates within the sediments also has implications for the dewatering behaviour of the system. If hydrates occur dominantly within pore spaces, or as semi-continuous layers, the resulting loss of permeability may be greater than if hydrates form as discrete nodules and lenses within the hydrate zone. As discussed below the effect of gas hydrates on fluid flow is not well known.

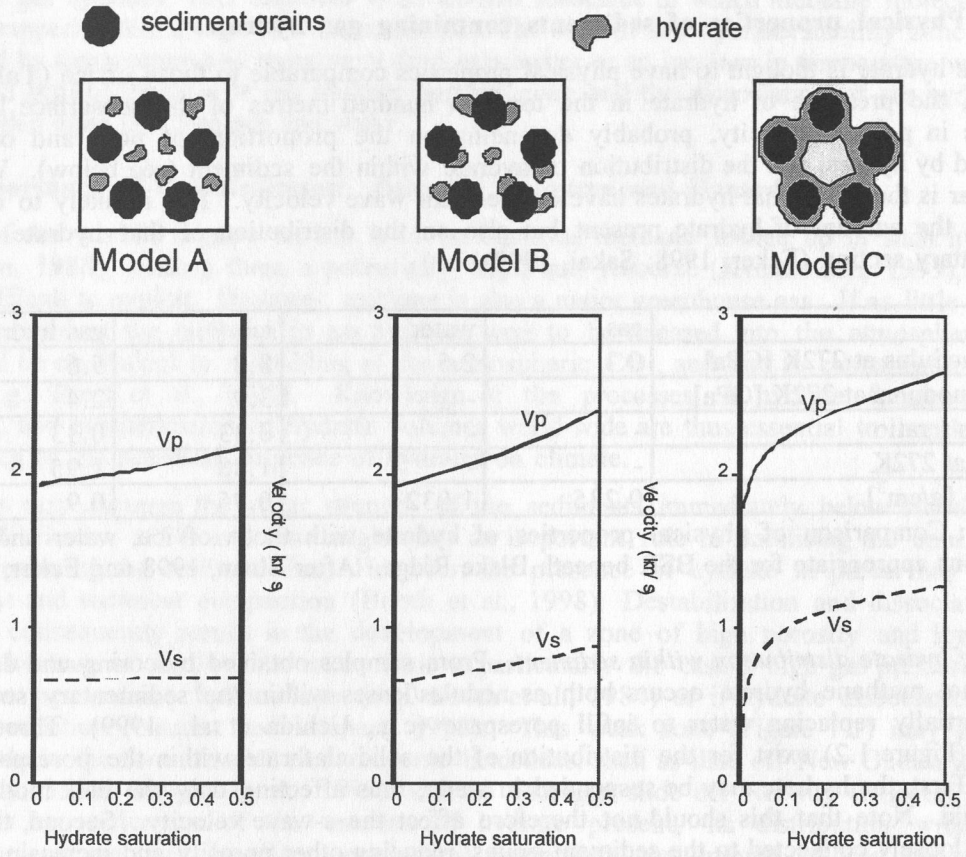

Figure 1.2: The variation of p- and s-wave velocities with hydrate saturation for three different models of hydrate distribution in the pore space (after Ecker, 1998). Collecting high quality s-wave data can allow us to distinguish between these different models and also quantify the volumes of hydrate present.

One problem with assessing the influence that gas hydrates have on the physical properties of sediments is in getting an undisturbed sample of hydrates within sediment to the laboratory: either the gas partly dissociates, or if the core is frozen, water within the pores space is replaced by ice. As a result, we are at the moment largely reliant on indirect geophysical determination of physical properties. However, as discussed below, the usual techniques, based on P-wave velocities, are non-unique and further constraints are needed.

1.1.3 Base of the hydrate stability zone and the BSR

The presence of gas hydrate bearing sediments beneath the sea floor is usually identified from a characteristic negative polarity p-wave reflection occurring sub-parallel to the seafloor (the bottom simulating reflection or BSR), and coming from the base of the hydrate stability zone (HSZ). For a long time it was assumed that the BSR reflection came from the contrast between high acoustic impedance hydrate-filled sediment and the hydrate free zone beneath (e.g., Stoll and Bryan, 1979). However, detailed seismic modelling studies, have shown that the development of a strong BSR requires the presence of small amounts of free gas beneath the hydrate (e,g,. Pecher et

al., 1996). This is supported by data from ODP drill sites: holes that have penetrated the BSR indicate that the BSR is mainly due to free gas trapped beneath the hydrate stability zone rather than to the presence of gas hydrate just above the phase boundary (Bangs et al., 1993; MacKay et al., 1994; Holbrook et al., 1996). For instance, ODP Leg 164 (Holbrook et al., 1996) found that where a BSR is observed (Sites 995 and 997), a zone containing free gas occurs immediately beneath the hydrate, whereas where no BSR is observed (Site 994), free gas is absent. As a result, although the presence of a BSR means that gas hydrates are present, the converse is not true: the absence of a BSR does not mean that there are no hydrates present. It is possible for instance that a BSR only forms where gas hydrate has dissociated and hence where either pressure has dropped (e.g. due to uplift such as might be expected at an accretionary margin) or the temperature has increased. Alternatively, the BSR might be an indication of a steady supply of free gas from below. Thus to quantify hydrate volumes worldwide, we need to develop a reliable and efficient method of identifying and mapping gas hydrates where no BSR is present.

The presence of free gas beneath the hydrates has implications for the mechanics of hydrate formation. If the methane in hydrates forms from the *in situ* breakdown of organic material, then the free gas beneath the hydrates may represent the accumulation of a large proportion of methane produced by microbial activity beneath the HSZ. However, the amount of methane trapped in gas hydrates (Kvenvolden, 1988) is thought to exceed the total amount that could be generated within the hydrate zone from the amount of organic matter present (e.g., Paull et al., 1994; Pecher et al., 1998). Thus gas hydrates probably form from methane generated microbially both within the stability zone and deeper within the section. This requires the upward transport of methane into the hydrate zone either as free gas (Sloan, 1990) or dissolved within percolating pore fluids (e.g., Hyndman and Davis, 1992; Brown et al., 1996). Much of the methane budget of the whole sedimentary section may be incorporated into the hydrate layer, and any free gas beneath the layer may represent a smaller volume of methane either trapped beneath the hydrate once an impermeability threshold has been reached, or formed by the dissociation of hydrate. Knowledge of the fluid flow regime associated with gas hydrates is thus critical in understanding the processes of hydrate formation and dissociation.

One area of particular interest will be the detailed study of hydrate formation and dissociation in regions of slumping and submarine landsliding. Here, the complex interplay between deformation, fluid flow, exhumation and burial is likely to lead to changes in the extent of the HSZ both immediately following the slide and during the subsequent return to equilibrium (e.g., Mienert et al., 1998). However, the time-scale of these processes is poorly understood and is clearly a subject for further research. Evidence for the time-lag in hydrate formation and dissociation may come from observations of "double BSRs" (e.g., Mienert et al., 1998). These are generally interpreted as representing an old and a new base of the HSZ: as the hydrate takes a finite time to form/dissociate (perhaps thousands of years - Delisle et al., 1998), there is a period when two BSRs may be present.

1.1.4 Seismic techniques for the exploration of gas hydrates

As discussed above, one of the main methods for mapping out hydrate zones is the BSR reflection from their base. However, such reflections are not always present and seem to only occur when the hydrated layer is underlain by a zone containing some free gas. Thus other methods are necessary to determine the presence of gas hydrates and hence to allow the global quantification of hydrate thicknesses.

The spectrum of seismic methods presently applied to the exploration of gas hydrates comprises mainly reflection imaging and P-wave amplitude consideration. Most studies to date have involved relatively standard surface seismic systems. INGGAS set out to expand the range of techniques by developing ocean floor sources and obtaining a multichannel deep-tow streamer system.

Deep-tow streamer systems offer one major advantage over conventional near-surface streamers: by towing the streamer near the seafloor, the Fresnel zone is greatly reduced in size (Figure 1.4). This improves the spatial resolution, in particular that perpendicular to the profile (the in-line resolution can be improved by migration). Previous work with deep-tow streamers (e.g., Gettrust et al., 1999) has shown that the improved resolution reveals the fine structure (e.g. faults) both within and at the base of the hydrated layer (Figure 1.5). As faults provide conduits for fluid flow, an understanding of their distribution is crucial for models of hydrate formation.

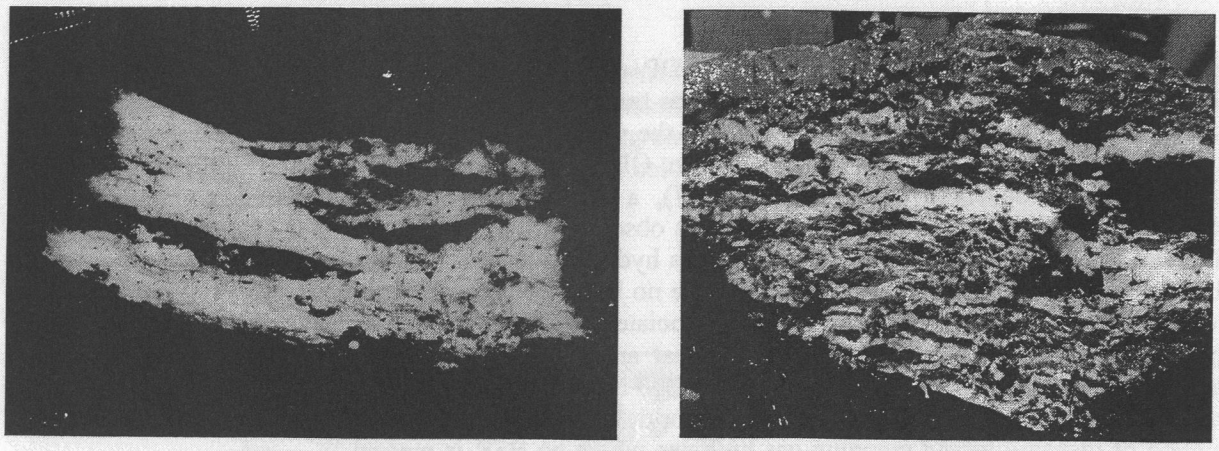

photographs of hydrate recovered from Hydrate Ridge (GEOMAR)

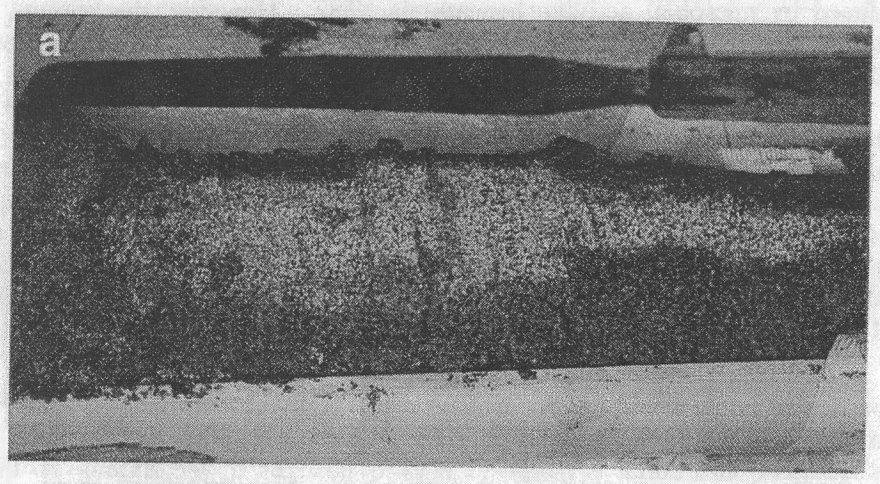

photographs of hydrate within pore space form the Mallik 2L-38 well
(N Canada - see Uchida et al., 1999; Sakai 1999)

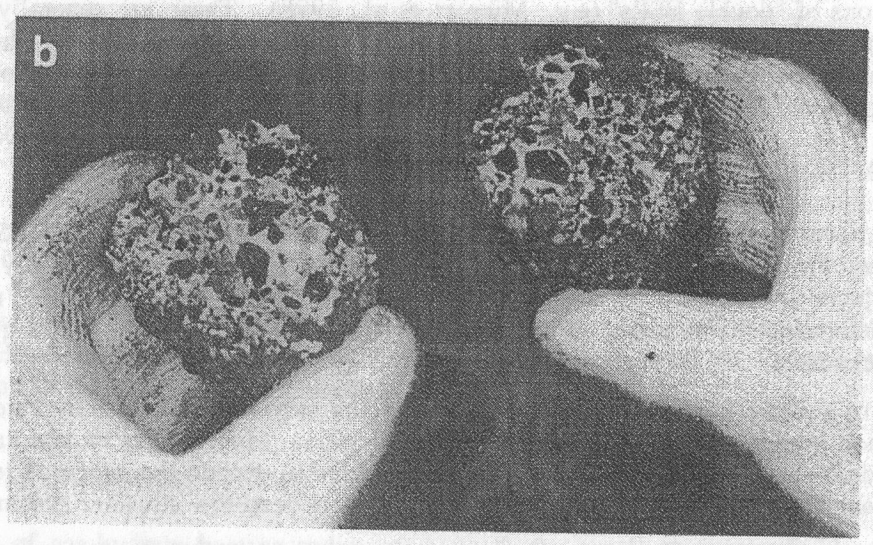

Figure 1.3. Photos of gas hydrates showing the variety of textures possible. The distributions of hydrates within the sediment is likely to strongly influence the physical properties of the hydrate bearing zone.

P-waves have also been used in attempts to deduce the physical properties of the hydrate and underlying gas zones. Some studies report the presence of high velocity layers within the HSZ and high velocity layers above the BSR (Hobro et al., 1998), interpreted as layers with a high concentration of hydrate. Better resolution of such layers will help improve our understanding of the distribution of hydrate within the HSZ. Other studies have focussed, for example, on the AVO behaviour of the hydrate BSR including 1-D inversion (e.g., Pecher et al., 1998), full waveform inversion (Yuan et al., 1999) and mapping of BSR reflection strength using seismic sources at different offsets (Fink and Spence, 1999). Another example is the study of Grevemeyer et al. (2000) who identified a low velocity channel associated with the BSR by joint inversion of refracted arrivals and wide-angle reflections. Lateral variation of BSR structure has been characterised by the computation of band-limited impedance logs from near-vertical incidence data, based on Born expansion and deconvolution (Grevemeyer et al., 2000). However, as the P-wave velocity depends not only on the amount of hydrate present, but also on its distribution within the sediment, the interpretation of such results is non-unique. Other tools are needed to constrain physical properties better: these include the use of S-waves.

S-waves

The approaches described above only loosely constrain the shear wave velocity. In particular the AVO behaviour of the BSR is only weakly sensitive to the shear modulus (e.g. Yuan et al., 1999). However, S-wave velocity is an important underground parameter, containing important information not only on the hydrate content of the sediment but also on its shear strength. For example, a correlation between shear strength and S-wave velocity could be verified for near surface sediments of the Barents Sea (Ayres and Theilen, 1999).

Shear waves have been used to investigate gas hydrates and also permafrost in the JAPEX/JNOC/GSC Mallik 2L-38 gas hydrate research well. Here, S-waves recorded during a multicomponent VSP survey were critical in distinguishing between possible models for hydrate distribution and hence allowing the quantification of hydrate volumes (Sakia, 1999; Walia et al., 1999). Furthermore, examination of the velocities of S-waves on the transversely and radially polarised components indicated that the gas hydrate - sediment composite was anisotropic, possibly related to fracture orientations. As such, detailed multicomponent work has the potential for mapping out fracture orientations and so constrain the stress regime. However, such VSP surveys can only be carried out when a suitable well exists, and as such do not provide a realistic way of surveying large volumes of gas hydrates. Instead, multicomponent OBS may present a more economical method of determining detailed physical properties, including anisotropy, and quantifying gas hydrate volumes.

A problem with shear-wave studies of the hydrate zone has been the reliance on P-S converted waves. Although both the seafloor and the base of the hydrate zone are candidates for the conversion of P-waves to S-waves, the necessary incident angle requires relatively large offsets before such converted waves are recorded. This in turn reduces the resolution of the method. An alternative, is the use of ocean-bottom sources to directly generate S-waves. Such sources, in conjunction with arrays of ocean bottom seismometers can provide information on S-wave velocities (hence on shear strength) and S-wave reflectivity (hence on changes in physical properties across key boundaries). As a result, they will increase the potential for controlled studies designed to investigate the physical properties of the hydrated layer and the underlying free gas zone.

PS-converted body waves can however yield valuable information about gas hydrates. In particular, it should be possible to use PS-transmitted waves to image converting interfaces and to quantify S-wave-contrasts within geological structure. This so-called receiver function method has successfully been applied in seismology for the investigation of structure at crustal scales since the 1980s (for example Vinnik, 1977, Kosarev et al., 1987, 1993; Yuan et al., 1997) but has never been applied to gas hydrate research. To determine receiver functions seismic signals have to be recorded with three-component instruments with adequate spectral bandwidth. The PS-converted waves have much stronger amplitudes on the horizontal than on the vertical component. The key element of data processing is a deconvolution of the vertical component signal from the horizontal component signal leaving a time series composed mainly of zero-phase PS-conversions and reverberations below the station. These traces can be inverted for a model of S-velocity layering but can also be used for imaging the PS-converting horizons.

As they rely on converted waves, receiver functions are sensitive to Poisson's ratio rather than to absolute velocity. The S-velocity determination is significantly improved if a reliable P-velocity model is known a priori. For the exploration of shallow sediments high spatial resolution is required. We believe that the receiver function method can be applied to this small scale target as well if signals of artificial impulse sources, such as airguns and water guns, are used providing a broad spectrum with sufficiently high frequencies, and if it is combined with reflection seismics. To develop this technique is one of the objectives of INGGAS.

Scholte waves

Recently, Bohlen et al. (1999a) successfully applied Scholte wave (seismic waves which follow the interface between the water and the sediment) analysis to determine the elastic properties of shallow submarine permafrost sediments. Scholte-wave dispersion curves are particularly sensitive to the shear modulus, and so provide information directly relevant to the stability of continental slopes. As such they have the potential of acting as a direct hydrate indicator, once the effect that hydrates exert on the shear strength of the sediments can be shown. They are best generated by a source near the seafloor (e.g. SeeBoSeis - SP1) and detected through the deployment of an array of closely spaced Ocean Bottom Seismometers (OBS - see SP2), or a streamer towed close to the seafloor. Although it is not yet clear whether Scholte-waves can be generated at the deep sea bottom by remote source near the sea surface, they can be excited by towed sources in shallower water regions (Bohlen et al., 1999a) which are one target of INGGAS. During the INGGAS-Test cruise, we planned to investigate the potential of detecting Scholte waves in deep water by using both OBS and a streamer towed close to the seafloor.

1.2 New Technology Developed within INGGAS

As is clear from the above discussion, the characterisation and quantification of gas hydrates requires an understanding of the physical properties of the hydrate and underlying gas zones, and improved imaging of both. More precisely, the quantification and characterisation of gas hydrates needs:

1. Capability of studying gas hydrates with S-waves to determine the complete wavefield, better constraining physical properties and thus allowing the determination of the amount and distribution of gas hydrates within the sedimentary section. This requires the development of ocean bottom sources and seismometers.
2. Development of a broadband frequency approach to cover frequency dependent reflection behaviour/characteristics of target horizons. This requires seismic sources that can illuminate the whole hydrate-sediment zone at frequencies ranging from below 10 Hz (traditional OBS/OBH refraction seismics - SP1 and SP2) to 1 and perhaps 3 kHz (e.g., high frequency surface sources in combination with a deep-tow streamer - SP3 - and broadband OBS - SP2).
3. Improved imaging, and in particular increased spatial resolution. This will be achieved through the use of high frequency sources (e.g., a watergun - SP1) in combination with a deep-tow streamer (SP3) and with OBS (SP2). In the former case, high resolution sampling with intervals of between 1 and 6.25 m will be important to avoid aliasing.

To address these needs, INGGAS has developed new ocean bottom seismic sources, new ocean bottom seismometer systems to record both p- and s-waves, and a deep tow seismic streamer.

1.2.1 Ocean Floor Seismic Sources

Conventional ocean bottom seismology using surface sources provides information on the P-wave velocity structure of the subsurface and on the AVA behaviour of key reflections which is better resolved than with surface seismics alone. However, some of the physical properties (shear velocities, near surface velocity gradients, shear modulus, seismic anisotropy) of the gas hydrate zone are best determined using ocean floor sources and receivers. Sources should be capable of generating P-waves, S-waves and perhaps surface waves: as water only transmits P-waves such sources must be deployed on the seafloor to avoid reliance on converted waves (P to S).

By developing ocean floor seismic sources and constructing sufficient 3 component ocean bottom seismometers (see SP2), Sub-project 1 of INGGAS set out to determine:

- the physical properties (P- and S-wave velocity structure, shear modulus) of the hydrate zone and of both the overlying and underlying section
- the variation with incidence angle and frequency of the BSR and hence quantify the nature of this reflector and the thickness of the gas hydrate / free gas transition

Two ocean-floor sources have been developed within this project:

- SeeBoSeis imploding glass sphere system - this generates P-waves, S-waves and surface waves
- Beatgun: a ship-operated ocean-floor weight-drop system within a high pressure cylinder. This is lower energy but more repeatable than SeeBoSeis. It can be configured to generate S-waves as well as P-waves and recordings from multiple "shots" at a single location can be vertically stacked to enhance S/N ratios.

SeeBoSeis has been successfully used and is commercially available, but has been modified so that shotgun cartridges rather than explosives can be used to inititiate the implosion and enlarged to increase power. The Beatgun is a new weight drop based seismic source for deployment on the seafloor.

1.2.2 Ocean Bottom Seismometers

High resolution shear-wave and velocity studies of the gas hydrates require dense deployments of ocean bottom seismometers. Within INGGAS, these were acquired by converting GEOMAR's existing tethered system to an instrument that actually rests on the seafloor, and the use of a three-component geophone package, including the development of a new method of deploying the geophone package from the main instrument.

The basic methods of use of OBS are fairly well-known. They include the polarisation analysis of the 3-component data, and the rotation of the two horizontal channels to provide in-line and cross-line data. After application of these routine procedures, the instruments will contribute to the study of gas hydrates in several ways:

- detailed P-wave velocity structure of the hydrate and underlying gas zones. This can help identify zones of hydrate concentration within the HSZ, and of free gas beneath it.
- detailed S-wave velocity analysis of the hydrate and underlying zones. As discussed above, the S-wave velocity of hydrates, in combination with P-waves, may hold the key to understanding their distribution within sediments and their connectivity into a semi-rigid framework. This has implications for hydrate volumes and for slope stability.
- investigation of the anisotropy (especially S-wave) of the hydrate-sediment system. This is likely to provide information on the orientation of fractures (Sakia, 1999) and hence on the past and present fluid flow regime of the subsurface (see SP4).
- AVA (AVO) studies of key reflections (e.g. the BSR) using both P-waves and S-waves. Closely spaced OBS provide the ideal tool to study the variation in amplitude with incidence angle and thus to quantify the change in physical properties across key structures.
- imaging of the BSR through prestack migration of reflected waves. By applying downward continuation of the source, it is possible to reconfigure the OBS data to allow prestack migration and hence to use the OBS for imaging. This technique requires knowledge of the far-field source signature, which can be provided by deep-tow streamer data (see SP3).
- imaging of the converting boundaries (e.g. base of the hydrates - equivalent to the BSR) through receiver function analysis of P-S converted waves.

It should be emphasised that these are long-terms aims of the INGGAS project and that the INGGAS-Test cruise SO-162 was simply to test the equipment and not to apply the full range of possible analytical methods.

1.2.3 Deep-tow seismic reflection methods

Deep-tow seismic has the potential to provide better vertical and spatial resolution than possible with near surface streamers. Spatial resolution is controlled by the size of the Fresnel zone footprint: for a near surface seismic source and a water depth of 4000 m., the Fresnel zone at the seafloor for a streamer towed 100 m over the seafloor is c. one eighth of the size of that for a streamer towed near the surface. Although 2-D migration can improve the spatial resolution of surface-streamer data in the inline direction, it does not improve that in the crossline direction. As a result, the lateral resolution of near-surface 2-D seismic reflection data recorded in deep water is rarely better than a few hundred metres. While this limitation can be overcome with 3-D seismic, the use of a deep-towed source provides a cost-effective solution where 3-D surveys are not required.

As a result, Subproject 3 of INGGAS purchased a digital deep-tow streamer as described in a following section. The only previous comparable system to that built in INGGAS was DTAGS, which belonged to the US Navy and was lost during a gas hydrate site survey in the Pacific. The USGS have purchased a similar streamer to the INGGAS system, but had not yet deployed it at the time of the SO-162 cruise. Thus the SO-162 cruise was the first deployment of a deep-tow digital streamer.

- determine the detailed internal structure, reservoir characteristics and stratigraphy of the gas hydrate zone. In particular deep-tow methods have demonstrated their potential for mapping out the small-scale faults that may act as fluid conduits within the sub-surface. Thus SP3 is closely linked to SP4.
- investigate the nature of the BSR through waveform modelling. Although the BSR is generally considered to be a simple decrease in P-wave velocity over a transition zone, it may exhibit small scale internal layering and structure that can be resolved using high frequency sources and a deep tow streamer.
- investigate the lateral variability within the hydrate zone and of the underlying BSR. The increase spatial resolution of a deep tow system can reveal small-scale variations in BSR structure not apparent on near surface data (Figure 1.5).
- determine the far-field signature of the seismic source for deterministic deconvolution and minimum phase conversion (see SP2), thus optimising vertical resolution with both the deep-tow and with OBS data.

Details of the deep tow streamer system acquired are described in a following section.

A strong link exists between INGGAS and the OMEGA project of Bohrmann and others. They have acquired a deep-tow high resolution side-scan sonar system (using the navigation system acquired within INGGAS proposal) to study the seafloor morphology and reflectivity in gas hydrate provinces. First, the high resolution imaging of the seafloor in OMEGA is clearly closely related to the high resolution imaging of the sub-surface in INGGAS. Furthermore, to keep costs to a minimum, the data storage and telemetry systems for the deep tow streamer have been incorporated into the sled of the side-scan sonar. Thus the two deep-tow units form a single integrated deep-tow system. This was to be tested on the cruise.

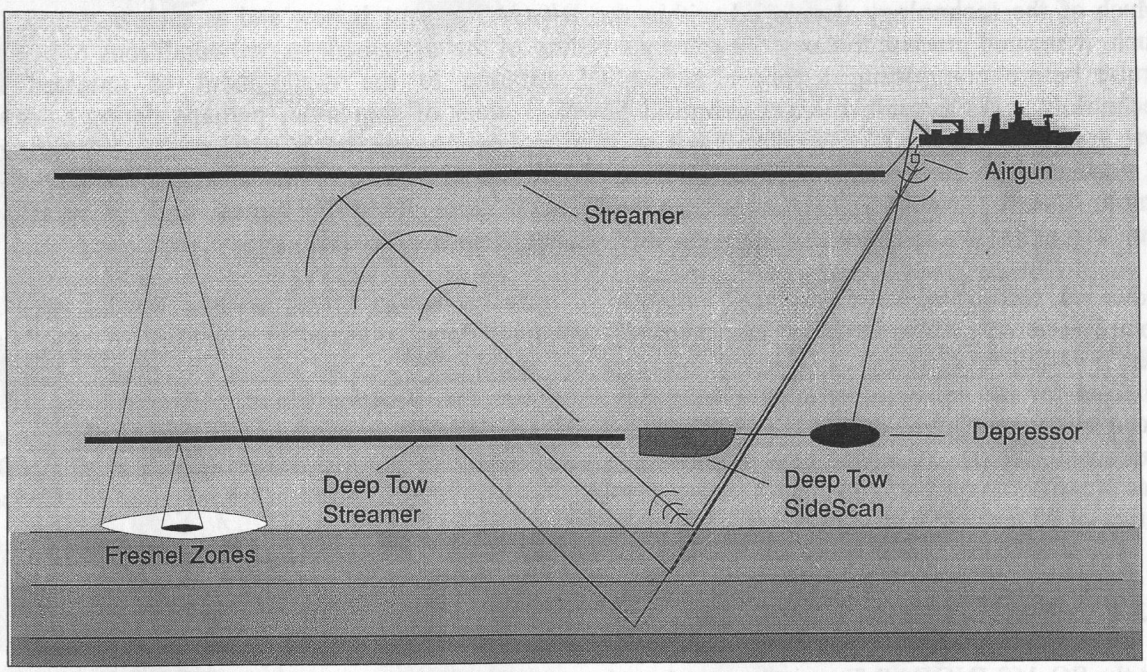

Figure 1.4 - Sketch of a deep towed streamer system. By towing the streamer close to the seafloor, the Fresnel Zone is reduced in size, improving spatial resolution in both the in-line and cross-line directions.

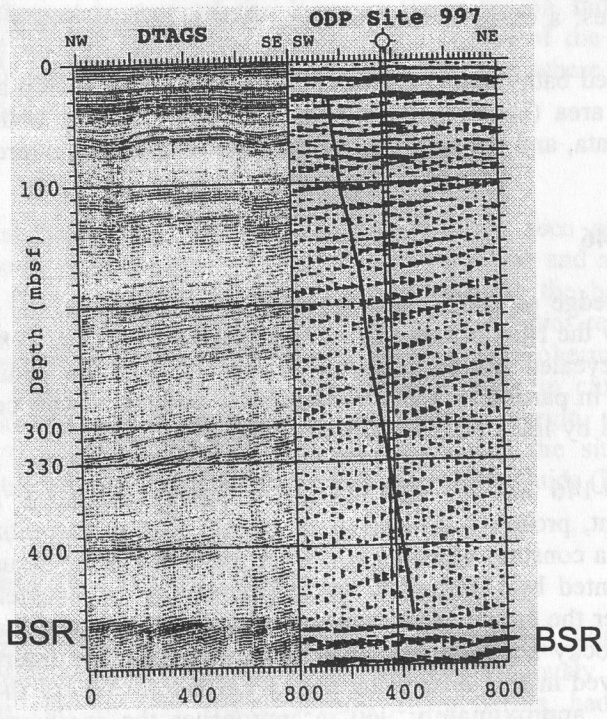

Figure 1.5: Comparison of Deep-tow seismic (left) with conventional surface seismic (right) from Blake Ridge (Rowe and Gettrust, 1993). The deep-tow seismic shows greatly improved resolution and allows the imaging of a whole array of normal faults. Only one could be tentatively identifed (inclined black line) from the near-surface seismic. Note also the fine structure and variation in character of the BSR resolved by the deep-tow seismic.

1.3 INGGAS-Test: Aims and Working Area

Much of the technology developed within the INGGAS project is new and as such untested. As such, it seemed prudent to carry out rigorous testing of the equipment in real conditions on a short cruise before committing a longer period of shiptime to the deployment of untested new technology. As a result, a cruise proposal for ca. 1 week of ship time, perhaps during a transit, was applied for to the BMBF. The result of this application was the SO-162 cruise, consisting of 7 working days during a 21 day transit from Valparaiso to Balboa. This arrangement gave both ample time for testing of the equipment during short stops along the transit, and for modifying and improving the equipment during the intervening periods of transit.

However, testing of some parameters requires a common target. This enables for instance the comparison of surface streamer and deep-tow streamer data, collected at a variety of speeds and with a variety of sources. As a result, most of the testing was carried out in one place. The site selected for the main experiment during this time was the Yaquina Basin, offshore Peru. This basin was investigated during the SO-146 1-2 cruises within the project GEOPECO (Bialas and Kukowski, 2000). A second area offshore Ecuador, the site of SO-159 Salieri (Flueh et al., 2001), was identified as a back-up. Both areas provide the bathymetric framework required to devise a series of experiments at various water depths.

1.3.1 Yaquina Basin (Figure 1.6)

As the SO-162 INGGAS-Test cruise was largely a transit cruise between Valparaiso and Balboa, the exact working area could be selected from a large part of the Andean margin. The area chosen for most of the work was the Yaquina Basin located on the continental slope offshore Peru. This basin may have formed by subduction erosion, is characterised by sediments ranging from Eocene to Plio-Quaternary (Ballesteros et al., 1988). Reasons for choosing this basin and the adjacent slope inslude:

- variety of water depths from 800 m to over 4000 m, allowing the testing of the deep-tow system at a variety of depths.
- presence of gas hydrates: a clear, if intermittent, BSR is observed (e.g. Bialas and Kukowski, 2000)
- reasonably well surveyed bathymetry, allowing precise planning of ship and deep-tow tracks
- previous work in the area (Bialas and Kukowski, 2000) allowing both comparison of test results with previous data, and the focusing of the tests on areas of interest.

Previous results - SO-146

Before SO-146, the knowledge of the stratigraphy of the Yaquina Basin was based on a single seismic profile collected by the Hawaii Institute of Geophysics (HIG), in 1985. Seismic reflection profiling during SO-146 revealed the presence of a clear BSR in the sediment at water depths greater than about 600 m. In particular, the BSR is clearly present in the central part of the SO-146 survey, in a box bound by lines HH00-009 and HH00-013.

Parasound data from SO-146 showed that in the Yaquina Basin, a continuous Holocene sedimentary cover is absent, probably indicative of strong coastal currents. Instead, mudwaves were observed: these have a constant wave length, from which it can be assumed, according to the mathematical model presented by Hopfauf & Spiess (University of Bremen, in prep.), that the current has been stable over the entire depth and corresponding time span that has been imaged by the data. In places, hummocky seafloor structures are present and are interpreted as chemoherm structures, like those observed in this area using the OFOS (s.b.). Where the wavy unconformity with the constant depth of approximately 960 m approaches the seafloor, gas migrates upwards toward the seafloor. The upper parallel reflections downlap onto that unconformity.

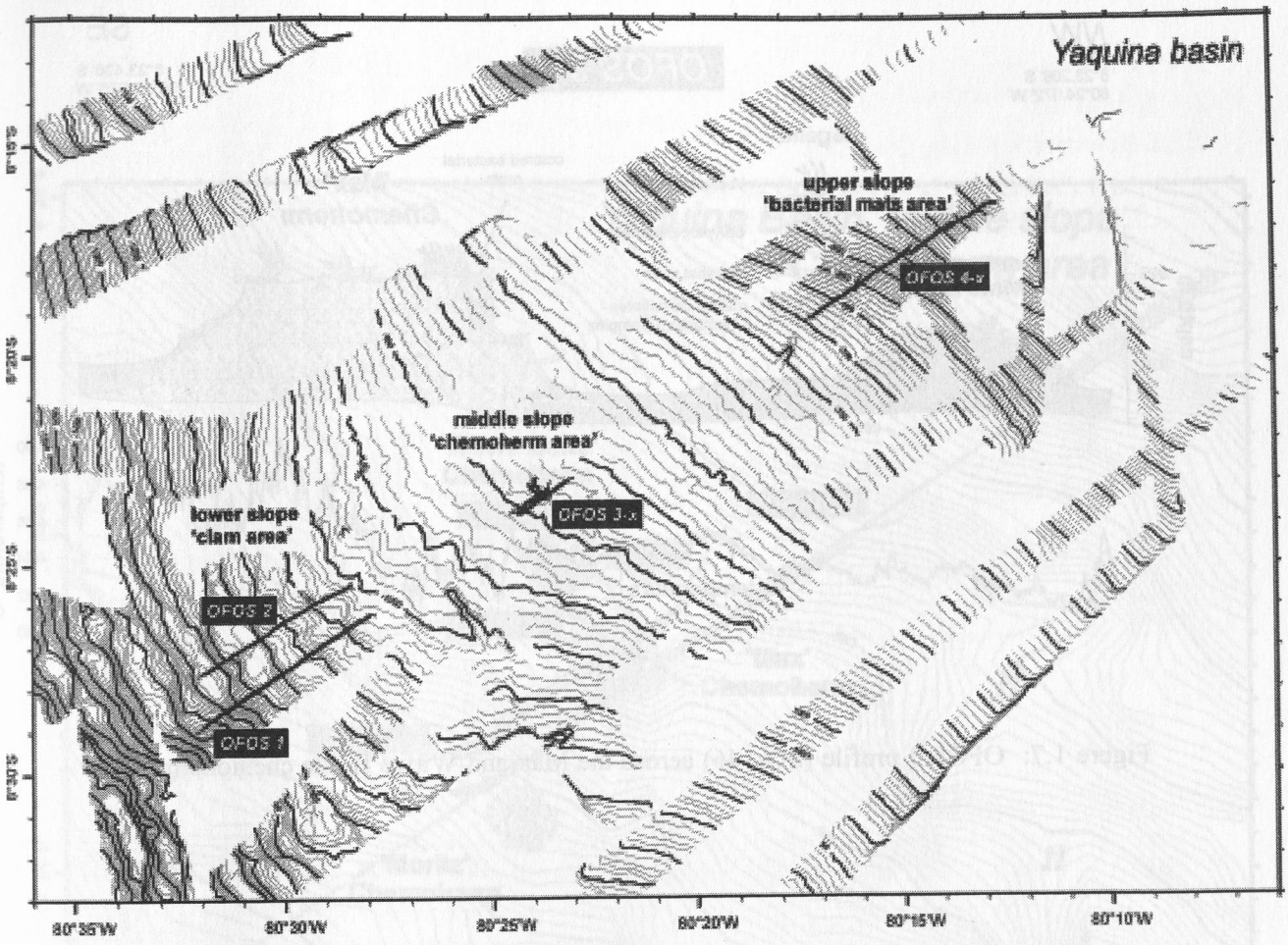

Figure 1.6: Bathymetric map of the Yaquina Basin region showing main seafloor features. During SO-162 we worked mainly in the region of the middle slope (water depths 800-1000 m) where a BSR had been reported and where chemoherms imply the cold-venting of methane rich fluids.

OFOS observations confirmed that the hummocky structure seen on Parasound were indeed chemoherms. Three such chemoherms were positively identified and named "Max" (Figure 1.7), "Moritz" and "Witwe Bolte", and the possibility raised based on the bathymetric data of several more in the same area. Chemoherms form when methane rich fluids react with seawater and lead to the deposition of carbonate (Figure 1.8). Consequently, chemoherms are an indication of the presence of upwelling methane rich systems. Their occurrence in clusters further suggests that this fluid upwelling is itself focussed into specific parts of the margin, perhaps related to increase permeability (faulting?) at depth. The chemoherms were also the site of significant biological communities, presumably also feeding of nutrient rich upwelling fluids (Figure 1.8).

Specific targets within the Yaquina Basin

Based on the results of SO-146 GEOPECO (Bialas and Kukowski, 2000), testing focussed on the region of about 900 m water depth where a clear BSR had previously been observed, and on the slightly deeper region (Figure 1.9) where several chemoherms had been identified ("Max", "Moritz" and "Witwe Bolte") and others tentatively interpreted from the bathymetric data. The chemoherms, as discussed later, also provided an alternative seafloor firmness for the testing of the environmentally friendly, non-destructive ocean floor source of the Beatgun.

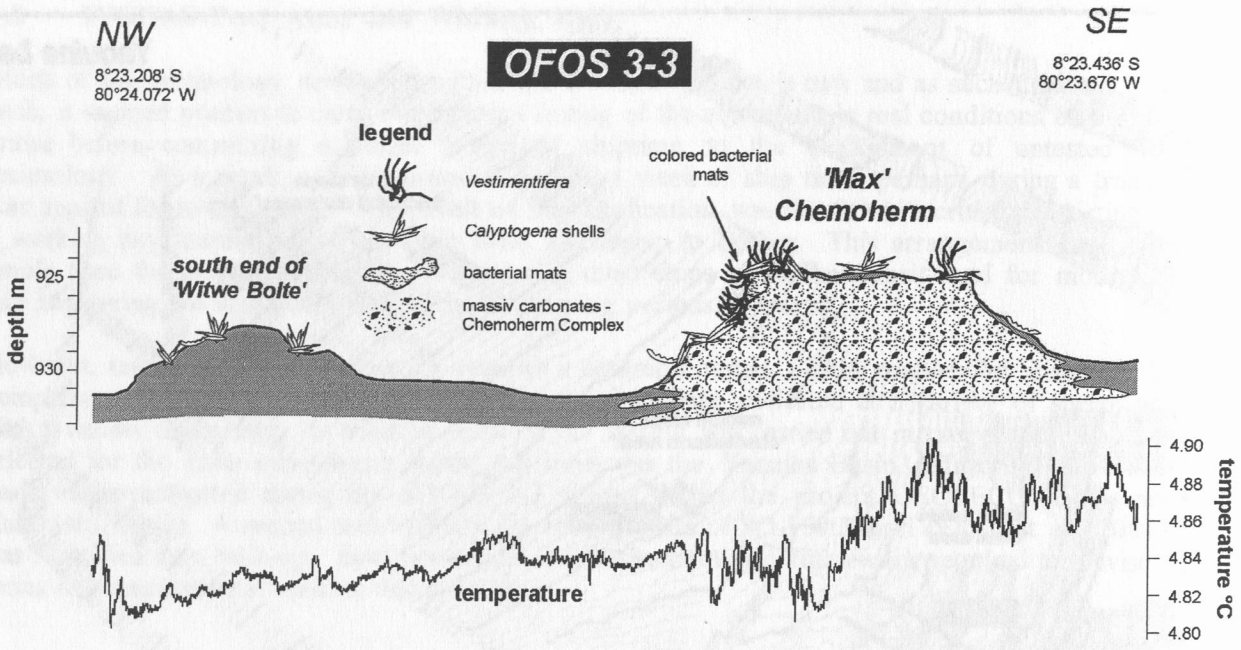

Figure 1.7: OFOS 3 profile (SO-146) across the Max and Witwe Bolde chemoherms.

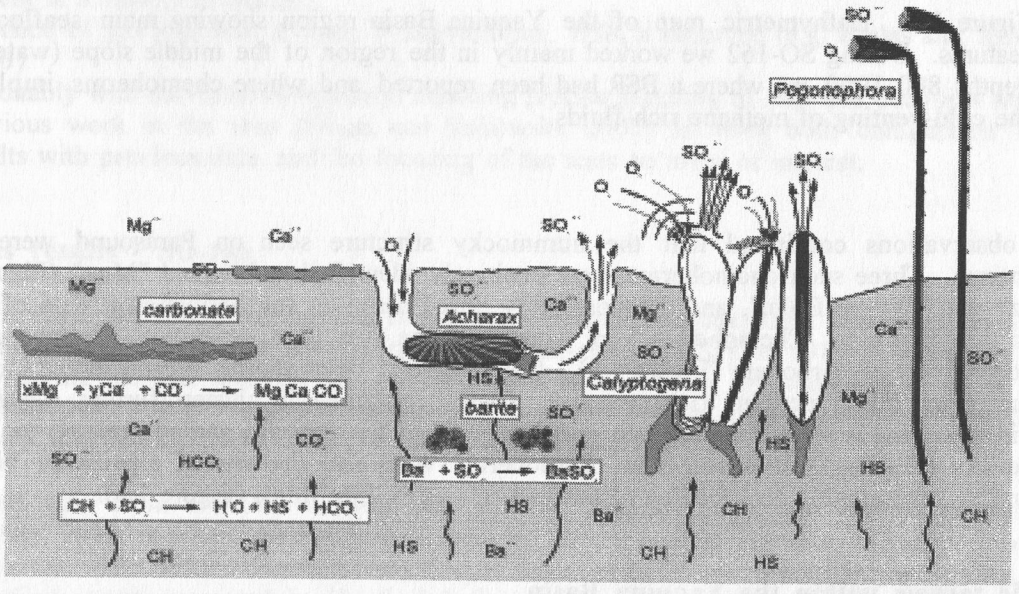

Figure 1.8: Schematic diagram of the chemical systems that lead to the formation of a chemoherm. As such structures rely on the venting of methane, they are closely related to gas hydrate research and hence to the INGGAS project.

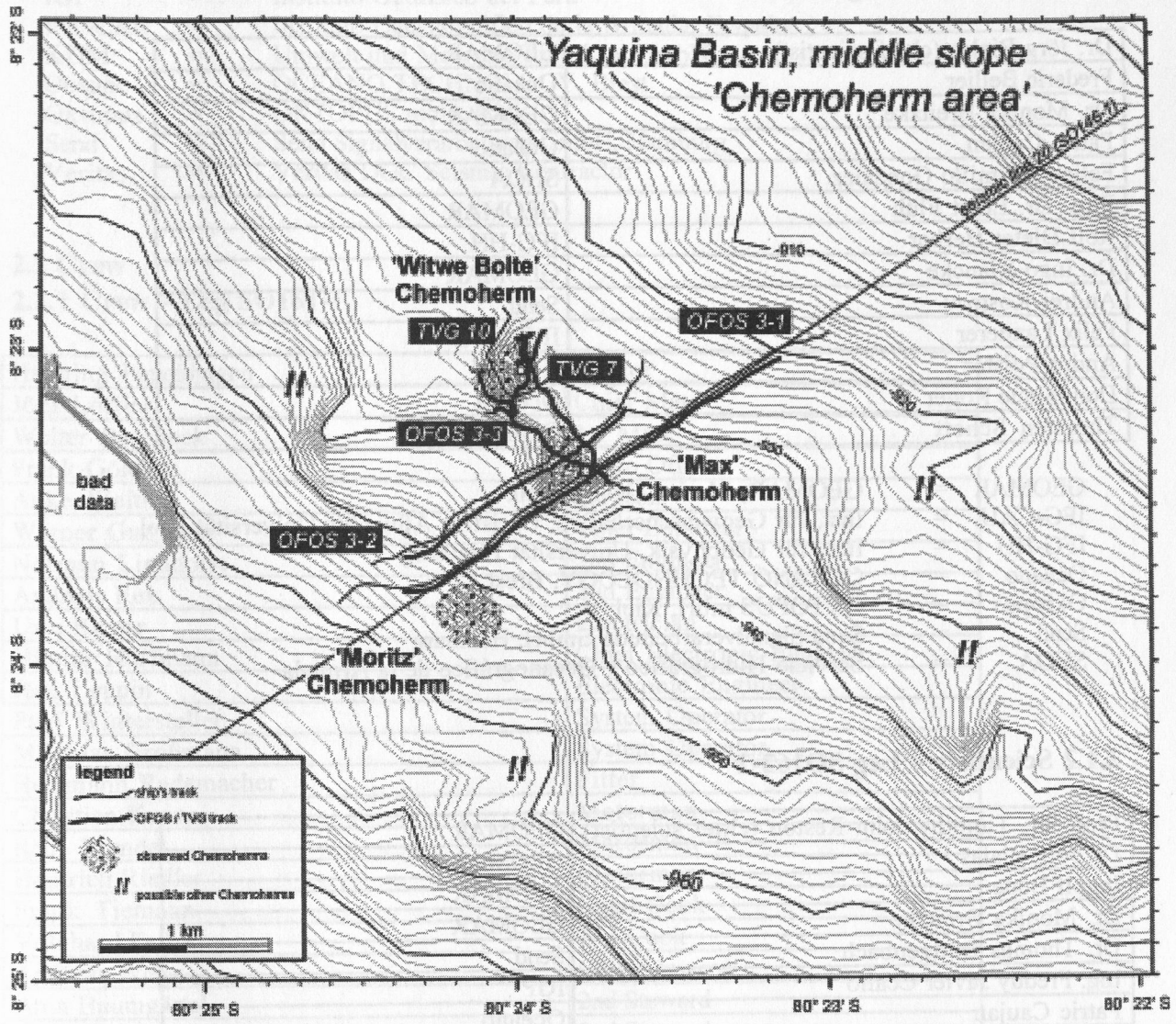

Figure 1.9: Map of the chemoherm field surveyed during SO-146. This was one of the working areas of SO-162 INGGAS-Test.

1.3.2 Carnegie Ridge area

A second working area was the region explored during SO-159 Salieri. Although this is not a gas hydrate region, swath-bathymetric data collected during this cruise, and earlier with the French vessel L'Atalante, provided the detailed information on seafloor morphology to allow identification of suitable, closely-spaced shallow and deep targets for testing equipment. Furthermore, the presence of a second working area allowed time during the northward transit for any necessary repair, modification and final preparation of the equipment between recovery in one site and redeployment. Other tests could effectively be made anywhere during the transit. As is clear in the Agenda of the cruise, we made full use of this flexibility.

2. Participants

2.1 Scientists

2.1.1 Scientists – Leg SO162-1

Dr. Jörg Bialas (chief scientist)	GEOMAR
Frederic Bellier	Oceano
Dr. Monika Breitzke	GEOMAR
Patric Caujan	Oceano
Felipe Jaramillo González	SHOA
Prof. Dr. Ernst Flüh	GEOMAR
Rolf Dieter Herber	IFG-HH
Dr. Ingo Klaucke	GEOMAR
Andrej Kostrov	Send
Felix Landerer	IFG-CAU
Andre Polster	IFG-HH
Dominique Roger	Oceano
Thorsten Schott	Oktopus

GEOMAR = GEOMAR, Marine Geodynamik
IFG-CAU = Inst. für Geowissenschaften, Christian Albrechts Universität Kiel
IFG-HH = Inst. für Geophysik, Universität Hamburg
Oceano = OCEANO TECHNOLOGY, Brest
Oktopus = OKTOPUS mbH, Kiel
Send = Send Signalverarbeitung GmbH, Hamburg
SHOA = Servicio Hidrográfico y Oceanográfico de la Armada

2.1.2 Scientists – Leg SO162-2

Prof. Dr. Timothy John Reston (chief scientist)	GEOMAR
Dr. Jörg Bialas	GEOMAR
Ingolf Bode	GEOMAR
Dr. Monika Breitzke	GEOMAR
Dr. Thomas Büttgenbach	Send
Ing. Freddy Javier Ccallo	IGP
Patric Caujan	Oceano
Prof. Dr. Ernst Flüh	GEOMAR
Rolf Dieter Herber	IFG-HH
Dr. Caroline Huguen	GEOMAR
Dr. Dirk Kläschen	GEOMAR
Dr. Ingo Klaucke	GEOMAR
Andrej Kostrov	Send
Felix Landerer	IFG-CAU
Patrick Nicholls	Veritas
Andre Polster	IFG-HH
Ing. Teofilio Rodríguez Cancán	IGP
Dominique Roger	Oceano
Dr. Joshua Ronen	Veritas
Ing. Essy Santana	INOCAR
Thorsten Schott	Oktopus
Klaus-Peter Steffen	KUM

GEOMAR	=	GEOMAR, Marine Geodynamik
IFG-CAU	=	Inst. für Geowissenschaften, Christian Albrechts Universität Kiel
IFG-HH	=	Inst. für Geophysik, Universität Hamburg
IGP	=	Instituto Geofisico del Perú
INOCAR	=	Instituto Oceanográfico de la Armada, Ecuador
KUM	=	Umwelt und Meerestechnik Kiel GmbH
Oceano	=	OCEANO TECHNOLOGY, Brest
Oktopus	=	OKTOPUS mbH, Kiel
Send	=	Send Signalverarbeitung GmbH, Hamburg
Veritas	=	Veritas DGC Seismic Contractor

2.2 Crew

2.2.1 Crew – Leg SO161-1

Henning Papenhagen	Master
Jörn Löffler	Chief Mate
Walter Bascheck	1st Mate
Frank Göldner	Radio Officer
Anke Walther	Surgeon
Werner Guzmann	Chief Engineer
Norman Lindhorst	2nd Engineer
Andreas Rex	2nd Engineer
Uwe Rieper	Electrician
Hilmar Hoffmann	Chief Electronic Engineer
Jörg Leppin	Electronic Engineer
Paul Wintersteller	System Operator
Matthias Großmann	System Operator
Herrmann Rademacher	Fitter
Christian Kunze	Motorman
Rene Brendel	Motorman
Heinrich Riedler	Motorman
Frank Tiemann	Chief Cook
Volkhard Falk	2nd Cook
Andreas Wege	Chief Steward
Anja Baumgärtel	2nd Steward
Maik Steep	2nd Steward
Karl-Heinz Lohmüller	Boatswain
Ulrich-Bruno Hampel	A. B.
Andreas Woltmann	A. B.
Peter Rosin	A. B.
Norbert Bosselmann	A. B.
Dirk Schachel	A. B.
Karsten Bosselmann	A. B.

Oktopus: OKTOPUS
Gesellschaft für angewandte Wissenschaft
Innovative Technologien und Service in der Meerestechnik mbH
Wischhofstr. 1-3, Geb. D5
24148 Kiel
Germany
Tel.: +49 - 431 - 7209 - 350
Fax: +49 - 431 - 7209 - 356

Send: SEND GmbH
Rostocker Str. 20
20099 Hamburg
Germany
Tel.: +49 - 40 - 375 00 823
Fax: +49 - 40 - 375 00 893
e-mail: office@send.de
Internet: www.send.de

SHOA: Servicio Hidrográfico y Oceanográfico de la Armada
Errazuriz 232
Playa Ancha
Valparaíso
Tel.: +56 - 32 - 266540
Fax: +56 - 32 - 266542
e-mail: shoa@shoa.cl - sitiof@starmedia.com

IGP: Instituto Geofísico de Perú
Calle Calatraba 216
Urbanización Camino Real, La Molina
Lima
Tel: +51 - 1 - 4361683
Fax: +51 - 1 - 4361683
e-mail: jtavera@geo.igp.gob.pe
Internet: www.igp.gob.pe

INOCAR: Instituto Oceanográfico de la Armada
Base Naval Sur, Av. 25 de Julio, Vía Puerto Marítimo
Guayaquil
Tel: +593 - 4 - 2481300 ext 4001
Fax: +593 - 4 - 2485166
e-mail: geologia@inocar.mil.ec
Internet: www.inocar.mil.ec

Veritas: Veritas DGC Seismic Contractor
Crompton Way, Manor Royal Estate
Crawley, West Sussex
UK RH10 9QN
Tel: +44 - 1293 - 44 3000
Fax: +44 - 1293 - 44 3010
e-mail: shuki_ronen@veritasdgc.com
Internet: www.veritasdgc.com

Figure 2.1: SO 162-2 Scientific Party

3. Agenda

3.1.Agenda of the cruise SO 162 – 1 INGGAS-TEST

SONNE left the pier of Valparaiso at 13:00 on February 22 and headed north for the port of Callao, Peru. During the transit, the vessel stopped several times to test the new POSIDONIA system, with variable success. An acoustic release transponder unit was lowered to several 100 meters and the receiving array was activated to communicate to the transponder. During the transit calm seas and mild winds allowed for an average cruising speed of about 13 kn. The Simrad system was activated when leaving the 3nm exclusive economic zone of Chile and was operated permanently before entering the 3 nm zone of Peru near Callao.
In the afternoon of 26. February, a water velocity profile to a depth of 2000 m was measured using the Simrad sensor. Soon after, the sidescan sonar was deployed for a test measurement, 2600 m of cable were released and the system reached a depth of 1500 m, while the ship steamed at 3 kn. We finally reached anchorage in Callao on February 27 at 11:00.

3.1.Agenda of the cruise SO 162 – 2 INGGAS-TEST

SONNE left Callao at 2 pm on the 27th of February, heading north toward the region of Yaquina Basin. During transit on 27th and 28th February, SIMRAD profiling was carried out, and the final preparations were made for the first combined deployment of the deep tow side-scan sonar and streamer (DTS). On 28.2.02, an OBH was deployed in water just over 1000 m deep and a "Figure of eight" Posidonia calibration test carried out. Subsequently a line of four OBH and four OBS were deployed along the first in water depths of between 800 and 900 m. During the night of the 28.2 - 1.3, this line was shot using the surface streamer and the GI gun. On the morning of 1.3. (08:00) an OBH was again deployed in water depths just over 1000 m for another calibration of the Posidonia system (Figure 3.1). This time, the Posidonia unit was suspended several tens of metres below the flotation buoy to improve the signal reaching the transponder. This resulted in a greatly improved calibration compared to previous attempts.

Following the successful calibration of the Posidonia system, the OBH was recovered and a short transit made to the end of the profile for the deployment of the DTS. After a first attempt went awry because an electrical connection came loose, the system was successfully deployed in the late afternoon, and the first deep tow profile collected. Over the next 24 hours, three deep tow profiles (Fig 3.1) were shot with the GI gun along the same profile at c. 100 m over the seafloor with varying speeds throught the water to both test the optimum speed for the stability of the instrument and for data quality, and to gain experience in the handling of the instrument. A fourth profile with the 32 litre gun was then carried out along the same track, towing the deep tow side-scan and streamer between 20 and 30 m over the seafloor as possible. This meant that the high resolution side-scan system could be tested, and gave a chance of picking up any Scholte waves generated by the large low frequency source.

The transect over the OBH-OBS was finished at about midnight of 2-3 March. After recovery of the 32 litre gun, we turned on a new profile with the GI gun, heading into deeper water to the southwest (Fig. 3.1), towing the deep tow system c. 100 m above the seafloor. The Posidonia positioning signal deteriorated at tow depths greater than about 2500 m, possibly because of low battery power, but both the side-scan and the deep-tow streamer functioned well until the latter suddenly failed a t a tow depth of c. 3500 m. Both were recovered on the morning of the 3rd March, and the transit made back to the OBH-OBS profile. After collection of two cross profiles over the instruments early in the evening of the 3.3 (at the end of which the GI-Gun failed), the OBH-OBS were recovered, and SIMRAD collected during the rest of the night to infill the previous Hydrosweep survey to the north of the study area.

On the morning of the 4th, a new Posidonia calibration was carried out (Site 2 - Figure 3.1) and a pattern of two OBH and 2 OBS put out in the area of the Max and Moritz Chemoherms, where we planned a deep tow survey as well as tests of the BeatGun and SeeBoSeis (Figure 3.2). The deep-tow streamer was by now being thoroughly tested in the laboratory. The Beatgun was then successfully tested in just over 900 m of water, and was followed by a short SeeBoSeis profile (7

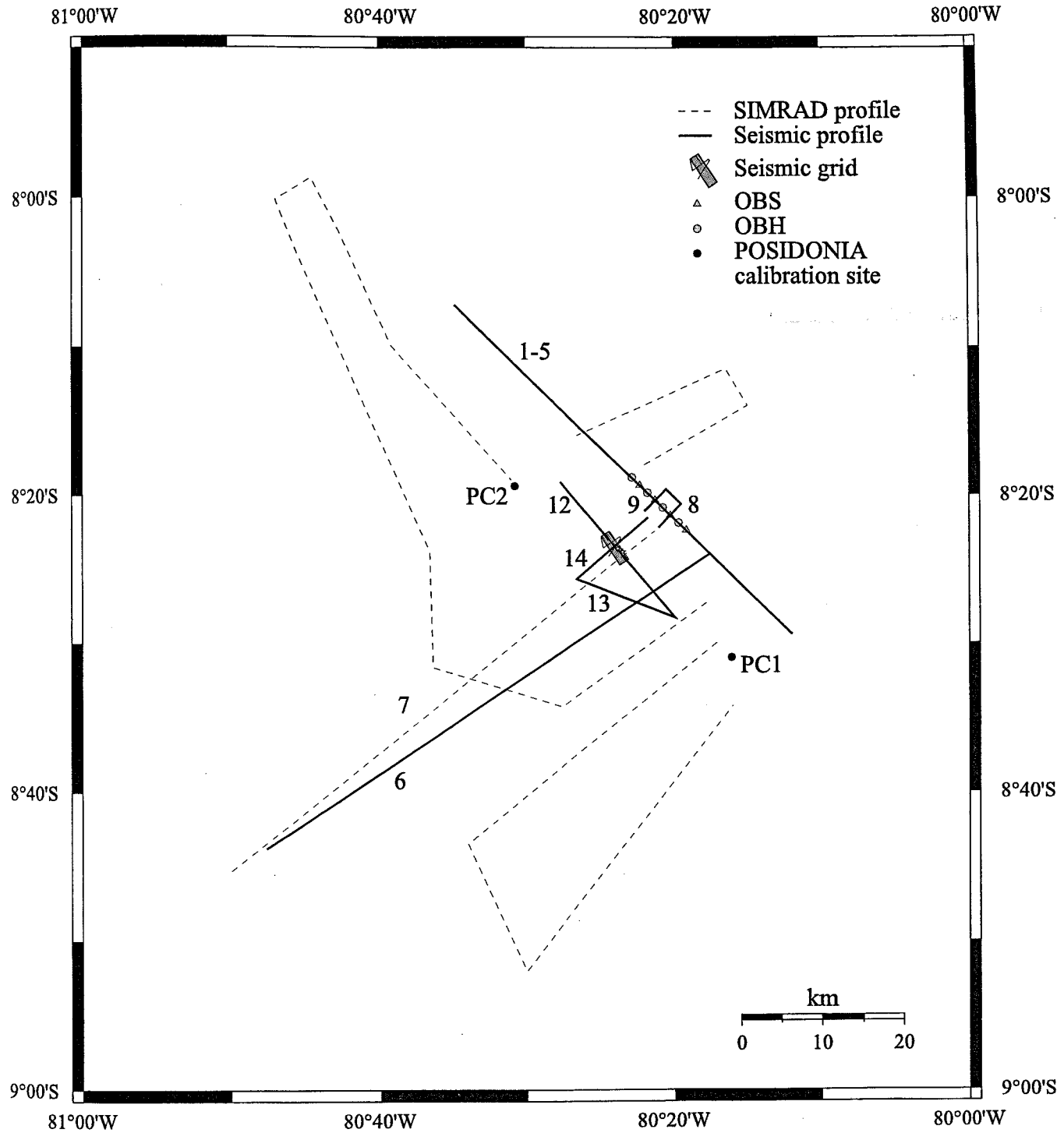

Figure 3.1 Overview of work carried out in the Yaquina Basin off Peru.

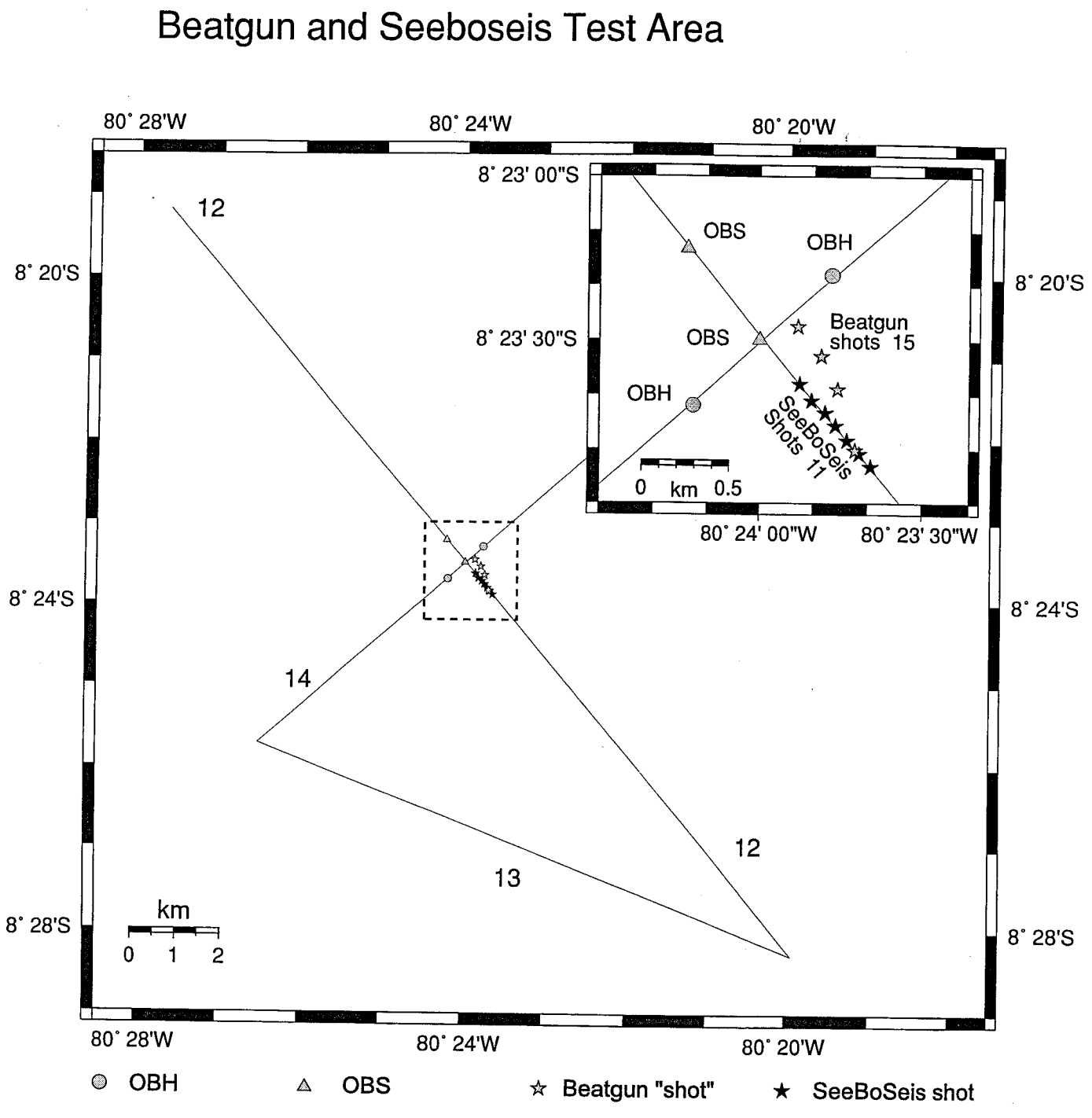

Figure 3.2 Map of profiles in the region of the Beatgun and SeeBoSeis tests.

shots, spaced 100m apart) (Fig. 3.2). After this, the magnetometer was tested for the first time: we plan to deploy it during the transit toward Balboa. The collection of a Beatgun profile was delayed until a less muddy site could be found, and in the evening of the 4th, further SIMRAD profiles were collected to the south of the study areas the DT streamer and Side-scan were assembled for a deployment just after midnight. However, the eventual deployment of the deep-tow streamer was aborted in the early hours of the 5th as streamer went dead at a depth of 400 m. Further SIMRAD profiles were shot during the early hours of the 5th, followed by three seismic profiles, 2 over the deployed OBH/S, 1 linking the other two, with the 32 litre gun and the short surface streamer. These were followed by a BeatGun weight-drop profile at c. 18:00 on 5.3.02, centred on the Max chemoherm, which was thought might provide a firmer seafloor for the test. After the test, the two OBH and two OBS were recovered, and a Posidonia (calibration test) and SIMRAD (acoustic velocity in water) measurements made in deep water.

The deployment of the DT Side-scan and streamer in the Max-Moritz area eventually took place in the early hours of the morning of the 6th. As the GI gun proved to be still inoperable, a single 1.6 litre Prakla airgun was used as source. Although the bubble from this single gun is quite strong, the deep tow streamer provides the ideal remedy, namely a whole array of deep-towed hydrophones recording the far field source signature, and allowing future source signature deconvolution. During the whole of the 6th, the deep tow system worked admirably and ten profiles over the Max-Moritz area were completed (Fig. 3.3). Unfortunately at the start of the final profile, the streamer went dead: on recovery, it was found that a hole had developed in the outer casing of the cable.

As soon as the streamer was on deck we set course for Ecuador, allowing repairs to be carried out in transit prior to another deep water test of the deep towed system. During the transit, SIMRAD data was collected. Following a final calibration of the Posidonia system with an OBH deployed on top of a conical seamount just southwest of Carnegie Ridge (Fig. 3.4), the deep tow system was deployed at 10:00, and lowered into the ocean trench, with water depths in places in excess of 4000 m. During this, the Posidonia gave very accurate and consistent readings until the sled was at a depth of about 3500 m, and 7000 m of cable had been deployed After a short profile along the bottom of the trench the whole system was recovered by 20:00 on 8.3.02. However, the deep tow streamer did not function properly and required further testing. As soon as the system was onboard, a generally northward course was set, but chosen to fill in gaps in the previous bathymetry and to survey some interesting bathymetric features (such as the Yaquina Graben off Columbia) on the way. The magnetometer was deployed at 8:15 on the 9th as we came off Carnegie Ridge, and again on the morning of the 10th, and the deep tow system was also deployed at 8:00 on the 10th for a final test of the streamer, in which the previous problems were solved and the streamer functioned perfectly.

We arrived off Balboa at 11:00 on the morning of the 12th, and docked by 15:00 on the same day.

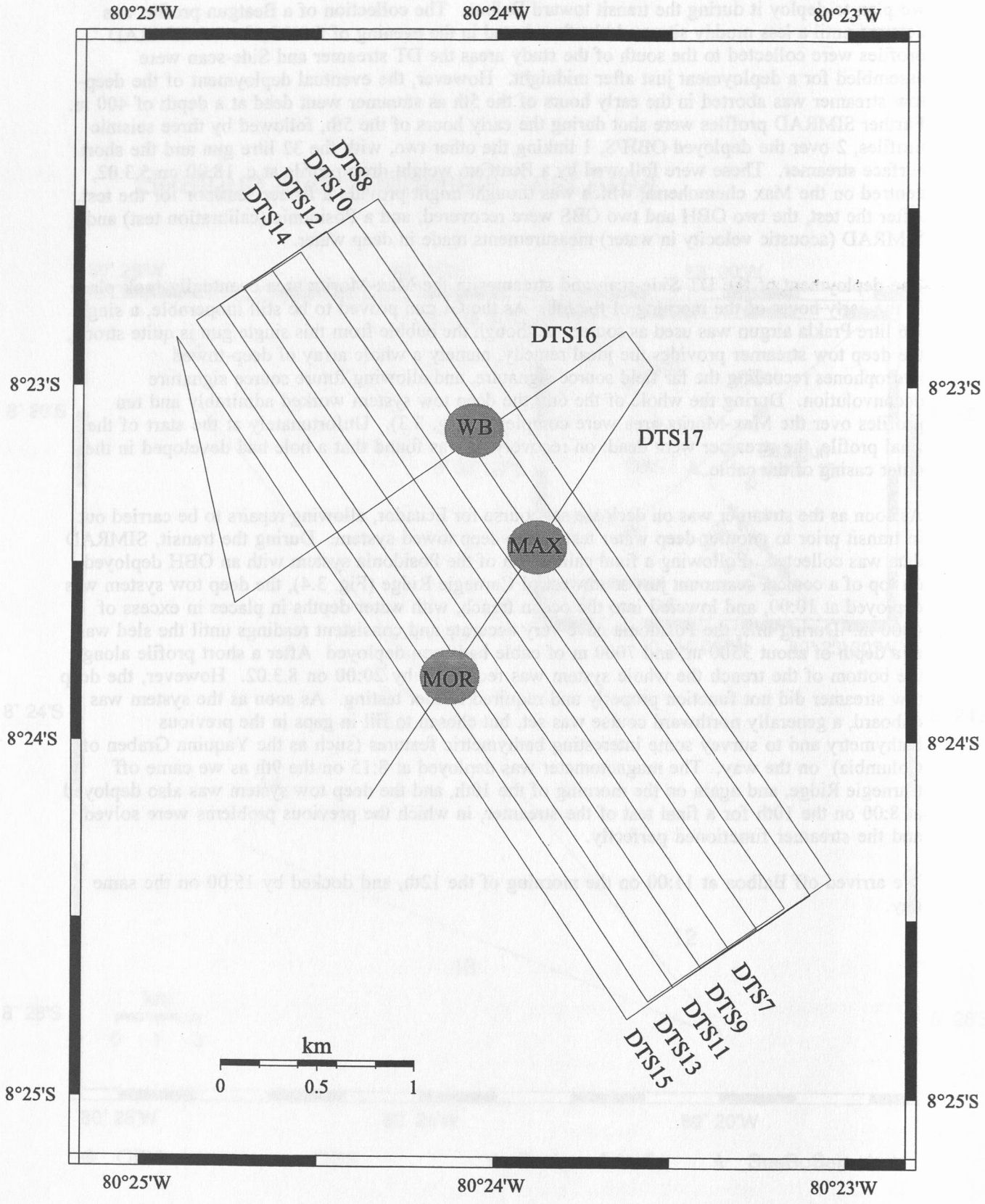

Figure 3.3 Deep-tow profiles shot in the Max-Moritz chemoherm area.
WB=Witwe Bolte chemoherm ; MAX = Max chemoherm; MOR = Moritz chemoherm.

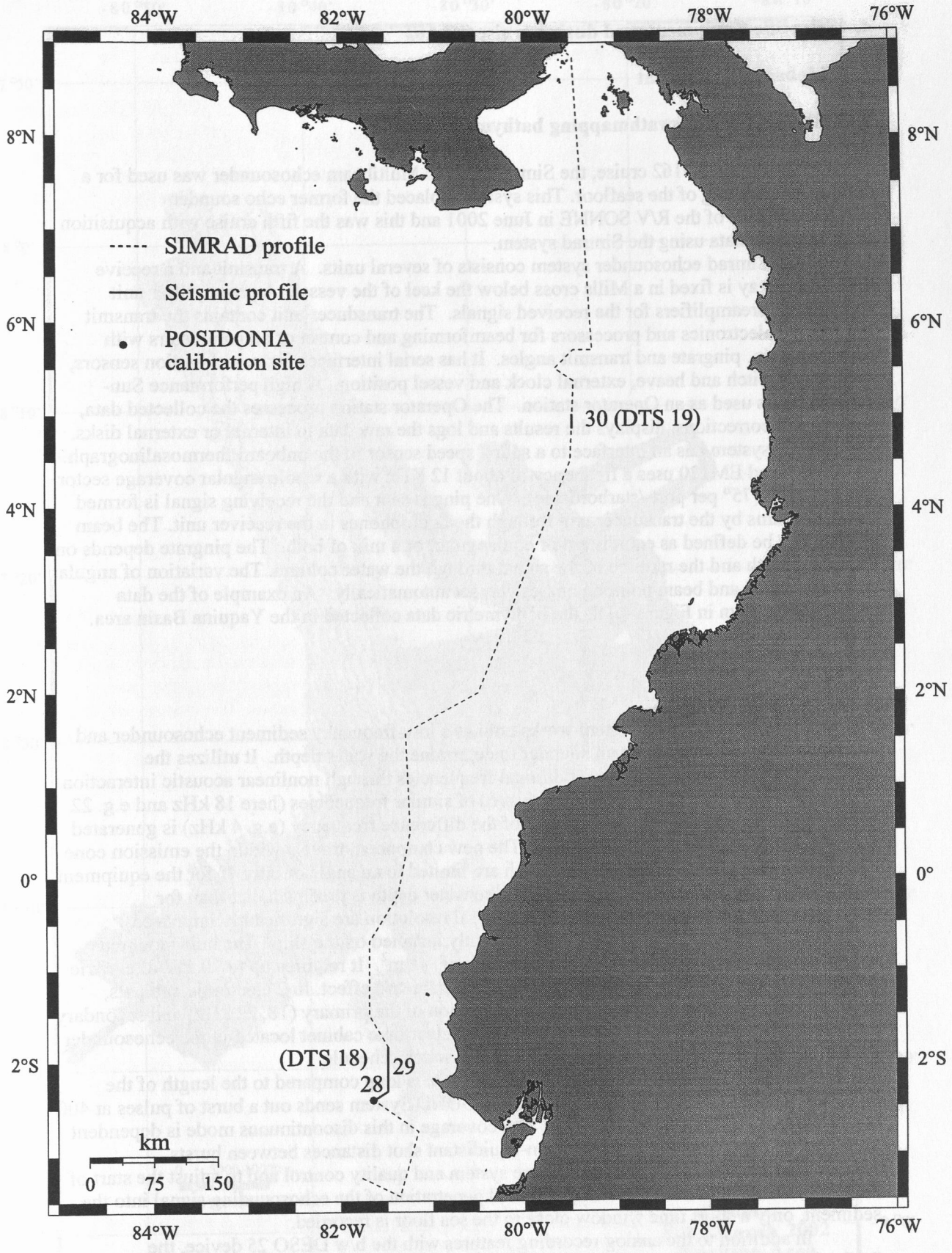

Figure 3.4 Map of work carried out north of 3°S. Apart from SIMRAD profiles (together with magnetics), one Posidonia calibration was carried out on top of a conical seamount, and short deep-tow test profiles were shot (numbered).

4. Scientific Equipment used during cruise SO-162

4.1 Shipboard Equipment

4.1.1 Simrad EM120 swathmapping bathymetry system

During the SO162 cruise, the Simrad EM120 Multibeam echosounder was used for a continuous mapping of the seafloor. This system replaced the former echo sounder HYDROSWEEP of the R/V SONNE in June 2001 and this was the fifth cruise with acquisition of bathymetric data using the Simrad system.

The Simrad echosounder system consists of several units. A transmit and a receive transducer array is fixed in a Mills cross below the keel of the vessel. A preamplifier unit contains the preamplifiers for the received signals. The transducer unit contains the transmit and receive electronics and processors for beamforming and control of all parameters with respect to gain, pingrate and transmit angles. It has serial interfaces for vessel motion sensors, such as roll, pitch and heave, external clock and vessel position. A high performance Sun-workstation is used as an Operator station. The Operator station processes the collected data, applying all corrections, displays the results and logs the raw data to internal or external disks. The EM120 system has an interface to a sound speed sensor in the onboard thermosalinograph.

Simrad EM120 uses a frequency of about 12 KHz with a whole angular coverage sector of up to 150° (75° per port-/starbordside). One ping is sent and the receiving signal is formed into 191 beams by the transducer unit through the hydrophones in the receiver unit. The beam spacing can be defined as equidistant or equiangular, or a mix of both. The pingrate depends on the water depth and the runtime of the signal through the water column. The variation of angular coverage sector and beam pointing angles was set automatically. An example of the data collected is shown in Figure 4.1.1, the bathymetric data collected in the Yaquina Basin area.

4.1.2 PARASOUND

The PARASOUND system works both as a low-frequency sediment echosounder and as a high-frequency narrow beam sounder to determine the water depth. It utilizes the parametric effect, which produces additional frequencies through nonlinear acoustic interaction of finite amplitude waves. If two sound waves of similar frequencies (here 18 kHz and e.g. 22 kHz) are emitted simultaneously, a signal of the difference frequency (e.g. 4 kHz) is generated for sufficiently high primary amplitudes. The new component travels within the emission cone of the original high frequency waves, which are limited to an angle of only 4° for the equipment used. Therefore, the footprint size of 7% of the water depth is much smaller than for conventional systems and both vertical and lateral resolution are significantly improved.

The PARASOUND system is permanently installed on the ship. The hull-mounted transducer array has 128 elements within an area of ~ 1 m^2. It requires up to 70 kW of electric power due to the low degree of efficiency of the parametric effect. In 2 electronic cabinets, beam formation, signal generation and the separation of the primary (18, 22 kHz) and secondary frequencies (4 kHz) is carried out. Using the third electronic cabinet located in the echosounder control room, the system is operated on a 24 hour watch schedule.

Since the two-way travel time in the deep sea is long compared to the length of the reception window of up to 266 ms, the PARASOUND System sends out a burst of pulses at 400 ms intervals, until the first echo returns. The coverage in this discontinuous mode is dependent on the water depth and also produces non-equidistant shot distances between bursts.

The main tasks of the operators are system and quality control and to adjust the start of the reception window. Because of the limited penetration of the echosounding signal into the sediment, only a short time window close to the sea floor is recorded.

In addition to the analog recording features with the b/w DESO 25 device, the PARASOUND System is equipped with the digital data acquisition system ParaDigMA, developed at the University of Bremen. The data is stored on removable hard disks using the standard, industry-compatible SEGY-format. The 486-processor based PC allows for buffering, transfer and storage of the digital seismograms at high repetition rates. Of the emitted series of pulses, usually only every second pulse can be digitized and stored, resulting in recording

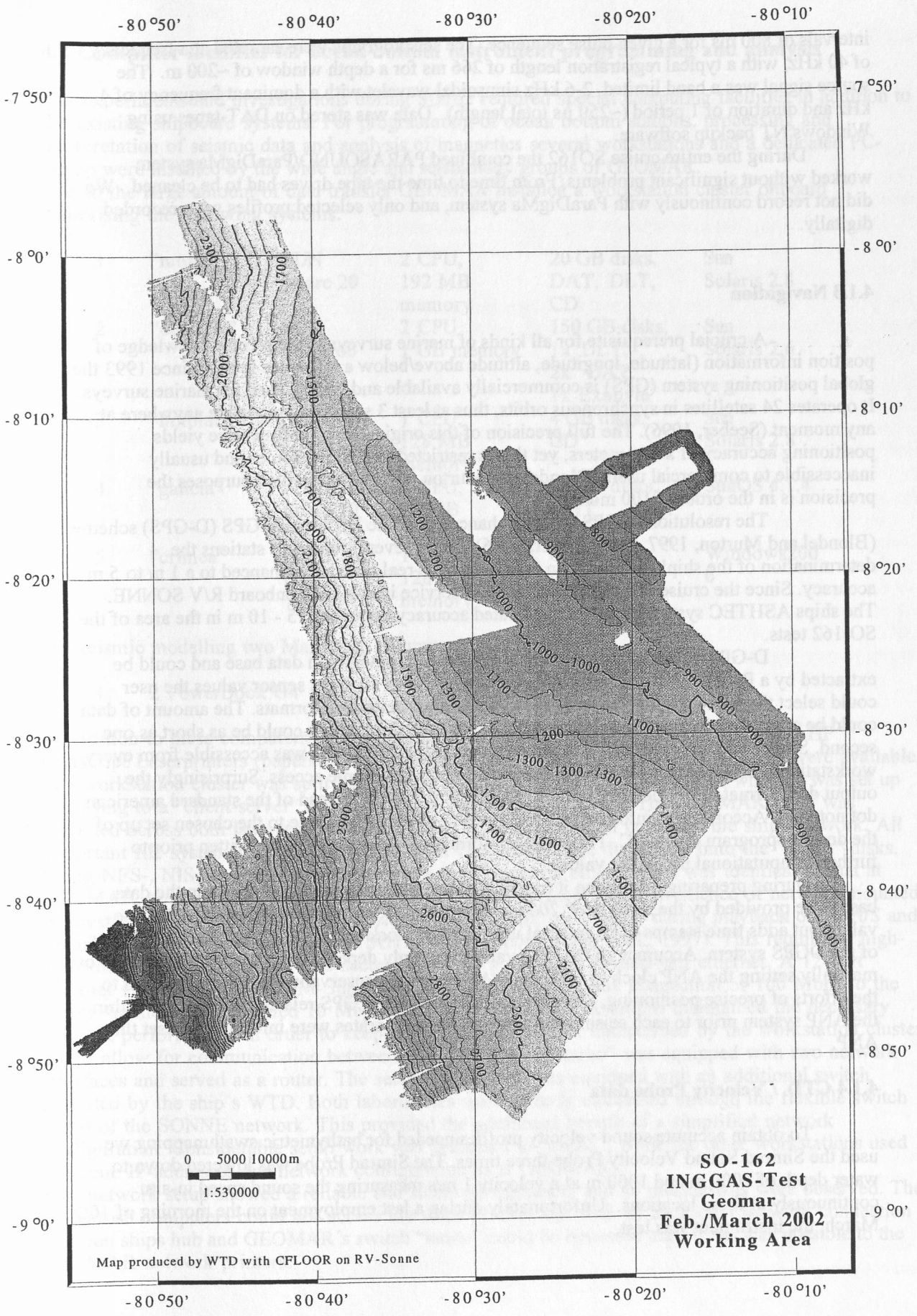

Figure 4.1.1 Bathymetric map of the Yaquina Basin region from data collected during SO162.

intervals of 800 ms for a given pulse sequence. The seismograms were sampled at a frequency of 40 kHz, with a typical registration length of 266 ms for a depth window of ~200 m. The source signal was a band limited, 2-6 kHz sinusoidal wavelet with a dominant frequency of 4 kHz and duration of 1 period (~250 µs total length). Data was stored on DAT-tapes using Windows NT backup software.

During the entire cruise SO162 the combined PARASOUND/ParaDigMa system worked without significant problems. From time to time the tape drives had to be cleaned. We did not record continously with ParaDigMa system, and only selected profiles were recorded digitally.

4.1.3 Navigation

A crucial prerequisite for all kinds of marine surveys is the precise knowledge of position information (latitude, longitude, altitude above/below a reference level). Since 1993 the global positioning system (GPS) is commercially available and widely used for marine surveys. It operates 24 satellites in synchronous orbits, thus at least 3 satellites are visible anywhere at any moment (Seeber, 1996). The full precision of this originally military service yields positioning accuracy of a few meters, yet this is restricted to military forces and usually inaccessible to commercial users (Blondel and Murton, 1997). For civilian purposes the precision is in the order of 100 meters.

The resolution of GPS can be enhanced with the Differential GPS (D-GPS) scheme (Blondel and Murton, 1997, Knickmeyer, 1996). Using several reference stations the determination of the ship's position can be corrected in real time and enhanced to a 1 m to 5 m accuracy. Since the cruise SO-109 (1996) D-GPS service is available onboard R/V SONNE. The ships ASHTEC system provides a validated accuracy better than 5 - 10 m in the area of the SO-162 tests.

D-GPS values were available from the ships navigation data base and could be extracted by a PC based end user interface program. Out of all ships sensor values the user could select the wanted variables and specify the output in various formats. The amount of data could be controlled by the desired interval of extracted values which could be as short as one second. Stored on the "wiss-data" directory the extracted ASCII file was accessible from every workstation connected to the shipboard network via ftp or volume access. Surprisingly the output data format writes decimal values separated by a colon instead of the standard american dot notation. According to information of the ships operator this is due to the chosen set up of the desktop program on the PC. Therefore a reformating program must be written prior to further computational use of the values.

During preparing discussion it turned out that the coordinates stored within the data base were provided by the *Atlas ANP 2000* system which does not copy the exact GPS time values but adds time stamps of its internal uncontrolled clock to the high precision coordinates of the DGPS system. Accuracy of the time values is mainly dependent on the operators skills by manually setting the ANP clock to GPS time. A somewhat conservative method compared to the efforts of precise positioning. To enable the most accurate GPS related time stamps within the ANP system prior to each seismic survey the system operates were informed to reset the ANP.

4.1.4 CTD / Velocity Probe data

To obtain accurate sound velocity profiles needed for bathymetric swathmapping we used the Simrad Sound Velocity Probe three times. The Simrad Probe was lowered down to water depth of 2000 m and 1000 m at a velocity 1 m/s measuring the sound speed in-situ continuously at these locations. Unfortunately during a last employment on the morning of 10th March, the instrument was lost.

4.2 Computer facilities for ocean bottom instrument programming and analysis

The experiments and investigations during SO162 required special computing facilities in addition to the existing shipboard systems. For programming of ocean bottom stations, processing and interpretation of seismic data and analysis of magnetics several workstations and a dedicated PC-laptop were installed by the wide angle and seismology groups of GEOMAR.
Due to the large amount of data transfer GEOMAR installed a workstation cluster onboard comprising the following systems:

1	"moho"	SUN Sparc 20	2 CPU, 192 MB memory	20 GB disks, DAT, DLT, CD	Sun Solaris 2.8
2	"devonia"	SUN Ultra 60	2 CPU 1 GB memory	150 GB disks, 1x DLT, 2x DAT, 1x Exabyte	Sun Solaris 2.6
3	"hotblack"	SUN Ultra 1	1 CPU, 128 MB memory	4 GB disks, CD	Sun Solaris 2.8
4	"galicia"	SUN Sparc 10	1 CPU, 96 MB memory	12 GB disks, DAT	SunOS 4.1.4
5	"crimea"	AMD Duron 700 MHz	1 CPU, 128 MB memory	68 GB disks, 6x PCMCIA	Windows2000

For seismic modelling two Macintosh computers were installed:

1	2 PowerBook G4

In addition to these computers several laptops were used. For plotting and printing two HP Postscript Laserprinters (papersize A3 and A4) as well as the shipboard color plotters were available. The workstation cluster was split between the Reinlabor and the Magnetiklabor where it was set up according to a "client-server" model, with "moho" being the server. The GEOMAR LAN was extended across both laboratories making use of the flexible patch boards of the ships network. All important file systems from the main server at GEOMAR were duplicated onto the "moho"-disks. Using NFS-, NIS-, and automounter services the computing environment was identical to that at GEOMAR, so every user found his/her familiar user interface. The convenience of network mounted file systems has to be paid for with a heavy network load, particularly during playback of OBH/S and streamer-data from tape to disk (c.f. SO123 cruise report, Flueh et al., 1997). This required a high-performance network, which was accomplished by a switched twisted-pair ethernet. A 12-port ethernet switching-hub (3COM-SuperstackII 1000) with an uplink connection of 100 Mbps to the server "moho" and dedicated 10 Mbps ports for the client workstations maintained the necessary network performance. In order to keep the shipboard network undisturbed by the workstation cluster, but to allow for communication between them, the server "moho" was equipped with two network interfaces and served as a router. The second laboratory was equipped with an additional switch provided by the ship´s WTD. Both laboratories were directly connected through the flexible switch board of the SONNE network. This provided the additional benefit of a simplified network configuration. Considerable setup work was dedicated to "moho", while the other workstations used the same IP-addresses and network configuration as at GEOMAR.
This network setup showed a reliable and stable performance, and no breakdowns were observed. The Macintosh computers could not access the ships printers but with an additional network connection between ships hub and GEOMAR´s switch "moho" could be bypassed and access was possible to the GEOMAR network printers.

4.3 The GEOMAR Ocean Bottom Hydrophone / Seismometer (OBH/S)

The Ocean Bottom Hydrophone

The first GEOMAR Ocean Bottom Hydrophone was built in 1991 and tested at sea in January 1992. This type of instrument has proved to have a high reliability; in fact more than 1800 successful deployment have been carried out since. A total of 4 OBH and 4 OBS instruments were used during SO162. In addition, the OBH-frames were used to calibrate the Posidonia System in three instances. Altogether 12 sites were occupied during the SO162 cruise, and 5 instruments were deployed for Posidonia calibrations and test purposes.

The principle design of the instrument is shown in Figure 4.3.1, and a photograph showing the instrument upon deployment can be seen in Figure 4.3.2. The design is described in detail by Flueh and Bialas (1996).

The system components are mounted on a steel pipe at the top of which the flotation buoy is mounted. The buoy is made of syntactic foam and is rated for a water depth of 6000 m, as are all other components of the system except for the pressure cylinders holding the recording electronics. Here, various models are available for variable depths (2500 m, 3000 m, and 6000 m). Attached to the buoyant body are a radio beacon, a flash light, a flag and a swim-line for retrieving from aboard the vessel. The hydrophone for the acoustic release is also mounted here. The release transponder is a model *RT661CE* or RT861 made by *OCEANO Technology (*formerly *MORS Technology)*. Communication with the instrument is possible through the ship's transducer system, and even at maximum speed and ranges of 4 to 5 miles release and range commands are successful. For anchors, we use pieces of railway track weighing about 40 kg each. The anchors are suspended 2 to 3 m below the instrument. The sensor is an *E-2PD* hydrophone from *OAS Inc.*, and the recording device is an *MBS recorder of SEND GmbH*, which is contained in its own pressure tube and mounted below the buoyant body opposite the release transponder (see Figures 4.3.1 and 4.3.2).

The Ocean Bottom Seismometer

The Ocean Bottom Seismometer (OBS) construction (Bialas and Flueh, 1999; Fig. 4.3.3) is based on the experiences with the GEOMAR OBH. For system compatibility the acoustic release, pressure tubes, and the hydrophone are identical to those used for the OBH. Syntactic foam is used as floatation again but of larger diameter due to the increased payload. In contrast to the OBH the OBS has three legs around a center post to which the anchor weight is attached (Fig. 4.3.4). While the OBH is floating about 1 m above the sea bottom, the OBS is positioned on the sea bottom to avoid collisions between the the seismometer cable and the anchor. The sensitive geophone package is deployed about 1 m to the side of the system once the OBS lands on the sea floor. During descent to the ocean bottom, the footplate of the geophone's release-lever is about one meter below the base of the anchor and therefore hits the seafloor first. At touch down the baseplate forces an upward movement of the lever which lays out the geophone package hook until the geophone anchor is about 0.5 m above the seafloor. At about 45 degrees to the vertical the seismometer is released from its hook and falls to the sea floor from about 1 m height, ensuring coupling between the seismometer and the sea floor. At this time the only connection from the seismometer to the instrument is a cable and an attached wire which retracts the seismometer during ascent to the sea surface. An oscillation of the main instrument caused by possible near-bottom currents is therefore not transmitted mechanically to the geophone package. All three channels are recorded by the MBS recorder as used in the OBH units. Parallel to these three channels the standard hydrophone is recorded on the fourth channel. A new self-levelling geophone package with 4.5 Hz geophones was successfully tested during SO162. The levelling of the three component geophones (termed A01) is done at a preset time by unlocking springs that clamp the geophones against the titanium housing.
Beside the standard OBS type used for active seismic recording broadband seismometer are available and routinely deployed within the profiles. During SO162 we deployed a *PMD-113* sensor. This

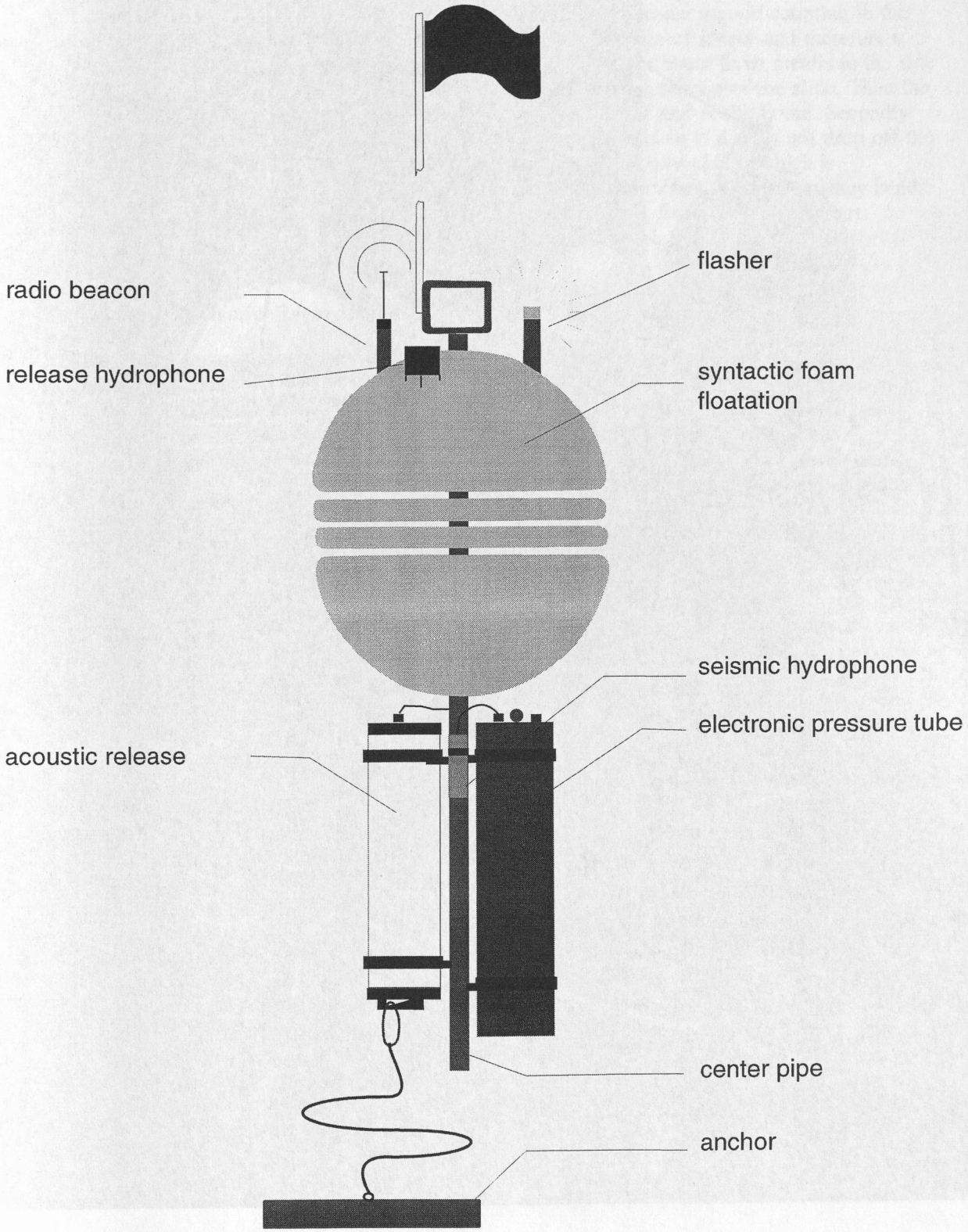

Figure 4.3.1: Principle design of the GEOMAR OBH (after Flueh and Bialas, 1996)

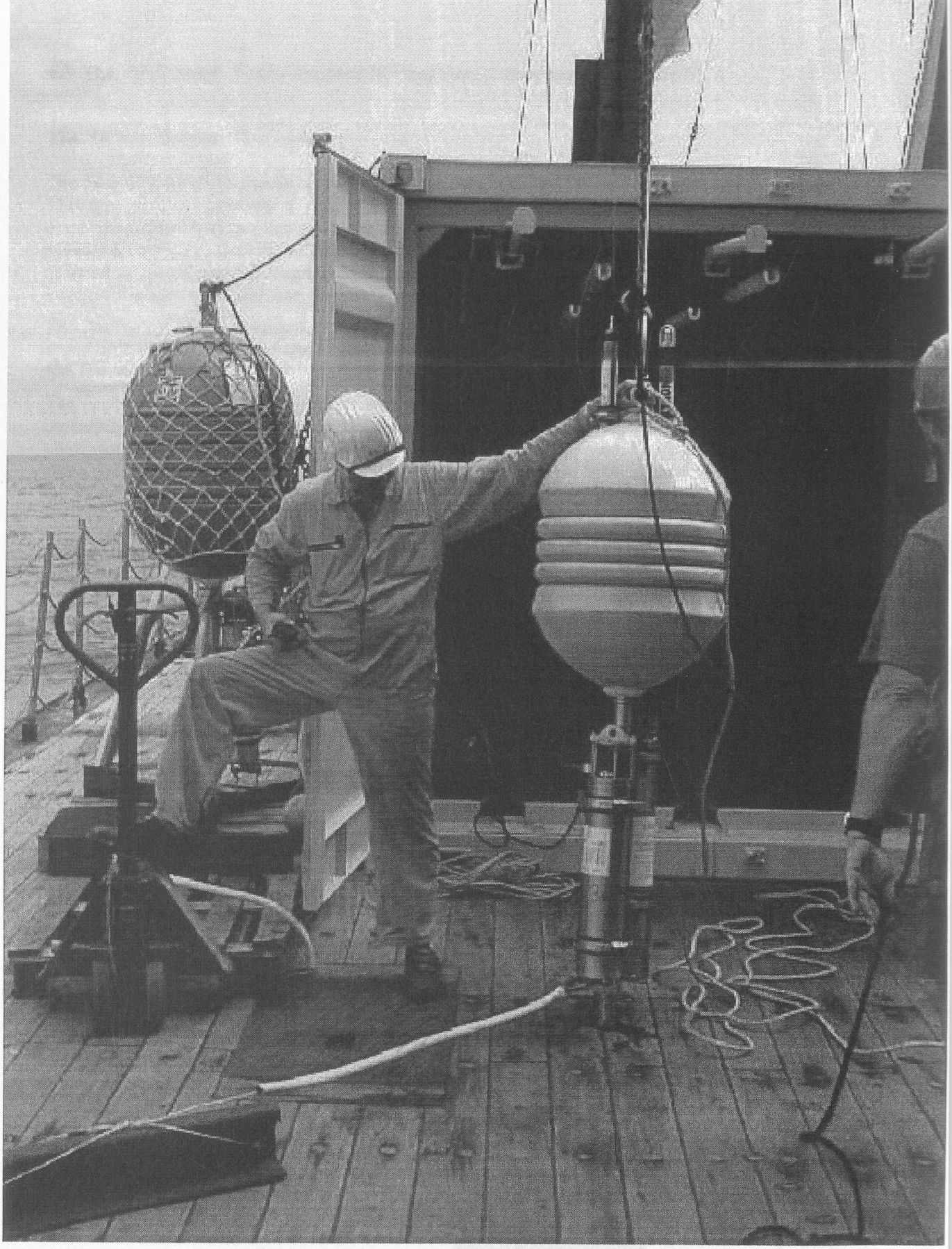

Figure 4.3.2: The GEOMAR OBH ready for deployment
Background left: GEOMAR OBS
Background right: OBH container

sensor has a flat frequency response curve from 95 sec. up to 30 Hz. This sensor type operates on the base of measuring levels within electrolytical tubes. This principle is less sensitive to its horizontal adjustment. The sensor is fixed like a pendulum while its lower third is surrounded by a viscous oil that gives freedom to very slow movements (through an angle of 18°) but which can assumed to be solid within the measured frequency range. The sensor is mounted within a 17" glass sphere with an additional weight at the bottom (20 kg weight in water) which should ensure a good coupling to the ground. The above discribed lever system was not able to handle this size of sensor and therefore a slide system was designed (Fig. 4.3.5) which allows to deploy the sensor about three meters to the side of the instrument carrier. A clock controled burning wire is used first as release of the slide. Then the sensor is pulled by an elastic rope along the slide until he falls off at the end of the boom. Secondly the clock releases the sledge itself to enable deployment of the sensor even if it does not drop off the slide for any reason. Signals are recorded by the *Marine Longtime Recorder (MLS)* which is manufactured by *SEND GmbH* and specially designed for longtime recordings of low frequency bands. Together with the broadband sensors the fourth channel records signals from either a standart hydrophone or a Differential Pressure Gauge (DPG) build by Spahr Webb at SCRIPPS.

Marine Broadband Seismic Recorder (MBS)

The so-called *Marine Broadband Seismic recorder (MBS;* Bialas and Flueh, 1999*)*, manufactured by *SEND GmbH*, was developed based upon experience with the DAT based recording unit Methusalem (Flueh and Bialas, 1996) over the last few years. This new recorder avoids a mechanically driven recording media, and the PCMCIA technology enables static flash memory cards to be used as unpowered storage media. Read/write errors due to failure in tape handling operations should not occur with this system. In addition, a data compression algorithm is implemented to increase data capacity. Redesign of the electronic layout enables a decreased power consumption (1.5 W) of about 25% compared to the *Methusalem* system. Depending on the sampling rate, data output could be in 16 to 18 bit signed data. Based on digital decimation filtering, the system was developed to serve a variety of seismic recording requirements. Therefore, the bandwidth reaches from 0.1 Hz for seismological observations to the 50 Hz range for refraction seismic experiments and up to 10 kHz for high resolution seismic surveys. The basic system is adapted to the required frequency range by setting up the appropriate analog front module. Alternatively, 1, 2, 3 or 4 analogue input channels may be processed. Operational handling of the recording unit is similar to the *Methusalem* system or by loading a file via command or automatically after power-on. The time base is based on a DTCXO with a 0.05 ppm accuracy over temperature. Setting and synchronizing the time as well as monitoring the drift is carried out automatically by synchronization signals (DCF77 format) from a GPS-based coded time signal generator. Clock synchronization and drift are checked after recovery and compared with the original GPS units. After software preamplification the signals are low-pass filtered using a 5-pole Bessel filter with a -3 dB corner frequency of 10 kHz. Then each channel is digitised using a sigma-delta A/D converter at a resolution of 22 bits producing 32-bit signed digital data. After delta modulation and Huffman coding the samples are saved on PCMCIA storage cards together with timing information. Up to 4 storage cards may be used. Currently, up to 640 MB per card are available. Data compression allows allows to increase this capacity. Recently technical specifications of flashdisks (disk drives of PCMCIA technology) have been modified to operate below 10 °C, therefore 2 GB drives are now available for data storage. After recording the flashcards need to be copied to a PC workstation. During this transcription the data are decompressed and data files from a maximum of four flash memory are combined into one data set and formatted according to the PASSCAL data scheme used by the *Methusalem* system. This enables full compatibility with the established processing system. While the *Methusalem* system did provide 16 bit integer data, the 18 bit data resolution of the *MBS* can be fully utilized using a 32 bit data format.

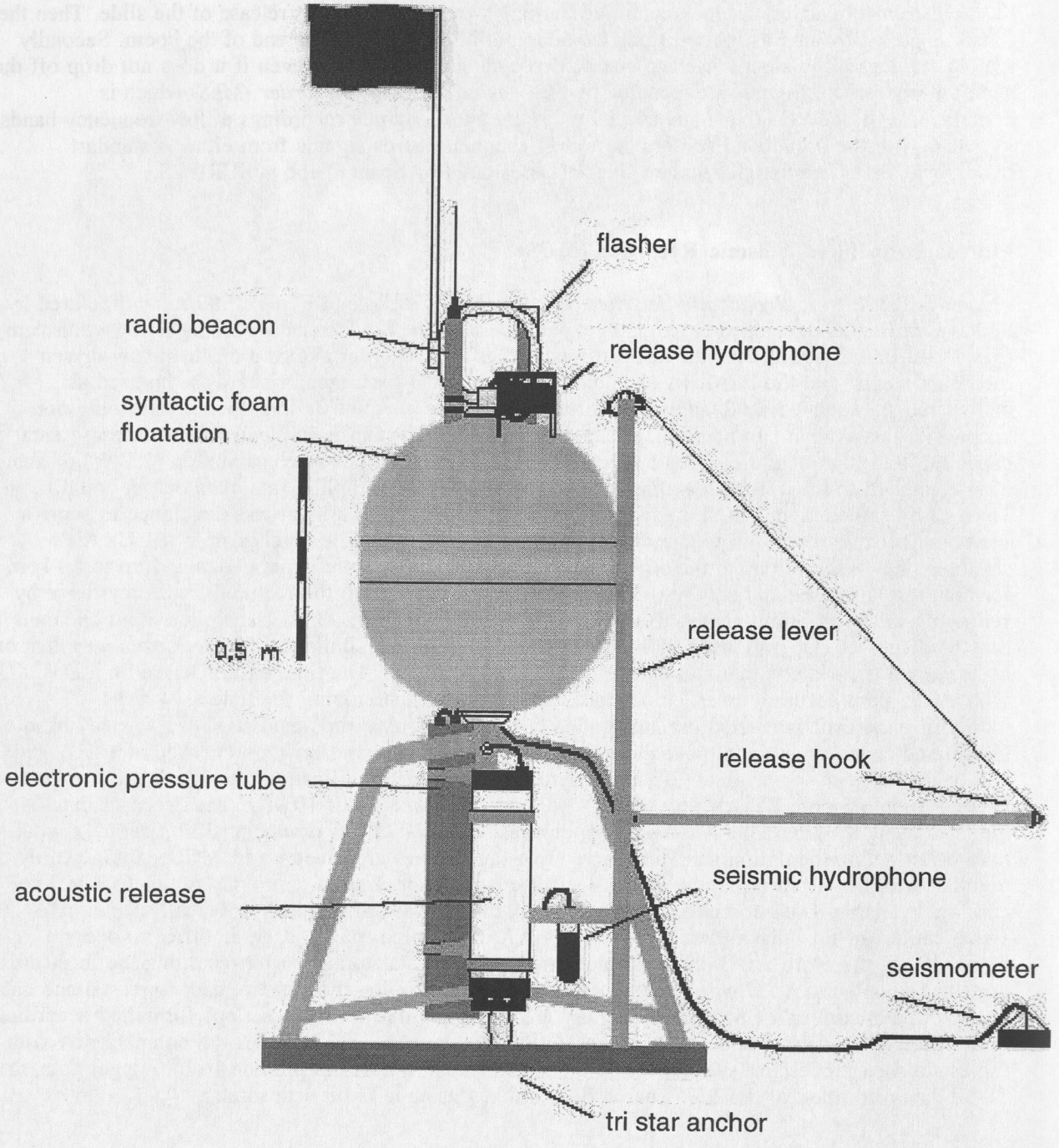

Figure 4.3.3: Priciple of the GEOMAR OBS (after Bialas and Flueh, 1999)

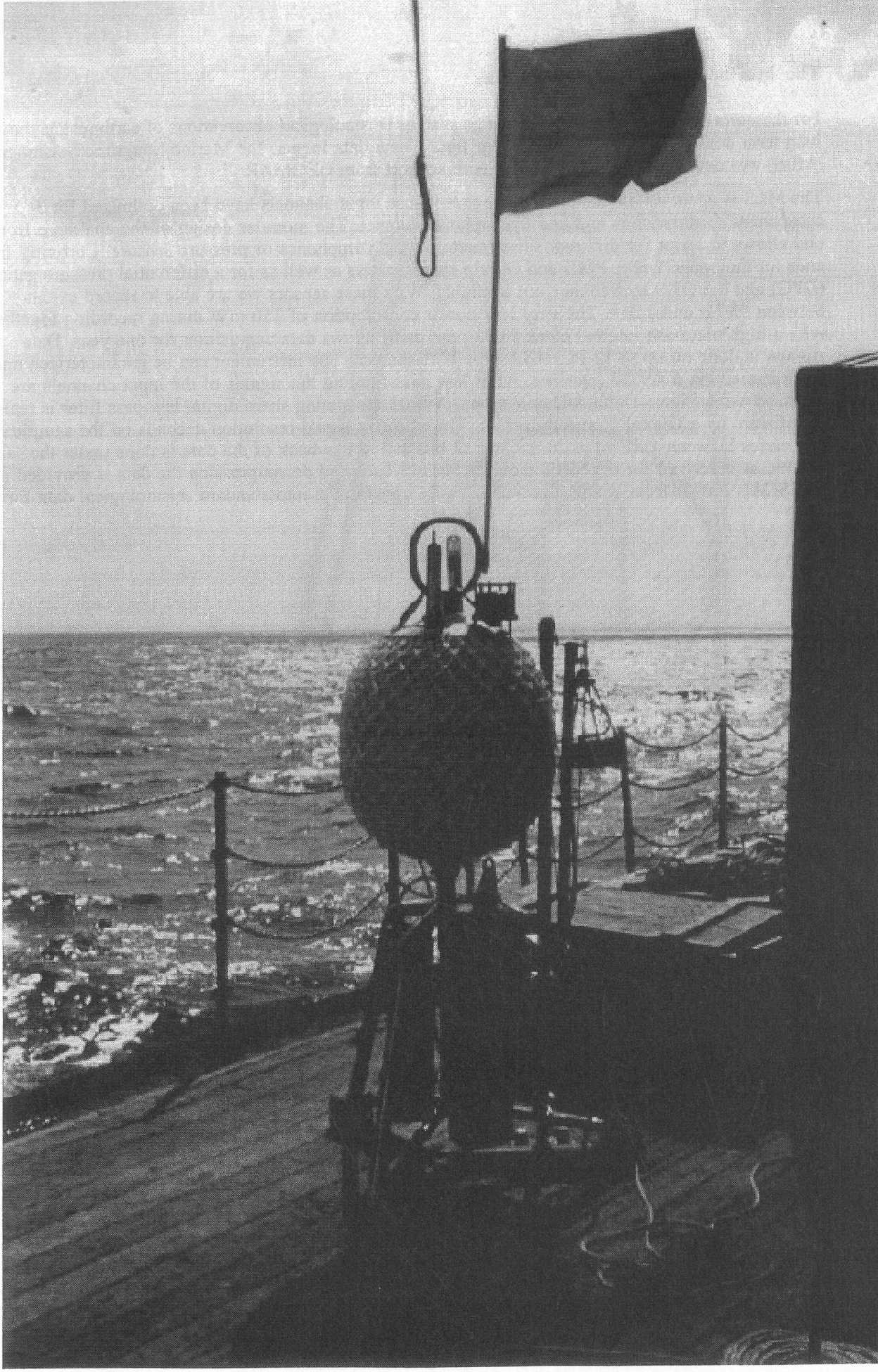

Figure 4.3.4: The GEOMAR OBS ready for deployment

The Marine Longtime Seismograph

For the purpose of low frequent recordings such as seismological observations of earthquakes during long term deployments of about one year time a new data logger, the Marine Longtime Seismograph (MLS) was developed by *SEND GmbH* with support from GEOMAR.

The MLS is again a four channel data logger whose input channels have been optimized for 3-component seismometers and one hydrophone channel. The modular design of the analogue front end allows to adopt for different seismometers and hydrophones or pressure sensors. Currently front ends for the Spahr Webb, PMD and Guralp seismometers as well as for a differential pressure gauge (DPG) and the OAS hydrophone are available. With these sensors we are able to record events between 50 Hz and 120 s. The very low power consumption of 250 mW during recording together with a high precision internal clock (0.05 ppm drift) allows data acquisition for one year. Data storage is done on up to 12 PCMCIA type II flashcards. The instrument can be parameterized and programmed via a RS232 interface. After low pass filtering the signals of the input channels are digitized using Sigma-Delta A/D converters. A final decimating sharp digital low-pass filter is realized in software by a Digital Signal Processor. The effective signal resolution depends on the sample rate and varies between 18.5 bit at 20 ms and 22 bits at 1 s. Playback of the data is done under the same scheme as described for the MBS above. After playback and decompression the data is provided in PASSCAL format from where it could be easily transformed into standard seismological data formats.

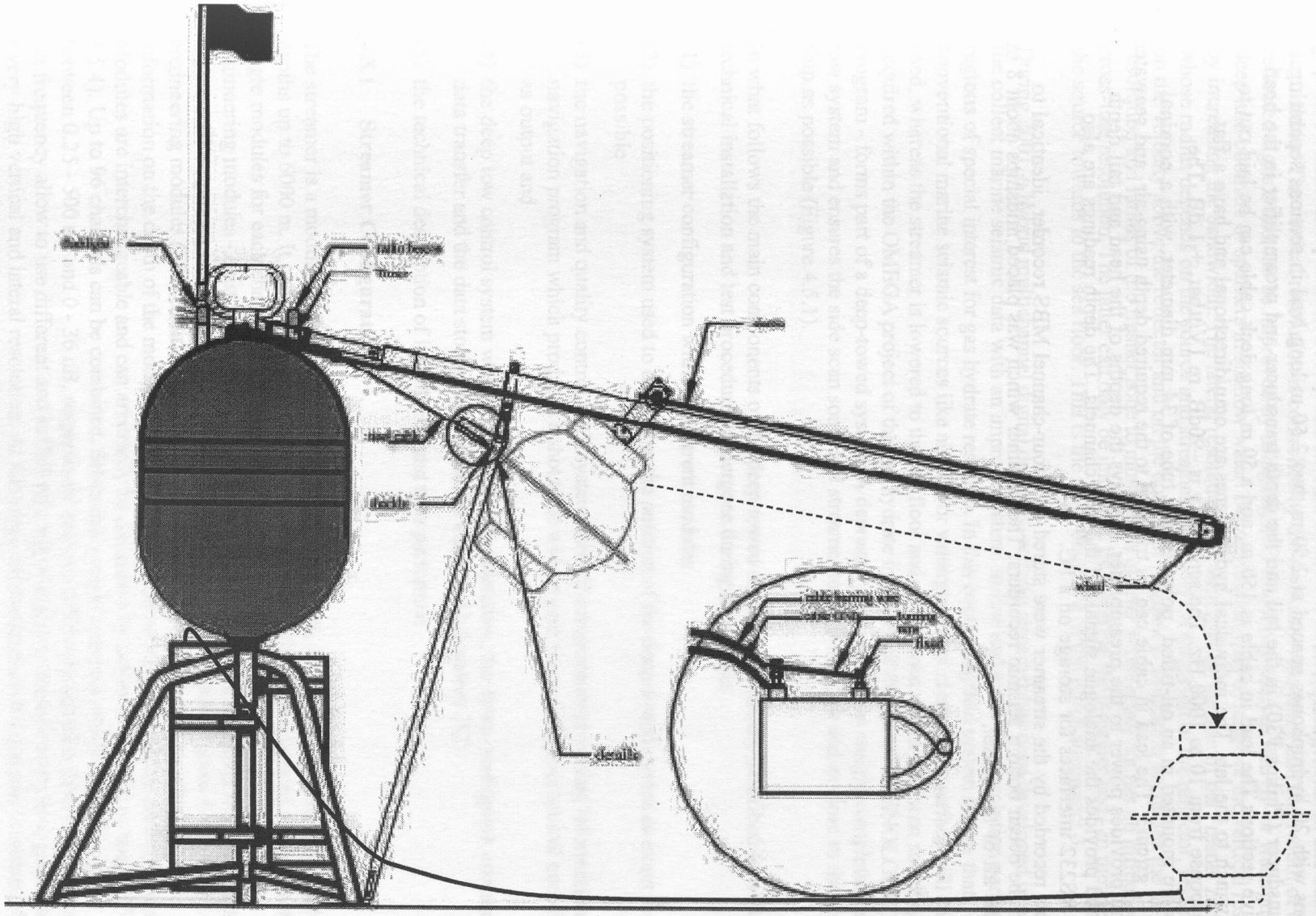

Figure 4.3.5: Scetch of GEOMAR broadband seismometer
dashed lines indicate deployment of the external broadband sensor at the seafloor

4.4 The SIG-Streamer

During this cruise a short four channel streamer was used. This streamer was manufactured by SIG (Service et Instruments de Geophysique, Framce) The system comprises several parts: four 50 m long active sections with 20 hydrophones spaced at 2.50 m, two 2.50 m long lead in sections separating the depth transducer (Philips P30) in the tail and the depth transducer and preamplifier in the head from the active sections.The lead in cable is 150 m, and a 50 m long deck cable can be laid out to connect the winch to the lab. The individual hydrophones are omnidirectional and have a flat frequency response from 10 to 1000 Hz. The sensitivity is –90dB, re 1V/μbar, +-1 dB. The hydrophones are mounted in an oil-filled polyurethane tube of 34 mm diameter, with a nominal density of 1.12 gr/cm3. The lead in cable can be trimmed to the required depth using air and seawater. A control unit provides power to the preamplifier, displays the depths of the head and tail depth transducers and provides the analogue signals of the four channels. The depth readings are also available on RS232 interfaces for storage on a PC.

The signals recorded by the streamer were stored on a four-channel MBS recorder, identical to those used in the ocean bottom seismic recorders. The streamer winch was placed midships about 8 m away from the aft of the vessel.

4.5 The DeepTow Streamer

The vertical and lateral resolution of marine subsurface structures in reflection seismic images strongly depends on the marine seismic source and streamer system used for signal generation and data acquisition. The vertical resolution is controlled by the dominant frequency and bandwidth of the reflected signals and can be improved by using high(er)-frequency sources like GI- or waterguns in deep and boomers or sparkers in shallow water. Deconvolution tries to improve the vertical resolution by increasing the bandwidth. The lateral resolution is determined by the size of the Fresnel zone whose radius depends on the source and streamer depth and on the depth of the reflector, respectively, on the velocity above the reflector and on the dominant frequency. Migration decreases the in-line resolution and radius of the fresnel zone to minimum a quarter wavelength but has no influence on the cross-line resolution. The latter can only be improved by lowering the streamer and - in the ideal case - the source towards to the sea floor. This is the main objective of INGGAS subproject 3.

During 2001, a hybrid multichannel digital deep tow seismic streamer has been developed in order to the collect marine seismic data with an improved lateral in-line and cross-line resolution particularly in regions of special interest for gas hydrate research. In this context, hybrid system means that conventional marine seismic sources like air-, GI or waterguns shot close to the surface will still be used, whereas the streamer is lowered to the sea floor and - combined with a side scan sonar system acquired within the OMEGA project of the gas hydrate initiative of the GEOTECHNOLOGIEN program - forms part of a deep-towed system. A depressor of about 2 tons weight completes the deep tow system and ensures the side scan sonar and streamer to keep in depth and as close to the towing ship as possible (Figure 4.5.1).

In what follows the main components of the deep-towed streamer system are described as well as the technical installation and test procedures undergone during this cruise:

(1) the streamer configuration with its different modules

(2) the positioning system used to determine the position of the deep-towed device as exact as possible

(3) the navigation and quality control (QC) system with all components providing information to a navigation program which produces a shot table with trigger times and geographical coordinates as output and

(4) the deep tow control system which coordinates the telemetry, the down- and uplink command and data transfer and the data storage on both underwater and laboratory PC's

(5) the technical description of installation and tests performed

4.5.1 Streamer Configuration

The streamer is a modular digital seismic array (HTI, High Tech, Inc.) which can be operated in water depths up to 6000 m. It consists of a 50 m lead-in cable towed behind the side scan sonar fish and single modules for each channel (Figures 4.5.2, 4.5.3). Two different modules - acoustic and engineering modules - exist. Each acoustic module (AM) houses a single hydrophone and a low- and high-cut filter, preamplifier and 24-bit AD converter in a pressure vessel (Figures 4.5.2, 4.5.4). Special engineering modules (EM) additionally include a compass and pressure sensor which provide information on the depth of the module below sea surface and on its geographical position (heading). Modules are interchangeable and can arbitrarily be connected by cables of 1 or 6.5 m length (Figure 4.5.4). Up to 96 channels can be combined. Selectable sample intervals and preamplifier gains between 0.25 - 500 ms and 0 - 36 dB, respectively and two different high-pass filters with 4 Hz low-cut frequency allow to use different and sufficiently high-frequency seismic sources to guarantee both a very high vertical and lateral resolution. At this stage of development the streamer consists of 26 modules including three engineering modules.

4.5.2 Positioning System

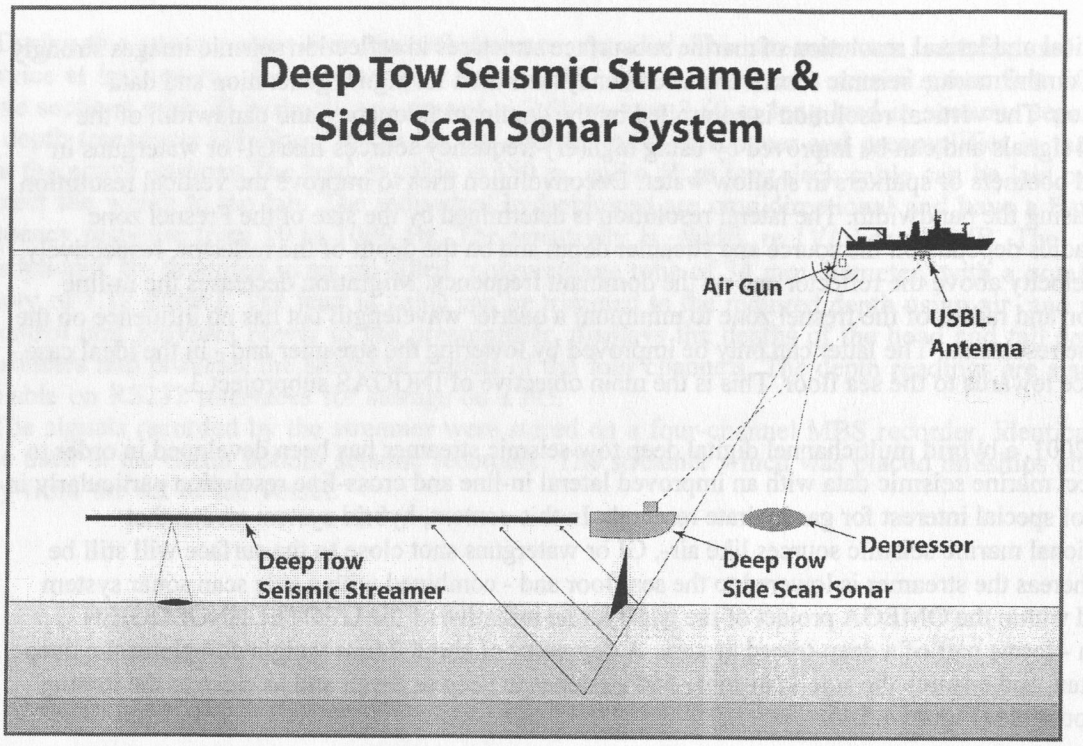

Figure 4.5.1: Sketch of the digital deep tow seismic and side scan sonar system

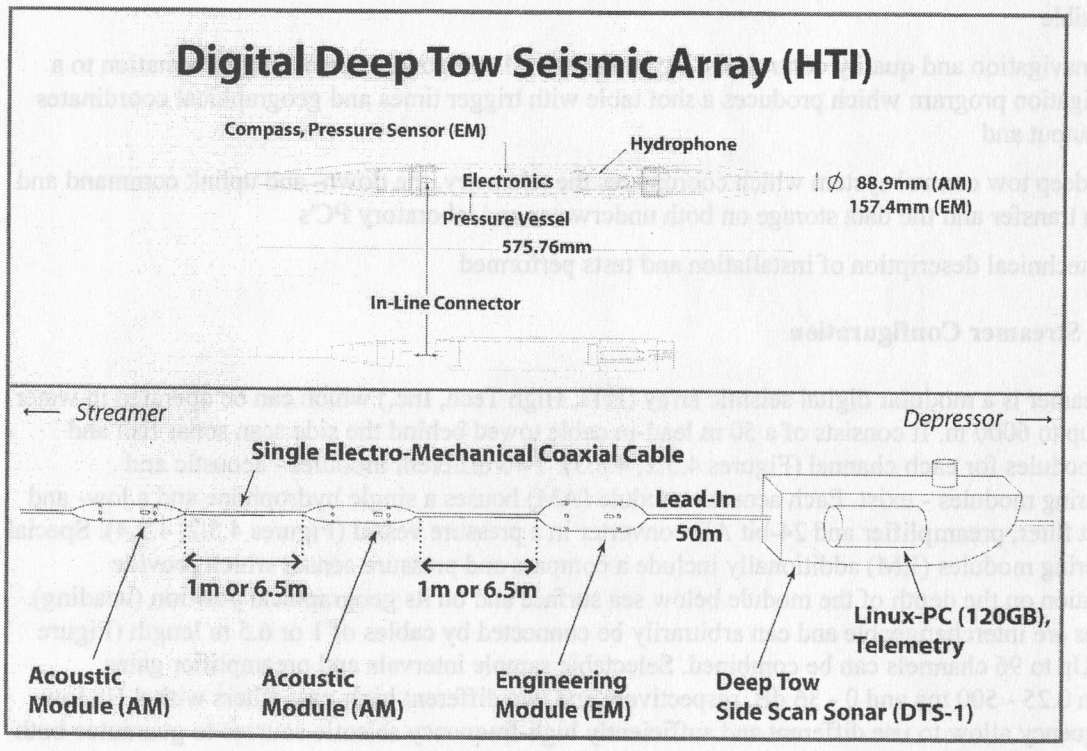

Figure 4.5.2: Configuration, components and dimensions of the digital seismic streamer array (HTI, High Tech Inc.)

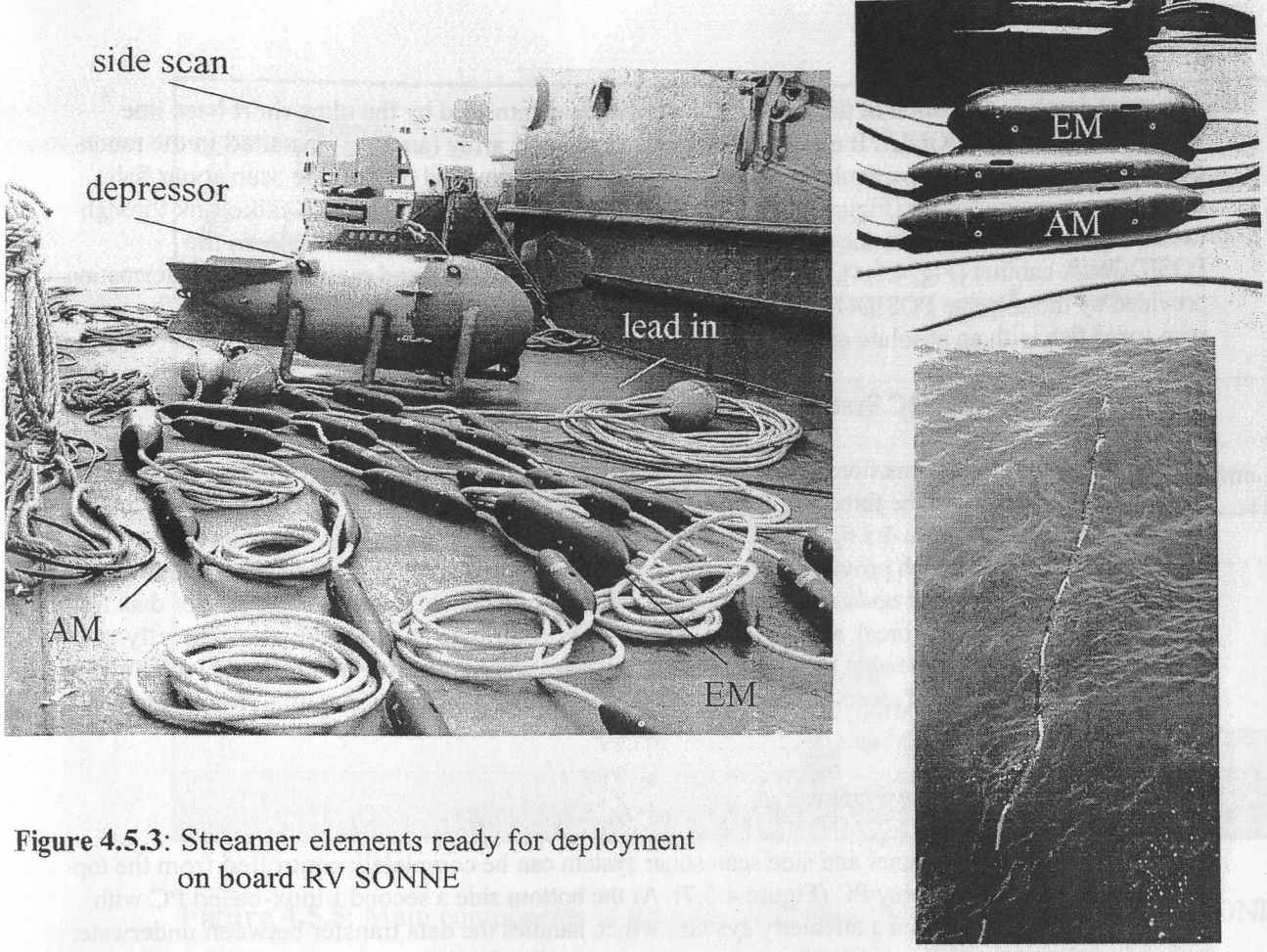

Figure 4.5.3: Streamer elements ready for deployment on board RV SONNE

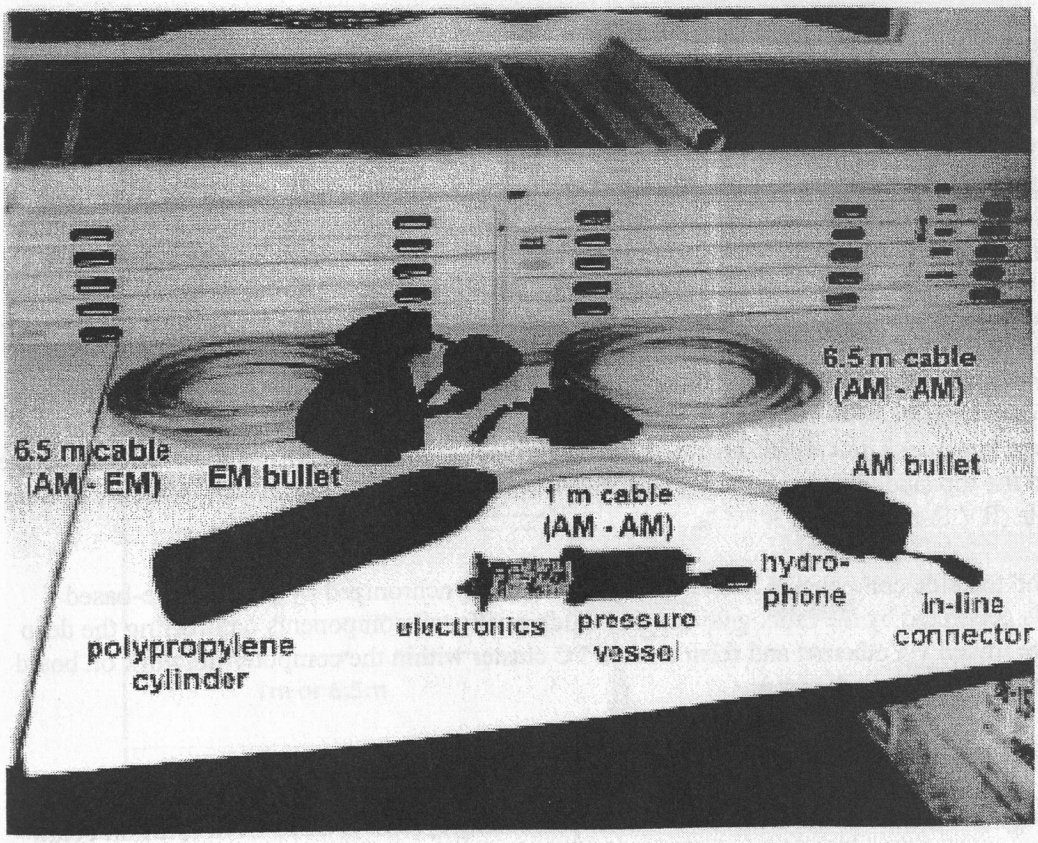

Figure 4.5.4: Streamer elements during inspection in the laboratory

The exact depth and position of the side scan sonar fish is determined by the ultra-short base line (USBL) system POSIDONIA. It mainly consists of an acoustic array (antenna) installed in the moon-pool and calibrated for its particular position, and a responder mounted on the side scan sonar fish including a pressure sensor (Figure 4.5.5). The responder function is triggered via cable link through Linux-based gateway PC into the coaxial or fibre optic sea cable by interrogations from the POSIDONIA cabinet (Fig. 4.5.4). Together with DGPS, gyro compass and motion sensor information provided by the ship the POSIDONIA system allows to determine the depth and position of the side scan sonar fish with an absolute accuracy of 0.5 - 1% of the water depth.

4.5.3 Navigation and QC System

The depths, geographical positions and heading values determined by the ultra-short base line (USBL) system POSIDONIA and the three engineering modules of the digital seismic streamer are fed into a navigation program (Figure 4.5.6). Together with the DGPS based trigger times this program generates a shot table which provides information on the depth and geographical position (latitude, longitude) of each streamer node at each shot/trigger time. Gyro compass and motion sensor data from the ship and, possibly first break and multiple arrival times contribute to this program, indirectly. During seismic profiling the shot table is stored on hard disc and thus serves a log file which allows to assign the exact source and receiver geometry to the seismic data header later offline, for subsequent data processing steps.

4.5.4 Deep Tow Control System

The deep tow seismic streamer and side scan sonar system can be completely controlled from the top side by a linux-based gateway PC (Figure 4.5.7). At the bottom side a second Linux-based PC with 120 GB storage capacity and a telemetry system, which handles the data transfer between underwater and on board systems and provide all necessary power supplies for the bottom electronics, are installed in a pressure-proofed housing mounted on the side scan sonar fish.

An online display of the engineering data from the streamer (depth, heading, pitch and roll) allows for a permanent status overview about the behavior of the streamer and the current depth. Records of the seismic data from the streamer are transmitted via ethernet connection to a PC running GEOMETRICS Strata Visor quality control and data storage module. A permanent online display of shot gather and frequency spectra as well as a monitor display of a selectable single trace allows to check signal quality and data transmission all the time. Seismic data are stored both underwater on the linux-based PC and on board on the QC-PC where two DLT devices are connected for infinite data storage in daisy chain operation. Side scan sonar data are stored underwater in the pressure case of the side scan sonar electronics and on board on a PC (HYDROSTAR) which provides various displays for data and tow fish control. These units are described in detail in chapter 4.8. Commands which control seismic recording parameters like sample interval, record length or preamplifier gain, and which initialize the data transfer between underwater and on board systems, are sent from the top to the bottom side via low-speed downlink, whereas seismic and side scan sonar data are transferred from the underwater to the top side via telemetry and high-speed uplink through a coaxial (RV Meteor) or fibre optic sea cable (RV Sonne).

All bottom and top side components and air gun shooting are synchronized by DGPS time-based trigger signals generated by the linux gateway PC. Additionally, all components controlling the deep tow device are linked via ethernet and form a small PC cluster within the computer network on board the research vessel during each cruise.

4.5.5 Technical installations and tests performed

Besides the mobile antenna of the OCEANO USBL positioning system (POSIDONIA) all on board equipment was set up in the Geolabor of RV Sonne. Eight PC´s with additional cabinets occupied all of the port side bench of the laboratory. Although data formats have been exchanged between all participating suppliers during development of the system components it turned out that several parts of

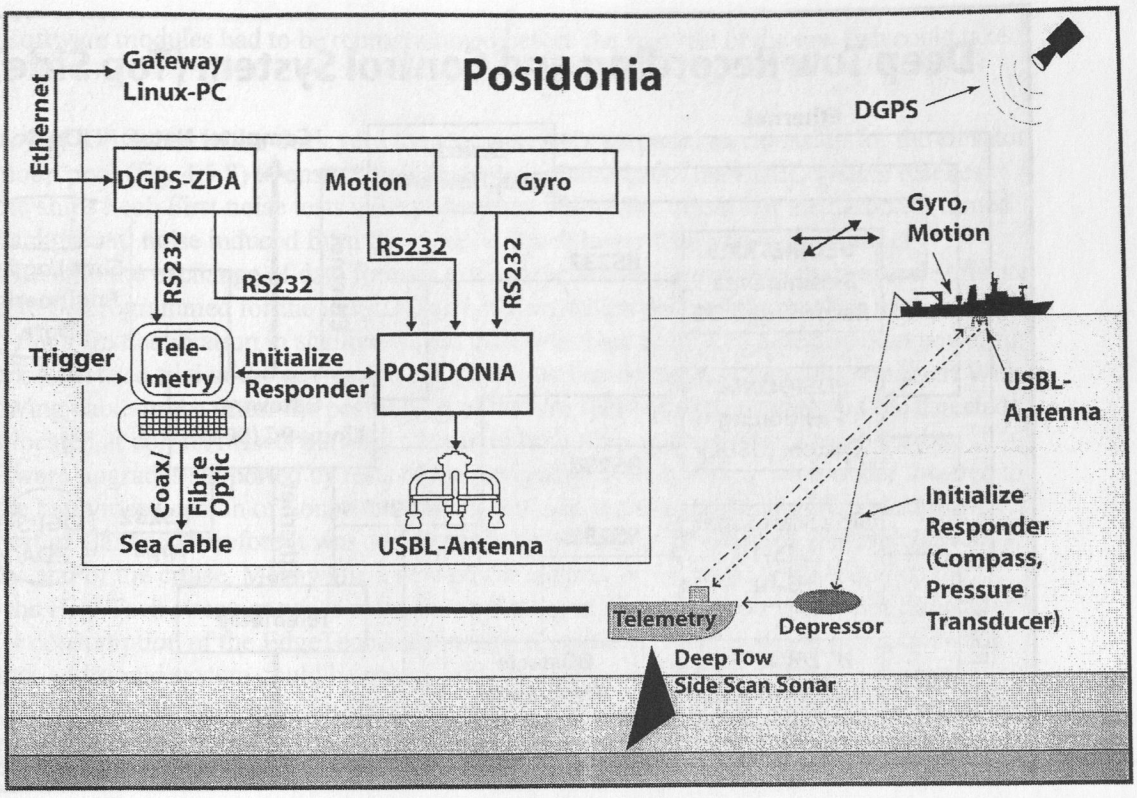

Figure 4.5.5: Main components of the ultra short base line (USBL) system POSIDONIA

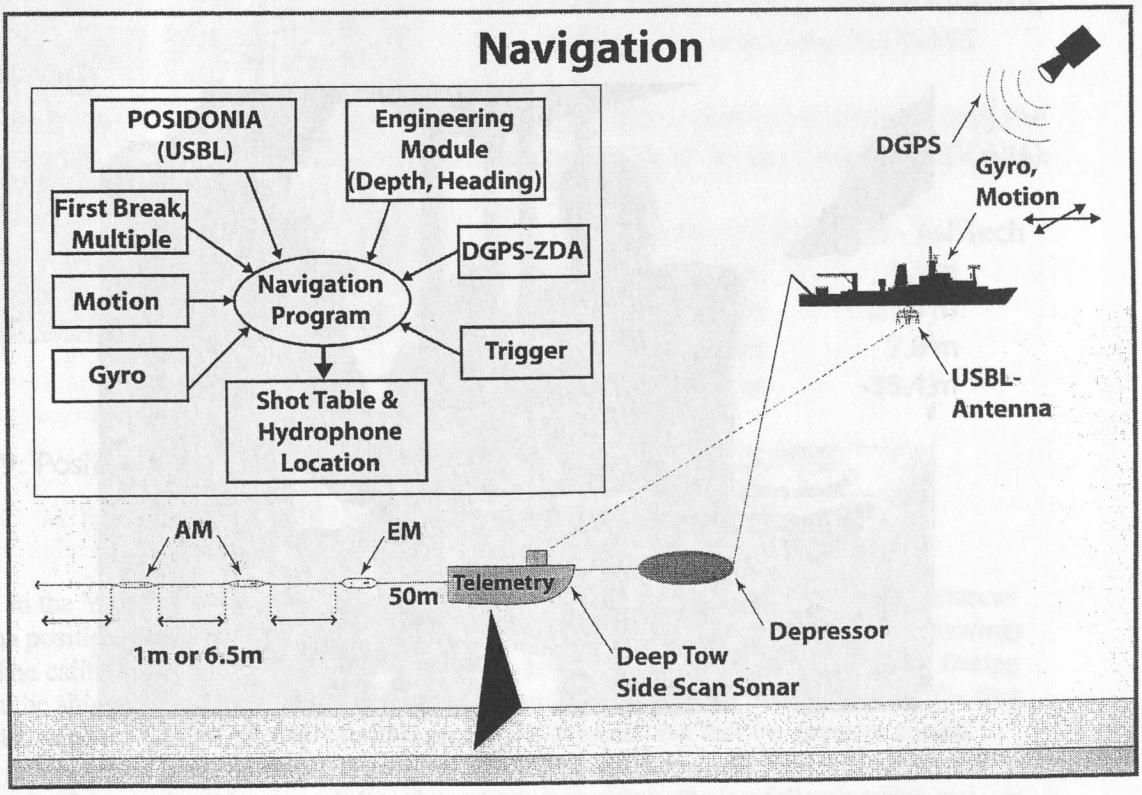

Figure 4.5.6: Main data components contributing to the navigation program

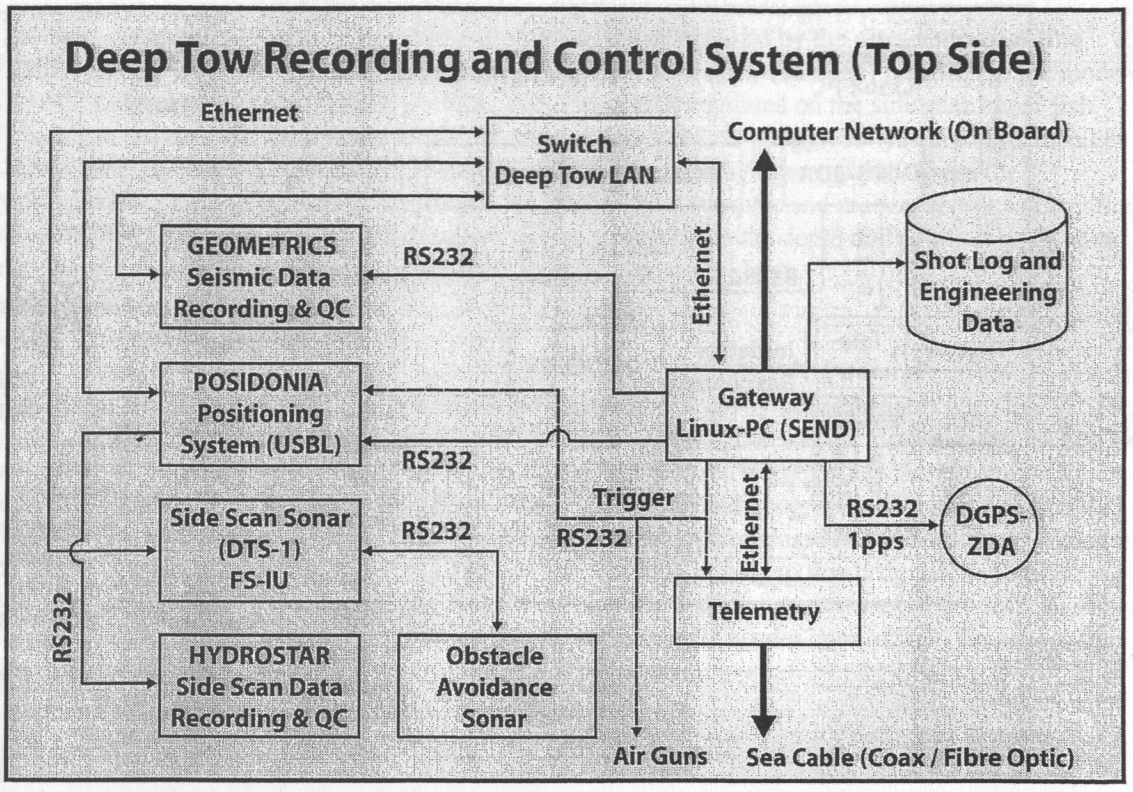

Figure 4.5.7: Block diagram of the top side data recording and control system for the deep towed device

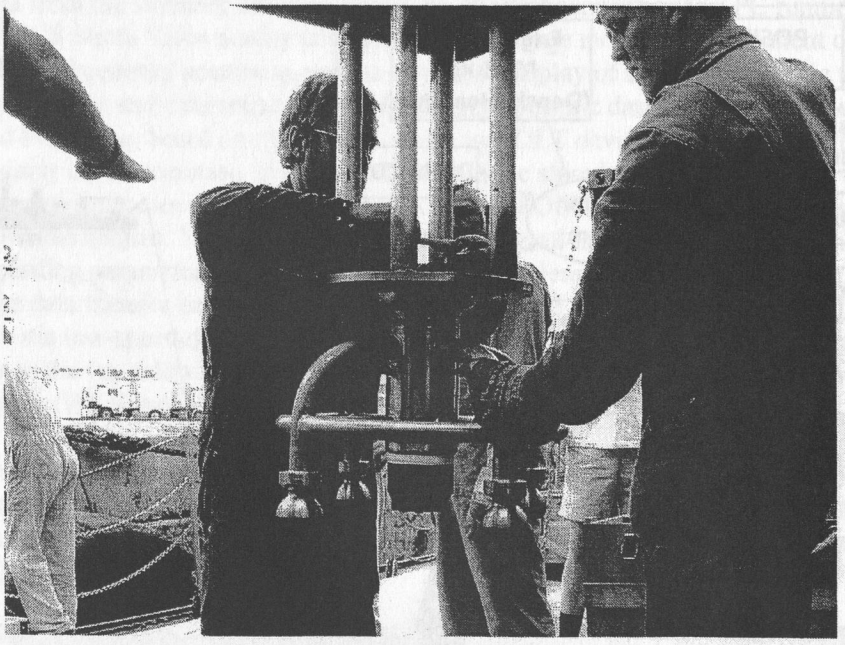

Figure 4.5.8: Mounting the POSIDONIA antenna under the elevator of the moon pool

the different software modules had to be reprogrammed before the first test of the tow fish could take place.

During the stay of RV Sonne in the dock yard the ship operators prepared an extension for the elevator cage of the moon pool (fig. 4.5.8) to ensure that the deployed antenna of the USBL system reaches well below the ships keel. First noise tests were undertaken before the vessel left the harbor. It turned out that the background noise induced from the vessel is much lower than known from other installations. Despite the exchange of data formats prior to the cruise it turned out that several software upgrades had to be programmed for the POSIDONIA system which delayed the first sea trials and did not enable to run a first calibration in shallow waters off Chile. Due to limited time and man power for all set up work a first sea trial of the navigation equipment was undertaken without the streamer. With 2500 m of towing cable in the water the positioning of the tow fish became unstable and the detected position was located at correct offsets but varies between both sides of the vessel. Due to further intensive software upgrades supported by tests of the navigation system with a transponder lowered to depth from the bathymetry winch of Sonne the training and sea acceptance could not be performed prior to the port of Callao. Therefore it was decided to keep two of the POSIDONIA technicians on board until the end of the cruise. Meanwhile a new power support board could be installed on the telemetry as the HighTech streamer needs more power than specified before. In addition it turned out that the power consumption of the EdgeTech sonar drains too much current in the moment of switch on that no other additional system could be booted simultaneously. Therefore a delay circuit was designed and tested. During later test sequences this simple circuit was converted into an IC circuit as the relay controlled solution seems not to work stable enough.

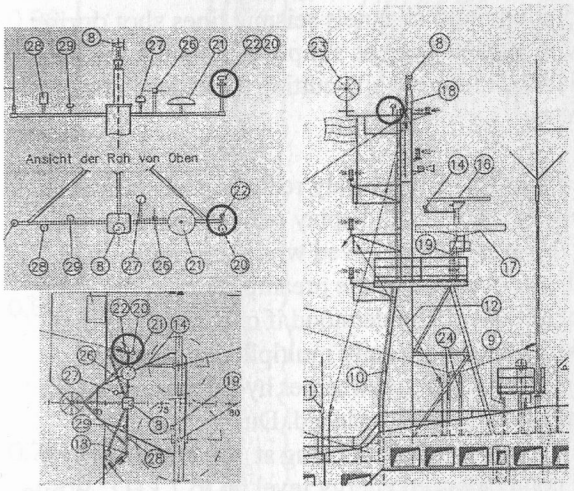

Positions of the GPS antennas
in the main mast of RV SONNE

22 - D-GPS antenna using Trimble-Inmarsat
20 - AshTech antenna using GLONASS

Offsets to the antenna instalation using the front moon pool (as used with POSIDONIA):

	22 - D-GPS	20 - AshTech
transverse	4.3 m	4.3 m
longitudinal	-21.3 m	-21.6 m
draft	7.8 m	7.8 m
vertical	-35.4 m	-35.4 m

Figure 4.5.9: Positions of the GPS antennas in the main mast of RV SONNE

Upon arrival in the Yaquina basin a calibration run was done for the POSIDONIA antenna. Distances of the antenna position relative to the ships GPS antennas were read from the ships technical drawings (fig. 4.5.9). The calibration should be done in water depth between 1000 m and 2000 m depth. During the operation the ship sails two figures of eight across a previously deployed transponder. For the first time we used a standard GEOMAR OBH for this procedure. It turned out that the acoustic signals were securely transmitted between ship and transponder but the signal to noise ratio was very poor. Consequently the first results did not result into the expected precision. During following runs the transponder was not directly attached to the OBH frame but a 30 m long rope separating transponder and OBH floatation ensured that the transponder hydrophone was not within the acoustic shadow of

the float. This does increase the signal to noise ratio significantly and lead to a calibration well within the expected 1 % accuracy of the water depth. Another feature that turned out during these calibration tests was the effect that the pings from the SIMRAD multibeam do disturb the measurements of the POSIDONIA system. Both of them cover the frequency range of 10 kHz to 12 kHz for acoustic transmission. During further test sequences it turned out that these influences could be efficiently reduced when POSIDONIA could be operated in responder mode. This is the case when the tow fish should be tracked as the POSIDONIA signal request could be transmitted via the deep tow telemetry to the deep tow vehicle and interrogate the transponder for acoustic signaling. At the same time a depth measurement is done by the transponder which could either be transmitted with the acoustic reply or via RS232 interface through the telemetry system. An other possibility offered by the USBL system would be the use of different interrogation frequencies which are well above the SIMRAD frequencies, unfortunately not all of these scheduled frequencies are available now. Interference from PARASOUND were not observed, the POSIDONIA electronics could filter these signals well.
After preparation of the switch-on delay in the telemetry system the streamer was tested on board. As known from the development of the streamer interface the synchronization of the digital output from the streamer is somewhat sensible and could only be done during power up of the complete underwater system at this time. Therefore several tests were done in the lab to check this feature. At the same time the power line for the POSIDONIA transponder was cut in order to operate the unit in battery mode. This was done due to the fact that during the first deployments severe interferences were observed with the side scan recording. As similar observations were made by the Oceano technicians during installation of a different EdgeTech sonar it was assumed that at this time again a PCB board from the EdgeTech unit does react to the power consumption of the transponder. After these preparations first deployments of the complete system were done (see. Chapter 5.3). As a high frequency source a GI gun was set up which comprised of a 1.7 l GI-gun on loan from AWI, Bremerhaven, a gun carrier and a pressure hose on loan from Institute for Geophysics, Bremen. For a first test deployment we chose a line crossing high resolution multi channels seismic lines shot during the SO146 GEOPECO cruise. In order to keep expectable maneuvering as simple as possible for the first deployment we set course along strike of the continental margin while cutting the older lines which still would allow correlation of reflection interfaces.

During winch operations the amplitudes of the streamer signals were severely reduced and seismic signals could no longer be detected for a time while the expected signal display reappeared after the streamer was kept in constant depth position again. As this was also observed while turning from one profile to the next one possible explanation seemed to be an overload of the preamplifiers in the cable. This was proved by the manufacturer HighTech and could easily be understood if one imagines that the change of one foot (30 cm) is .435 psi or 190 dB, which could be easily multiplied during fast changes in depth and turns. Later tests showed that amplification of the streamer hydrophones could be decreased and therefore these effects could be avoided or at least be reduced. During normal profiling we received good quality data. Application of a low cut filter opening at 100 Hz enabled a clear monitor display. The frequency spectra showed a good balanced energy level up to 1 kHz. While sailing along the line the depth transducers of the streamer and POSIDONIA transponder were cross checked with the multibeam depth values and the distance above sea floor that could be read from the sub-bottom penetrator of the side scan. These values were stable and in good agreement with the calculations from first arrival and POSIDONIA. According to the slight negative buoyancy of the streamer the cable was towed some 9 m below the side scan. Depending on the tow speed through water the last depth transducer of the streamer was some 2 m below the first one indicating the slight downwards directed orientation of the cable.

As each towed object will cause turbulence in the water it is to be expected that the tow speed through water will effect the signal to noise ratio at the hydrophones. Therefore the test line was shot several times with ship speeds varying from 1.0 kn to 4.0 kn through water. Up to about 2.5 kn to 3.0 kn the best results were achieved. Due to the better stability of the side scan a survey speed of 3.5 kn could be accepted. Figures 4.5.10 and 4.5.11 are displays of a single channel (15) of the data shwoing the very gigh signal to noise ratio and excellent resolution in the top 200 ms of the subsurface. The towing depth was chosen according to the bubble generated by the GI gun which occurred some 40 ms after the shot signal, in order to prevent overlap between sea floor reflection and the direct arrival. This

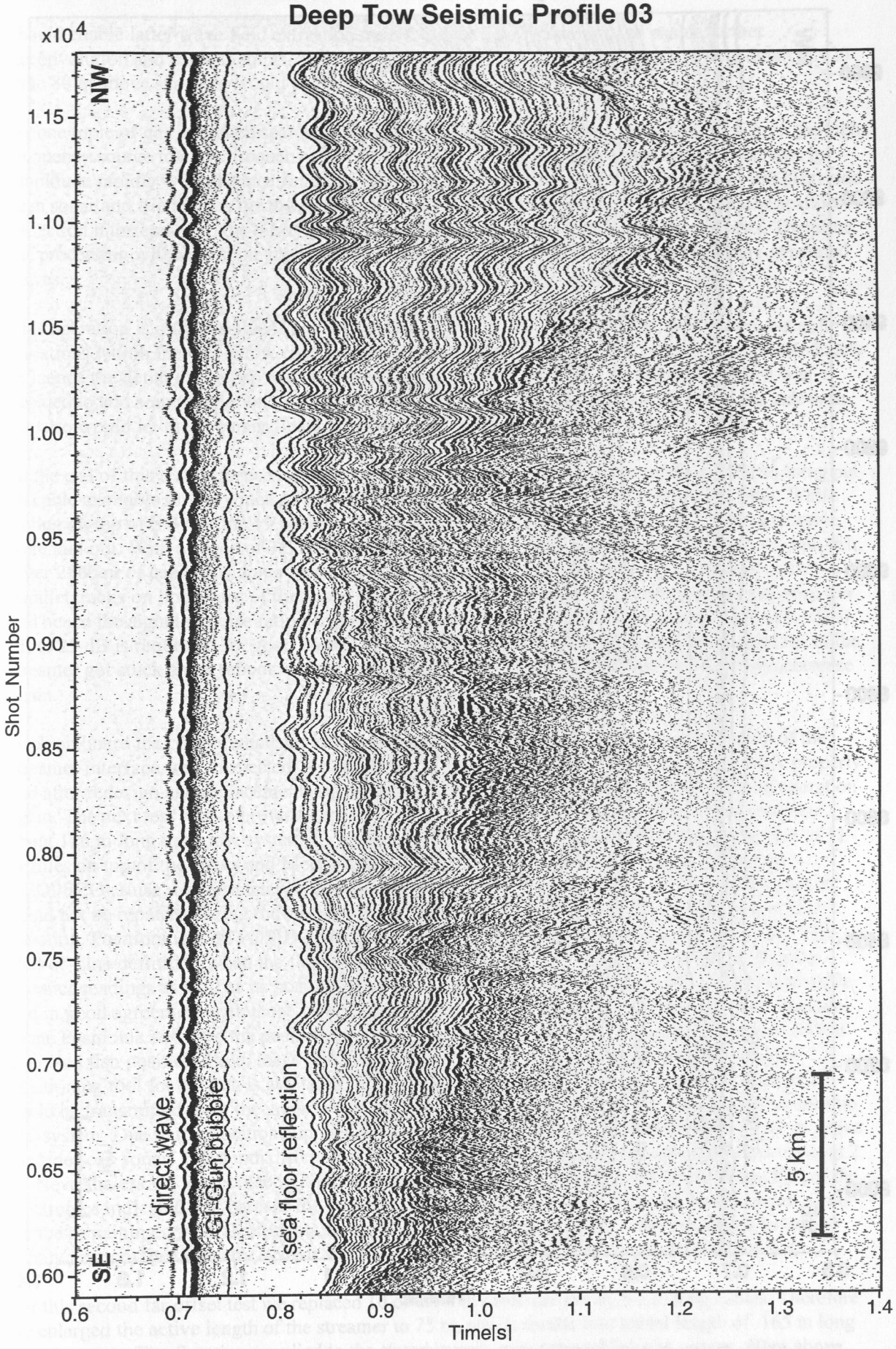

Figure 4.5.10. Deep tow seismic profile 3, shot parallel to the contours of the continental slope using a single GI gun as source. The streamer was towed about 100 m above the seafloor. Note good resolution of the upper 200 ms of the subsurface.

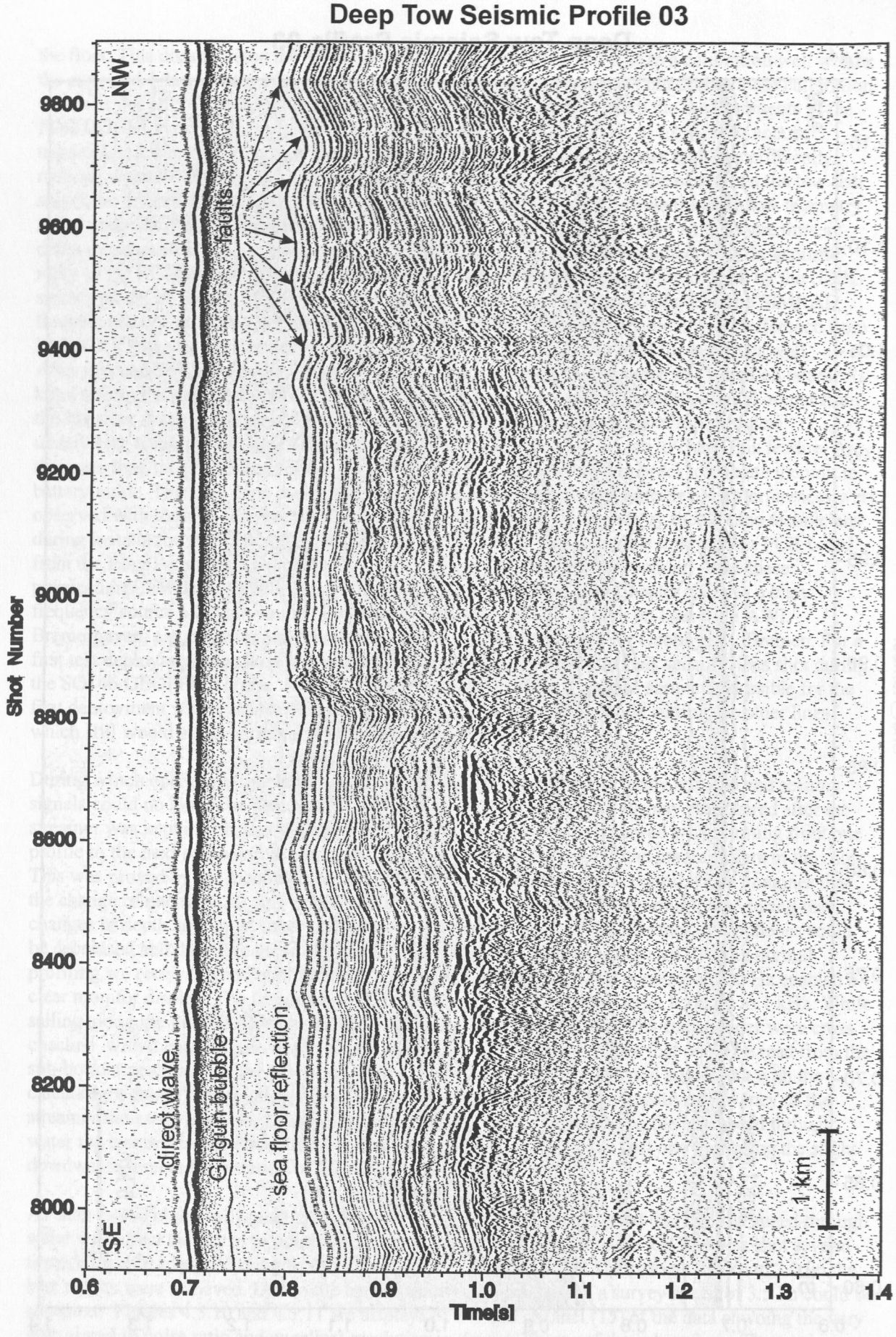

Figure 4.5.11: Detail of portion of Deep-tow profile 3. The improved resolution of the top 200 ms of the subsurface allows recognition of smal faults that may act as fluid pathways.

should enable latter wave field extraction from these far field recordings and enable further deconvolution and filter attempts. Together with the side scan it turned out that a towing depth of 120 m to 80 m above sea floor would be best.

As one topic of gas hydrate research is related to the study of Scholte waves we changed from the high frequency source to a low frequency 32 l Bolt gun. As the Scholte waves are known to decrease in amplitude rapidly with distance from the seafloor we decided to use the high frequency (400 kHz) side scan sonar and tried to run the towed system at about 20 m above seafloor. At this depth the seafloor reflection interferes with the direct wave as it is known from the ocean bottom instruments. Therefore the processing will need some time and application of special tools to detect these possibly generated waves.

This operation is only possible if one knows the topography of the profile well in advance, but still variations within the whole tow configuration of vessel, tow fish, wind and water currents immediately influence the depth of the fish and need a very precise winch operation. As a consequence it was decided to add some floatation to the streamer. This would not only lift the cable above the side scan but also would let the streamer float to the surface in the case of a broken cable.

At the end of this test sequences we set course from shallow water into the trench in order to bring out all cable available on the winch of RV Sonne for a depth and long distance test of Posidonia. While sailing on top of SO146 line 19 we used the GI gun again for seismic signals while 7000 m of cable were laid out. With a speed of 3.5 kn this brought us down to 3600 m of water depth with the tow fish. After 2500 m of cable Posidonia became slightly unstable and the tow fish was located along two parallel tracks on both sides of the vessel. We recognised that the battery power was already very low and hence the signal to noise ratio became as low as 15 dB to 17 dB, while a nominal S/N ratio of 20 dB to 25 dB is requested for good operation. Upon recovery of the towed system the control PC of the streamer got stuck and a reboot was necessary. After this operation the streamer failed to synchronise again.

Back on board the pressure housing of the telemetry system was opened and the connection of the streamer interface were inspected. It turned out that the power-on delay circuit does not work properly and after redesign and replacement (supported by the WTD of RV Sonne) the circuit was in operation again. The next test was to provide experience in terms of handling and operation of the complete about 126 m long deep tow system during 3D surveys. Therefore we defined a rectangular box of 11 profiles on top of the "Max and Moritz" chemoherms that were discovered during the SO146 GEOPECO cruise. Unfortunately the GI gun failed and despite replacement of O-rings and seals it could not be repaired during the stay on board. Therefore we chose a 1.6 l Prakla type airgun for shooting. Positioning with POSIDONIA worked well during the entire survey (Figur 4.5.12). The End-of-Line definition when the fish has passed the way point could easily be estimated from the distance readings as well as its position during turn could be well observed. Depth values were stable and in good agreement with those from the streamer and the side scan sonar. Due to further upgrades in the Posidonia software the positioning was very stable and only very few points were seen off the expected fish position. From these observations we are confident that with Posidonia a reliable positioning tool for the fish is available. The streamer worked well during the survey and all data could be transmitted from the under water PC to the top unit and hence into the storage of the seismic QC system. Due to the flotation supplied to the streamer the cable was now floating about 20 m above the side scan sonar. The depth difference between first and last engineering node decreased to about 2 m. Nevertheless we lost contact with the streamer at the end of the last profile. Later inspection of the electronics indicated that parts of the power-on delay circuit need to be replaced. It did not fail again for the remaining cruise. During this inspection the Posidonia transducer was turned back to power supply through the telemetry system as we were interested to complete a second far offset test.

For this second far offset test we replaced 10 of the 1 m cable section by 6.5 m long cables. Therefore we enlarged the active length of the streamer to 75 m, which results into a total length of 165 m long towed system. The flotation supplied to the streamer now raised the cable up to approx. 50 m above the side scan while the depth offset along the streamer could be kept within 5 m. This time Posidonia

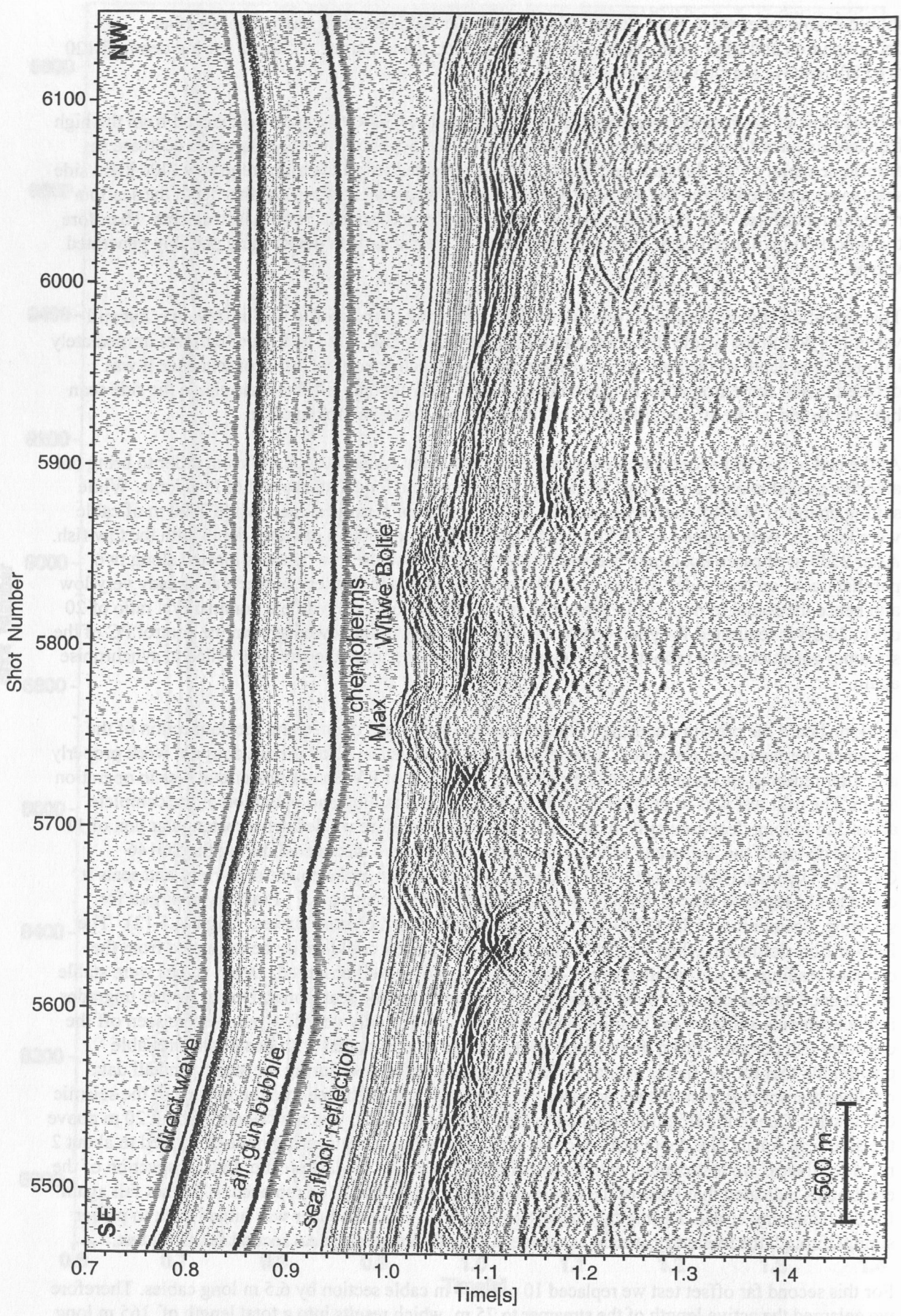

Figure 4.5.12 Single channel (lagely unprocessed) of deep-tow profile 12 recorded as part of a series of close parallel profiles in the region of the Max-Moritz Chemoherms. These profiles were shot using a single Prakla airgun. The bubble from the gun is quite evident, but will be suppressed during future processing.

could precisely track the tow fish up to the complete length of 7000 m cable. During winch operation, when the pitch of the side scan was well out of horizontal alignment the tracking became less stable. Obviously this time the directivity of the transponder hydrophone disabled a clear signal detection. Other than with battery powered transponder this time the signal to noise ratio was slightly better and splitting of the track line could not be observed. Surprisingly this time we did not observe disturbances with the side scan records which led us to the battery operation before. Obviously we could improve the wire pathways within the telemetry pressure housing to not induce disturbances into the other data cables.

During a final short deployment of the deep towed system on 10th March we could again test some improvements of the streamer control software. These include gain functions, delay options and others. Continuous reception of seismic data from the streamer verified the success of these modifications.

As a result from these test operations we could conclude that the deep tow streamer system is in principle available for survey operations. Future improvements which will be done during the coming months are further improvement of the streamer control software in terms of a more user friendly designed graphic interface including display of engineering values. The hardware need some modifications as the power supply boards generate too much heat. Parts of the PCB´s will be moved into an additional external pressure housing while the remaining electronic circuits need to be cooled by use of a small fan allowing to better release heat through the walls of the tube. During this cruise we needed to permanently cool the pressure case by seawater during test runs on board RV Sonne.

The master of RV Sonne already asked for the possibility to have a daughter display of Posidonia installed on the bridge in order to support future ship operations along survey tracks. This would enhance the crews possibilities to navigate the towed fish precisely above the scheduled profiles. This will become a need during 3D surveys as they are necessary and planned for future operations using the high frequency capabilities of the system.

4.6 The Beatgun, a new seismic source

(R. Herber, A. Polster)

4.6.1 Description of the instrument:

The prototype of the Beatgun has been tested for the first time in this experiment. It was built to do weight drop seismic on the seafloor. It consists of a pressure cylinder in which wound a 20 kg weight is wound up by an electric motor to an height of 2 meters. Then the weight is released and it falls 2 meters through the cylinder and hits the base of the cylinder (Figs 4.6.1; 4.6.2). This beat generates an acoustic pulse that is used as a seismic source. The process is then repeated every 20 sec, so that it is possible to stack the single events vertically.

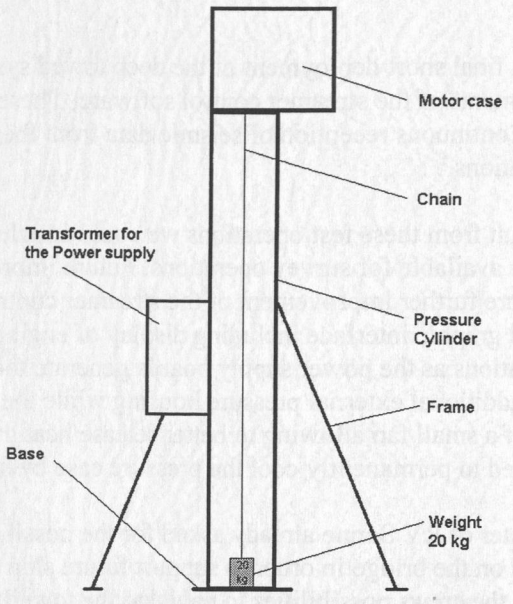

Fig. 4.6.1 The Beatgun, sketch

4.6.2 Tests:

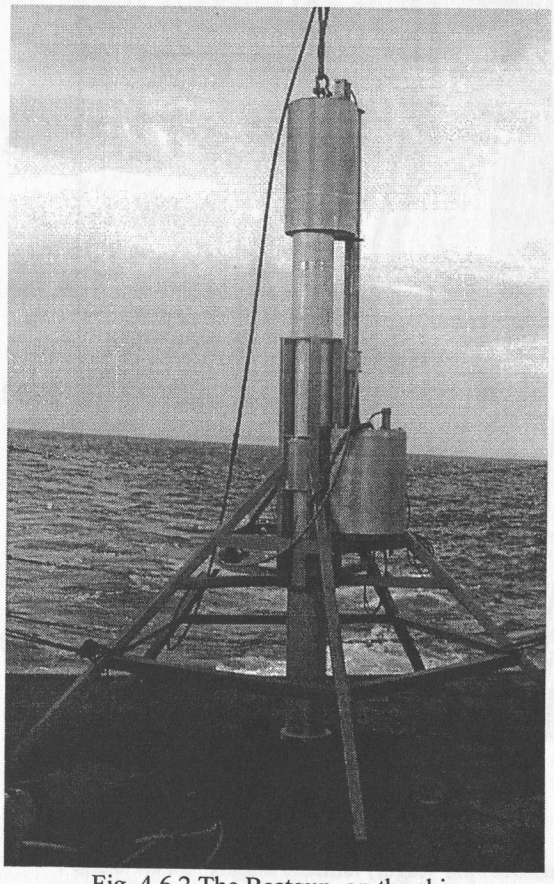

Fig. 4.6.2 The Beatgun, on the ship

First Test:

We made some test-beats on three different positions in the waterdepth of 945 meters. We lifted up and put down the source three times and each time shot 3 or 4 times. A problem was that we couldn`t identify exactly the moment of reaching the seafloor with the Beatgun. Having such soft sediments, you can not recognize on the tension instrument the release in tension. For this reason, we decided to use a transponder to know where the seafloor is in the next experiment. The parameters of this first test-shooting can be seen in Table 1.

Second Test:

The second test-shooting was 1 day later in the same area. 3 shotpoints with a spacing of 200 m, 400 m and 600 m from the OBS-Position were selected. On every shotpoint 13-15 Beats were carried out, the Beatgun was lifted up 100 m and then the ship moved to the next position. The parameters of this second test-shooting can be seen in Table 2.

Shooting-list 1, date: 04.03.2002:

Shooting No.	Local Time	UTC	Lat.	Log.	Depth
Test 1	15:35:00	20:35:00	8:23.838 S	80:23.704 W	945 m +-1
Test 2	15:40:00	20:40:00	8:23.838 S	80:23.704 W	945 m +-1
Test 3	15:44:40	20:44:40	8:23.838 S	80:23.704 W	945 m +-1

Shooting-list 2, date: 05.03.2002:

Shooting No.	Local Time	UTC	Lat.	Log.	Depth
1	18:40:00-18:45:00	23:40:00-23:45:00	8°23,45´ S	80°23,88` W	936 m +-1
2	19:06:32-19:11:02	00:06:32-00:11:02	8°23,55´ S	80°23,81` W	942 m +-1
3	19:28:00-19:32:19	00:28:00-00:32:19	8°23,65` S	80°23,76` W	943 m +-1

4.6.3 Experience:

The handling to assemble up the Beatgun with a crane could be done without problems. After connecting the high voltage (1000 Volts) to the transformer of the Beatgun, the motor of the gun started to wind up the 20 kg weight. The mechanical parts and the motor of the Beatgun worked from the start without defect.

The determination of the beat time must have an accuracy of 1 msec. There are two solutions possible:

a) fixing an OBH recording unit plus hydrophone to the frame of the Beatgun and recording the beats.

b) to measure the current consumption of the Beatgun. As the moment 20 kg weight releases the current drops down.

One of there solutions must be realised for the next experiment. Another unknown influence on the radiated signal is the footprint area of the Beatgun (Fig 4.6.3). In very soft sediments the area we have in use now seems to be much too small. Simple solutions can be found for this problem. The automatic switch for the Beatgun in the two extreme positions are:

a) hanging on the crane or cable
b) sinking more than 45 cm into the sediment.

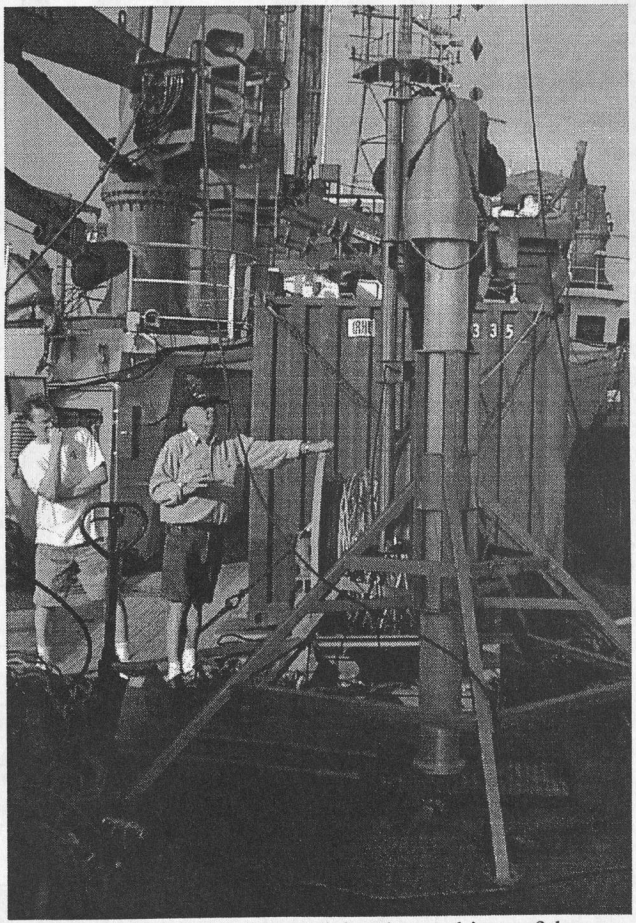

Fig. 4.6.3 R. Herber explains the workings of the Beatgun to the chief scientist

This is a good solution and helps the operator of the Beatgun to decide to stop the experiment or to repeat the experiment at the same position.

4.6.4 First results

In Figures 4.6.4 and 4.6.5, we show first examples of Beatgun shots. The traces displayed are the same time window for four different channels, corresponding to the hydrophone (channel 1), the two horizontal components and on the right the vertical component geophone (channel 4). The weight jumps and it produce a second signal after 170 ms. After 1.1 sec you can see the signal from the sea-surface. Other phases could not be unambiguuously identified as yet: this will require better control on shot time and position, and shots along a whole profile.

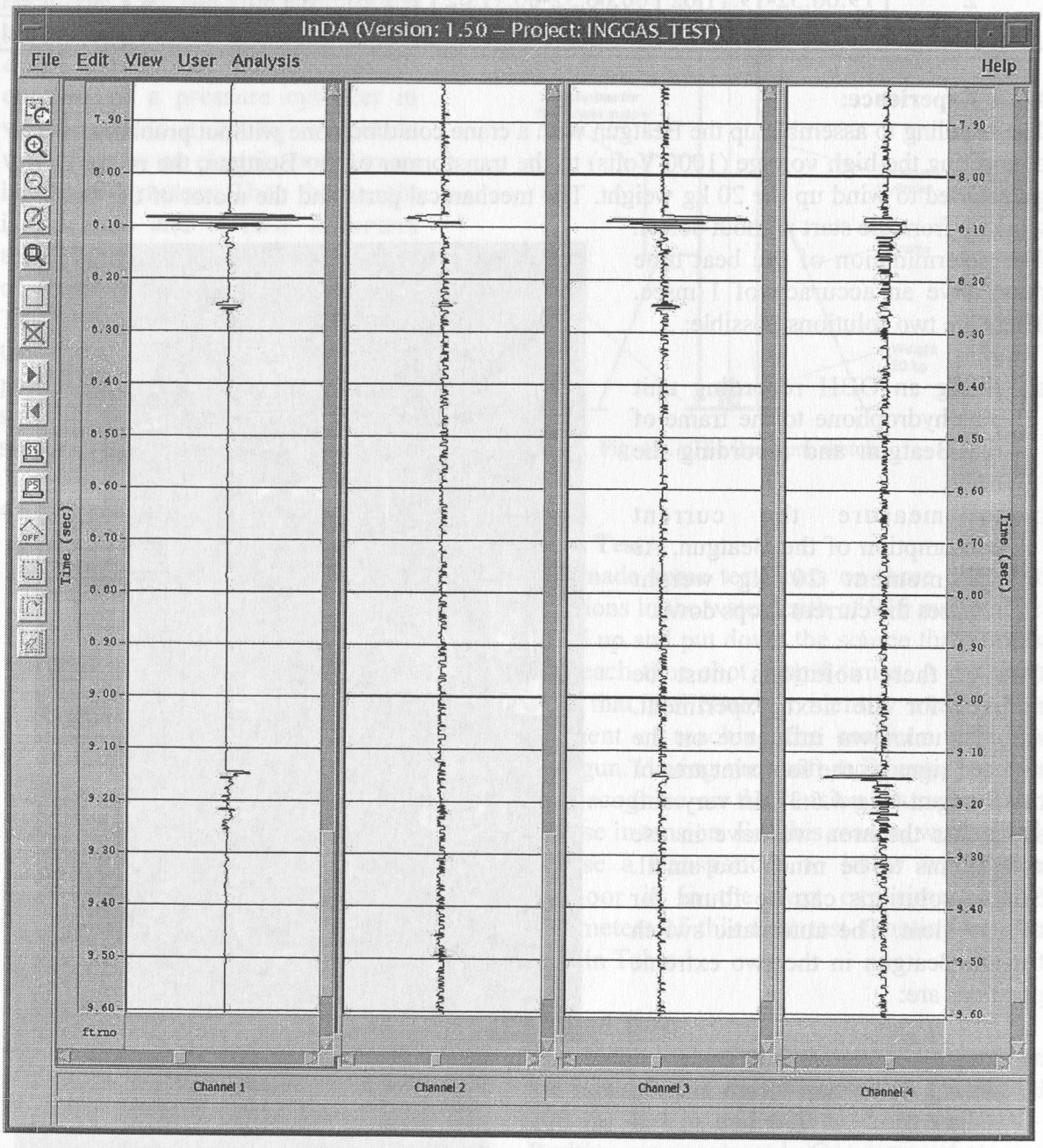

Fig. 4.6.4 Example of a Beatgun shot at source point 4 recorded by OBS 12.
Source ca. 500 m from the OBS.

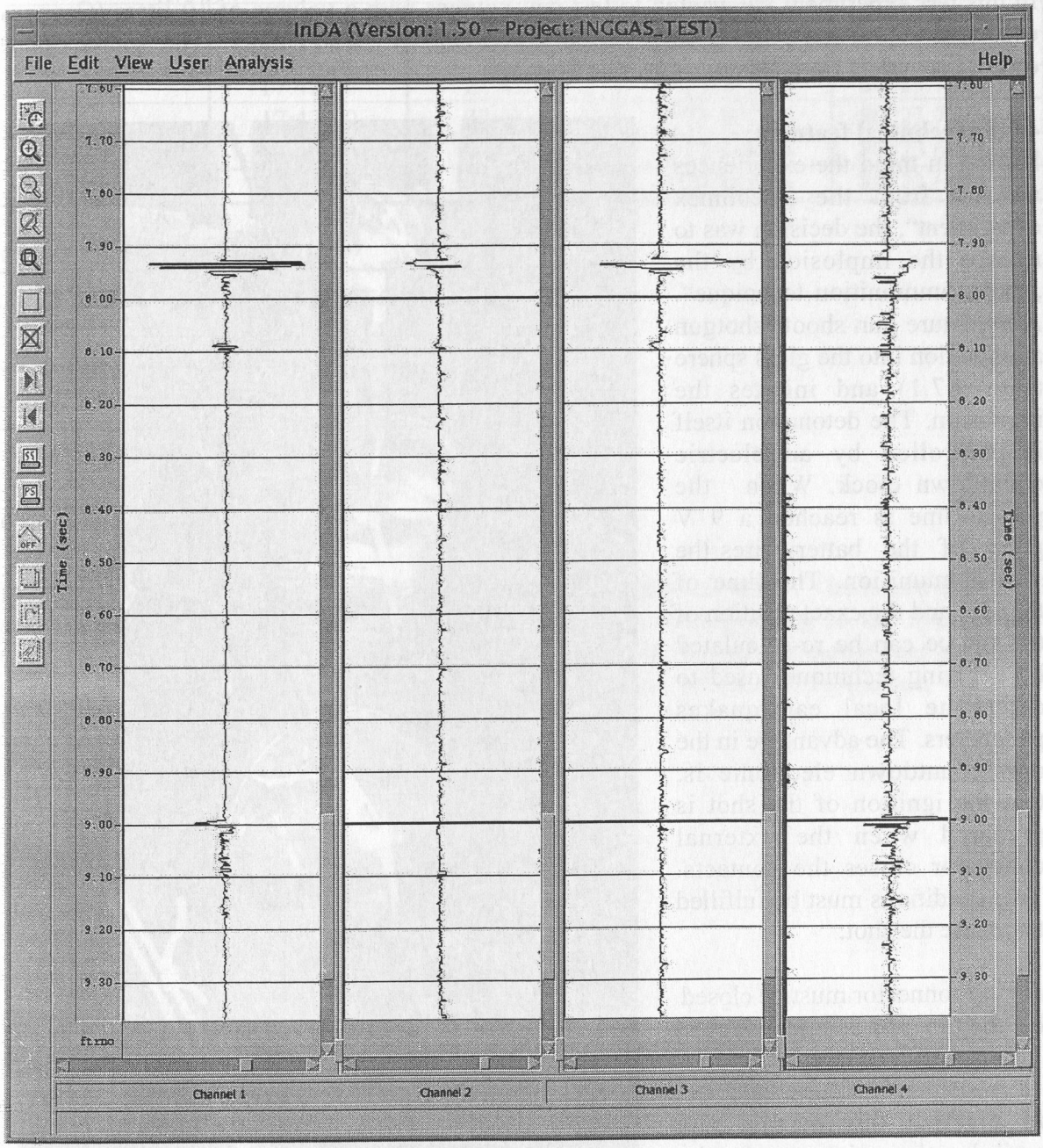

Fig. 4.6.5 Second example of a Beatgun shot at source point 4 recorded by OBS 12.
Source ca. 500 m from the OBS

4.7 The SeeBoSeis experiment (R. Herber, A. Polster))

4.7.1 Experiences

In this test experiment we wanted to test new sources with a volume of 10 litres (Geopeco experiment 5 lrs) and a new countdown electronic, built by „Send GmbH". The source can be ordered complete from „Nautilus Marine Service".

4.7.2 Technical features:

Having in mind the experiences we got from the „Geolimex experiment", the decision was to release the implosion by the „shot - ammunition technique". A miniature gun shoots shotgun ammunition into the glass sphere (Fig. 4.7.1) and initates the implosion. The detonation itself is controlled by an electric countdown clock. When the preset time is reached a 9 V pulse of the battery fires the shot ammunition. The time of the shot and the exact position of the source can be re-calculated by applying techniques used to determine local earthquakes parameters. The advantage in the new countdown electronic is, that the ignition of the shot is prepared when the external connector closes the contacts. Two conditions must be fulfilled to release the shot:

a) the connector must be closed
b) the timer of countdown must reach 0

In practice this means, you switch the timer of the countdown time depending from the water depth e.g. one hour, fill the shotgun with ammunition and close the glass sphere. An anchor weight of 20 kg is fixed 1 m below the sphere and just before dropping the source, the connector starts the countdown clock.

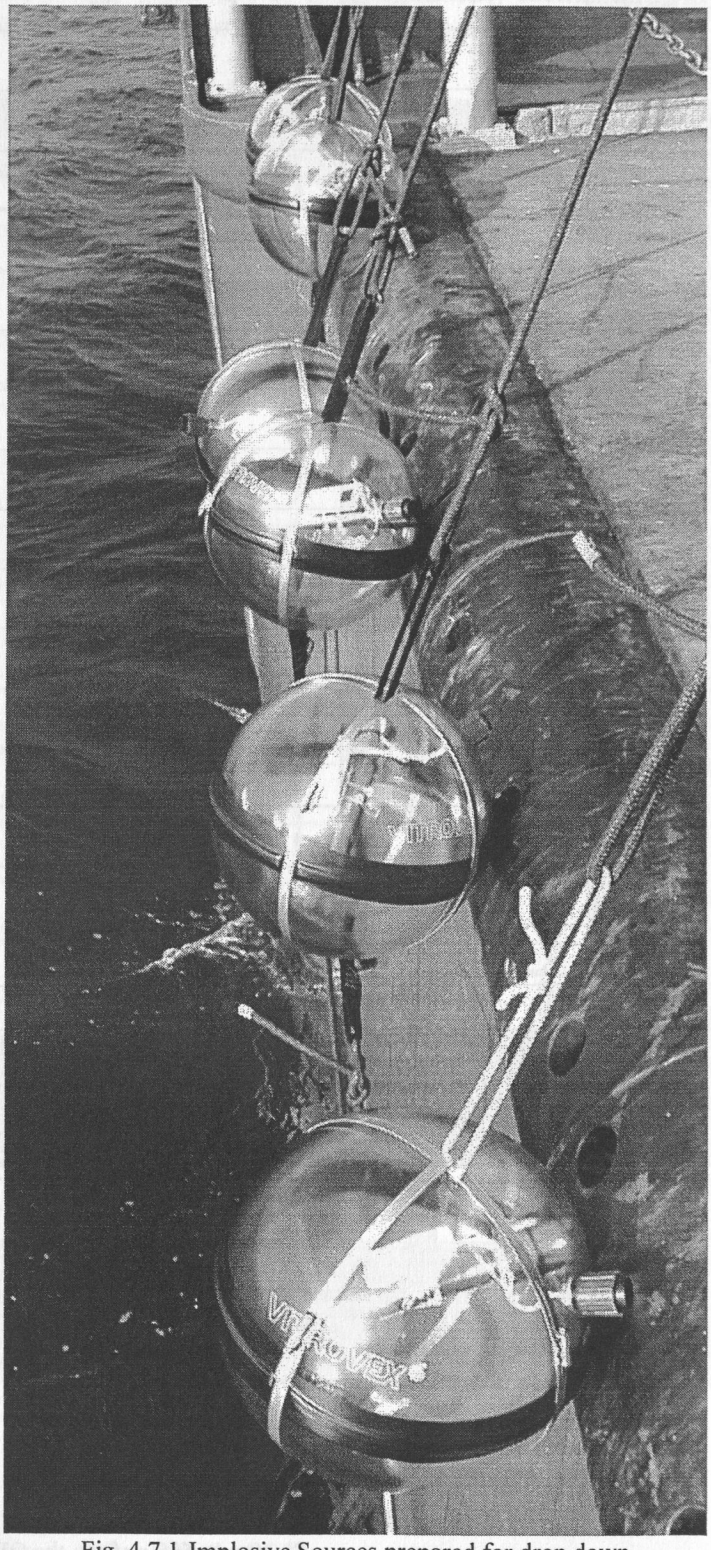

Fig. 4.7.1 Implosive Sources prepared for drop down

Implosion-Time, date: 04.03.02:

Glass sphere No.	Local Time	UTC	Lat	Lon
1	17:39:10	22:39:10	8°23.6350 S	80°23.8770 W
failed 2	17:40:00	22:40:00	8°23.6850 S	80°23.8399 W
3	17:41:00	22:41:00	8°23.7220 S	80°23.7960 W
4	17:42:00	22:42:00	8°23.7625 S	80°23.7635 W
5	17:43:00	22:43:00	8°23.8075 S	80°23.7325 W
6	17:44:00	22:44:00	8°23.8486 S	80°23.6963 W
7	17:45:00	22:45:00	8°23.8887 S	80°23.6604 W

Coordinates of the Tools:

Tools	Lat	Lon
OBH 9	8°23.701 S	80°24.207 W
OBH 11	8°23.303 S	80°23.778 W
OBS 10	8°23.500 S	80°24.010 W
OBS 12	8°23.36 S	80°24.15 W

C) First results:

In Figures 4.7.2 and 4.7.3, we show examples of two SeeBoSeis shots. The traces displayed are the same time window for four different channels, corresponding to the hydrophone (channel 1), the two horizontal components and on the right the vertical component geophone (channel 4). After 130 ms there is a strong onset that is not reflected from surface, while the first onset is reflected.

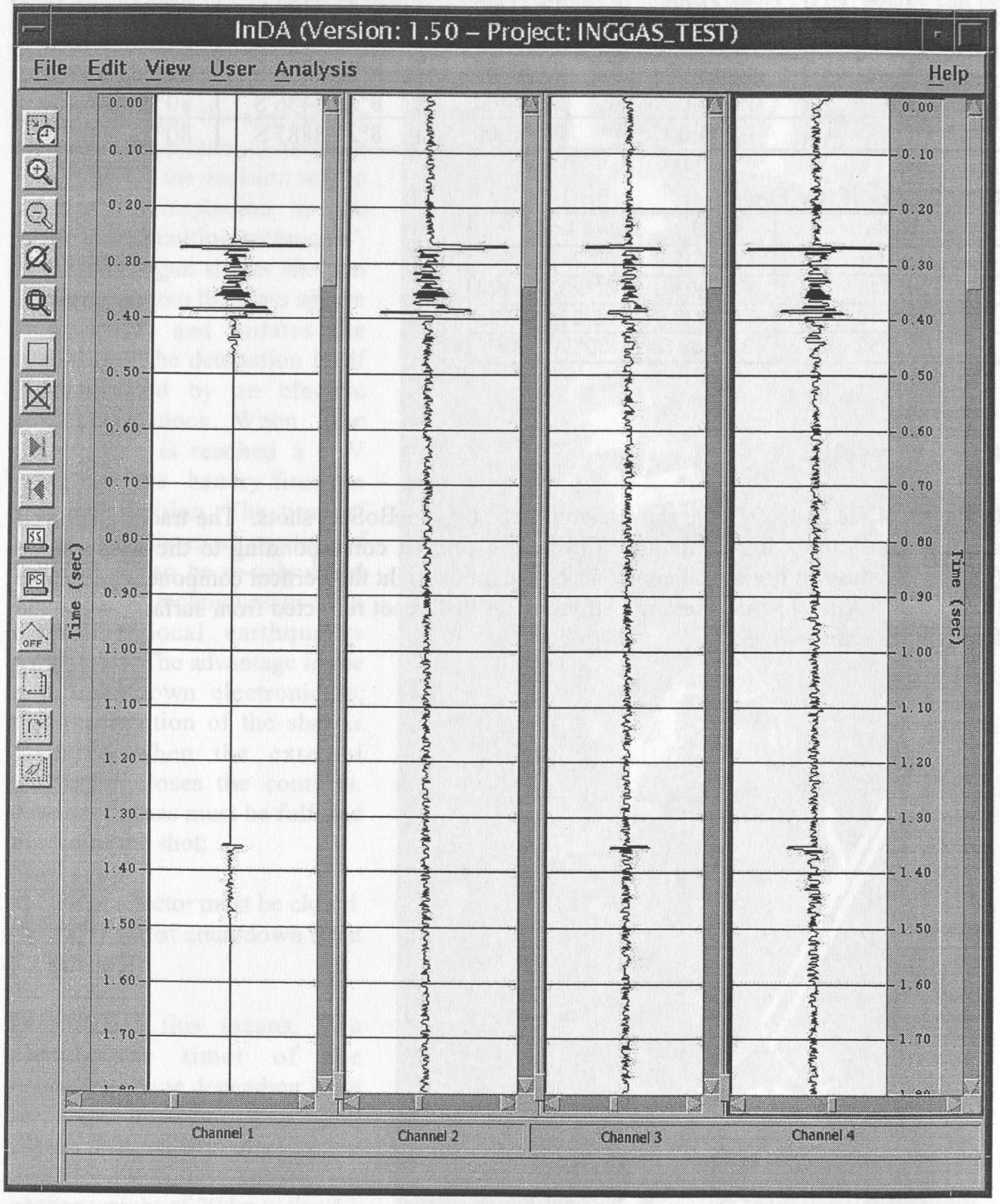

Fig. 4.7.2 Example of a SeeBoSeis implosive source shot (3) recorded by OBS 12. Shot ca. 900 m from OBS.

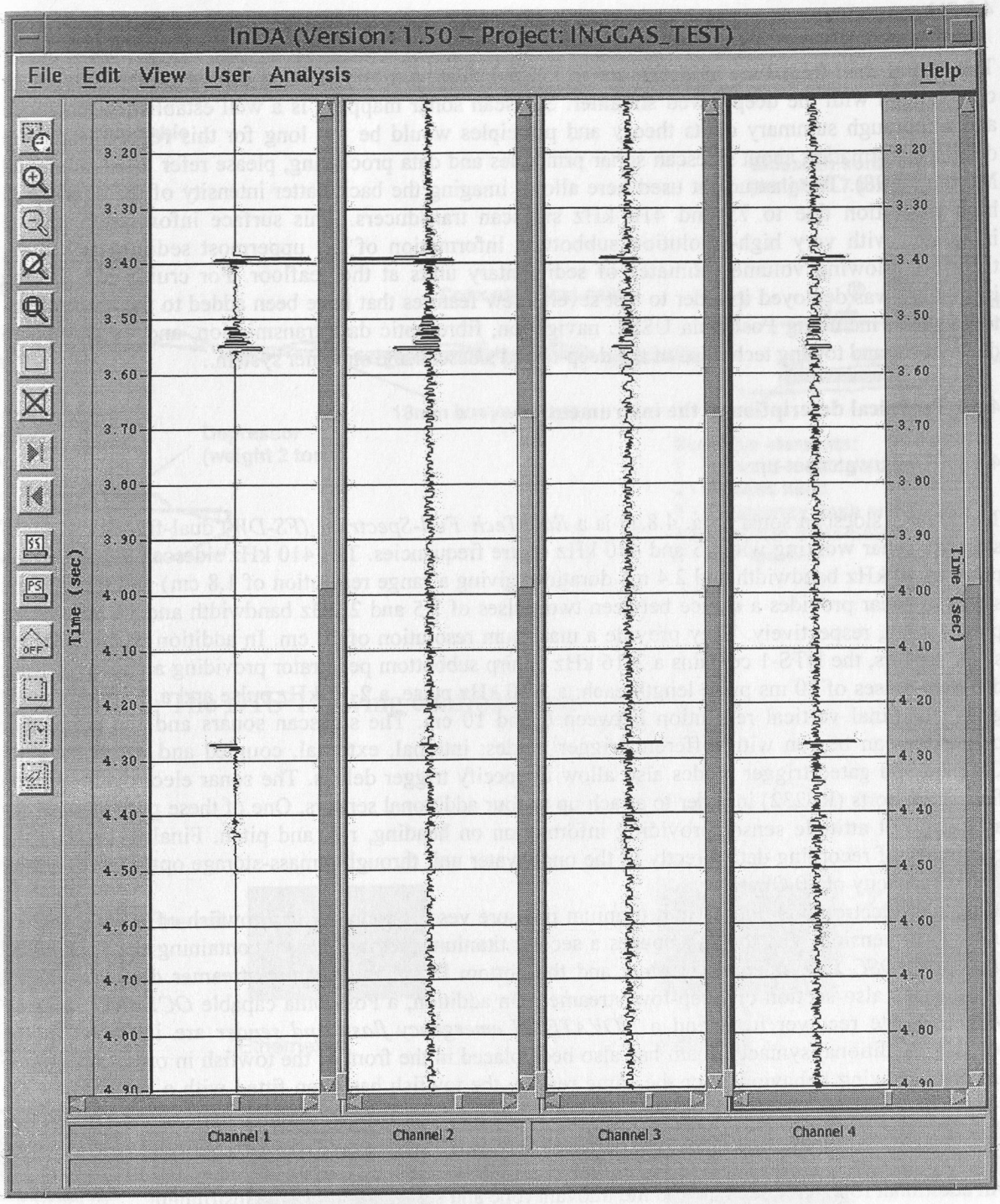

Fig. 4.7.3 Example of a SeeBoSeis implosive source shot (4) recorded by OBS 12. Shot ca. 1000 m. from source

4.8 Sidescan sonar

The digital dual-frequency sidescan sonar DTS-1 (Fig. 4.8.1) was used during cruise SO-162 in combination with the deep-towed streamer. Sidescan sonar mapping is a well established technique and a thorough summary of its theory and principles would be too long for this report. For more detailed information about sidescan sonar principles and data processing, please refer to Blondell and Murton (1998). The instrument used here allows imaging the backscatter intensity of the seafloor at high resolution due to 75 and 410 kHz sidescan transducers. This surface information can be integrated with very high-resolution subbottom information of the uppermost sedimentary layer, therefore allowing volume estimates of sedimentary units at the seafloor. For cruise SO-162 the instrument was deployed in order to test several new features that have been added to the entire deep-tow system including Posidonia USBL navigation, fibre-optic data transmission, and the combined deployment and towing technique of the deep-towed sidescan and streamer system..

4.8.1 Technical description of the instrument

4.8.1.1 Underwater set-up

The DTS-1 sidescan sonar (Fig. 4.8.1) is a *EdgeTech Full-Spectrum (FS-DW)* dual-frequency, chirp sidescan sonar working with 75 and 410 kHz centre frequencies. The 410 kHz sidescan sonar emits a pulse of 40 kHz bandwidth and 2.4 ms duration (giving a range resolution of 1.8 cm) and the 75 kHz sidescan sonar provides a choice between two pulses of 7.5 and 2 kHz bandwidth and 14 and 50 ms pulse length, respectively. They provide a maximum resolution of 10 cm. In addition to the sidescan sonar sensors, the DTS-1 contains a 2-16 kHz , chirp subbottom penetrator providing a choice of three different pulses of 20 ms pulse length each: a 2-10 kHz pulse, a 2-12 kHz pulse and a 2-15 kHz pulse giving nominal vertical resolution between 6 and 10 cm. The sidescan sonars and the subbottom penetrator can be run with different trigger modes: internal, external, coupled and gated triggers. Coupled and gated trigger modes also allow to specify trigger delays. The sonar electronics provide four serial ports (RS232) in order to attach up to four additional sensors. One of these ports is used for a Honeywell attitude sensor providing information on heading, roll and pitch. Finally, there is the possibility of recording data directly in the underwater unit through a mass-storage option with a total storage capacity of 30 Gbyte.
The sonar electronic is housed in a titanium pressure vessel mounted on a towfish of 2.8m x 0.8m x 0.9m in dimension. The towfish houses a second titanium pressure vessel containing the wet-end of the *SEND DSC-Link telemetry system* and the bottom PC of the seismic streamer data acquisition system (see also section on deep-tow streamer). In addition, a Posidonia capable *OCEANO releaser* with separate receiver head and a *NOVATECH emergency flash and sender* are included in the towfish. Additional syntactic foam has also been placed in the front of the towfish in order to improve the fish's towing behaviour. For the same reason, the towfish has been fitted with a deflector at the rear . This deflector has five positions from 0 to –5 and is designed to reduce the pitch of the towfish.
The towfish is connected to the sea cable via the depressor (2 tons weight) through a 40 m long umbilical cable. The umbilical cable is tied to a buoyant rope that takes up the actual towing forces. An additional rope has been taped to the buoyant rope and serves to pull in the instrument.

4.8.1.2 Laboratory set-up

The laboratory set-up consists of four elements: the dry-end of the *SEND DSC-Link telemetry*, the topside PC of the streamer acquisition system, the *Edgetech surface interface unit FS-IU* and the topside unit running *ELAC Hydrostar Online* software (Fig. 4.8.2). The only function of the bottom and topside PC of the streamer acquisition system is to provide a serial link between the *OCEANO* releaser operating in responder mode and the *Posidonia* topside unit. *Hydrostar Online* allows general running of the sidescan sonar and subbottom penetrator operations as well as onscreen display of a subset of the acquired data. Unfortunately some additional settings such as the trigger mode or data window size can only be changed by accessing the underwater electronics directly via the *FS-IU*. The

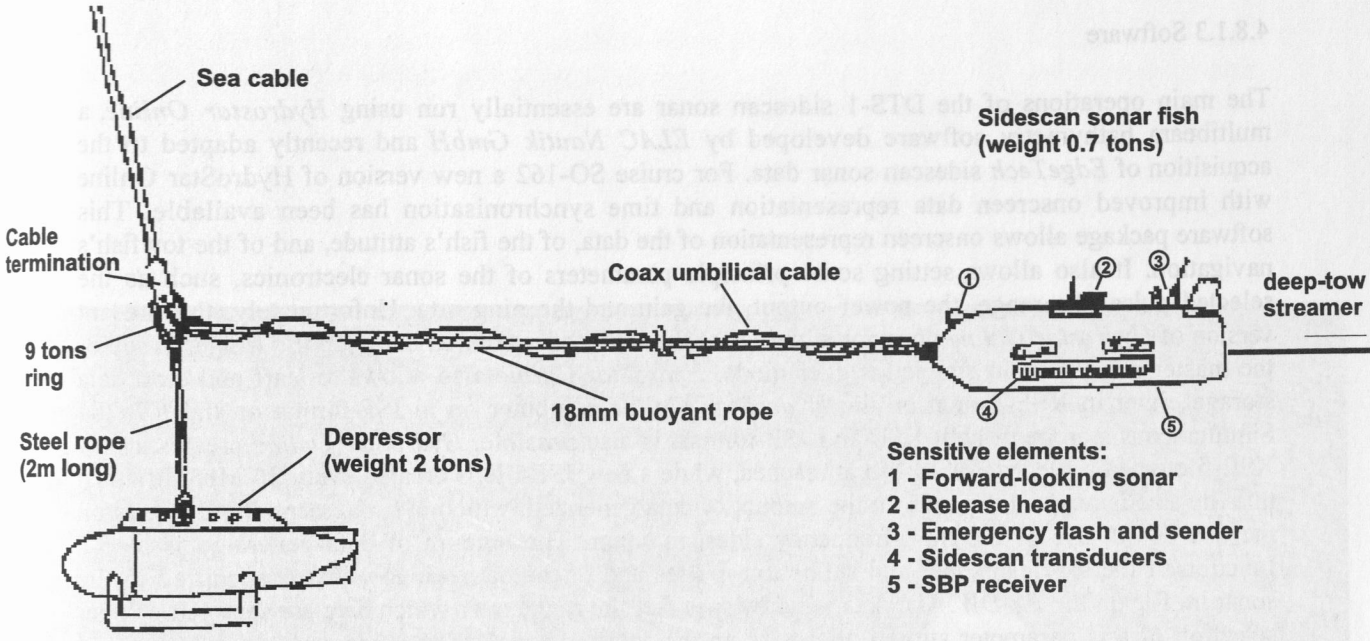

Figure 4.8.1: The DTS-1 towing configuration.

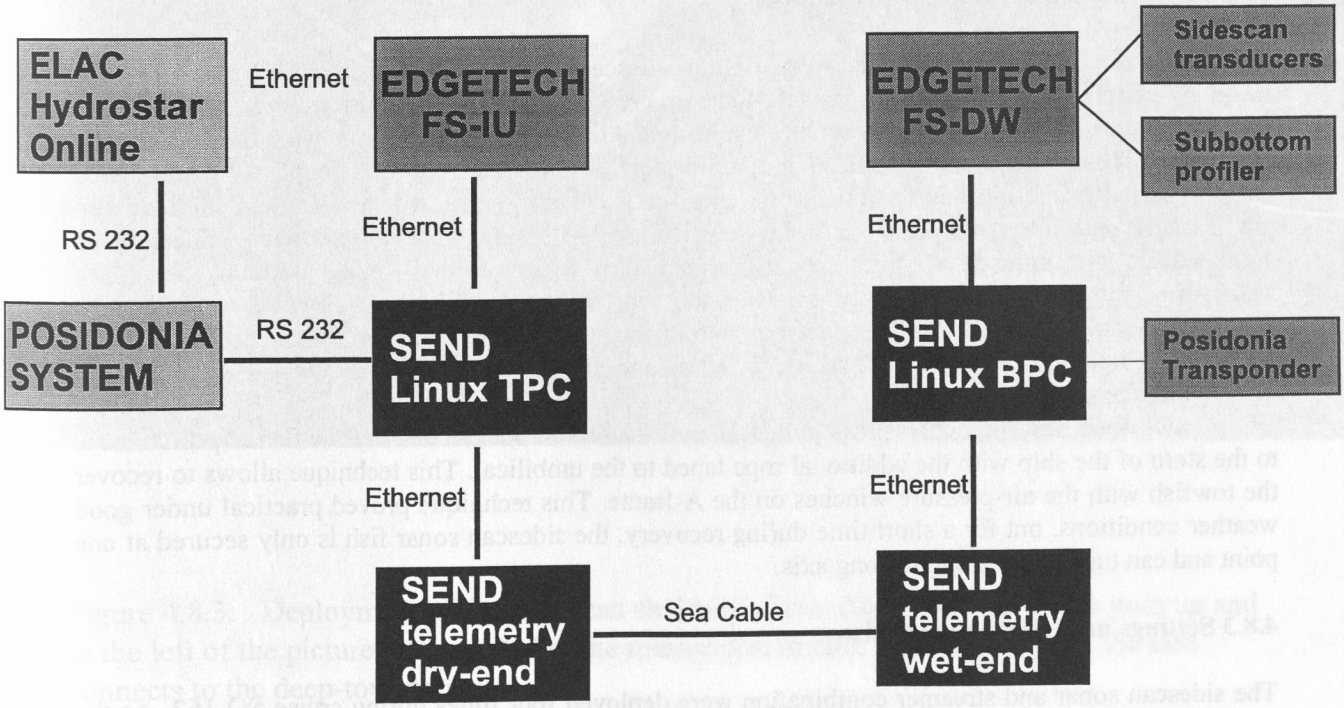

Figure 4.8.2: The DTS-1 electronics configuration.

FS-IU also runs *JStar*, a diagnostic software tool, that also allows running some basic data acquisition and data display functions.

4.8.1.3 Software

The main operations of the DTS-1 sidescan sonar are essentially run using *Hydrostar Online*, a multibeam bathymetry software developed by *ELAC Nautik GmbH* and recently adapted to the acquisition of *EdgeTech* sidescan sonar data. For cruise SO-162 a new version of HydroStar Online with improved onscreen data representation and time synchronisation has been available. This software package allows onscreen representation of the data, of the fish's attitude, and of the towfish's navigation. It also allows setting some principle parameters of the sonar electronics, such as the selected pulse, the range, the power output, the gain and the ping rate. Unfortunately, the present version of *Hydrostar Online* does not allow to set the range of registered data, nor the trigger mode or the master subsystem in coupled trigger mode. *HydroStar Online* also allows to start and stop data storage either in XSE-format on the *HydroStar Online* computer on in JSF-format on the *FS-DW*. Simultaneous storage in both XSE and JSF-formats is also possible. *HydroStar Online* creates a new XSE-file when a file size of 10 Mb is reached, while a new JSF-file is created every 20 Mb. How fast this file size is reached depends on the amount of data generated, which in turn essentially depends on the use or not use of the high-frequency sidescan sonar. The amount of data generated is also a function of the sidescan sonar and subbottom pulses and of the data window that is specified in the sonar.ini file on the *FS-DW*. The data window specifies the range over which data are sampled. Proper selection of this parameter strongly depends on the selected range of the sidescan sonar systems in order to avoid good data to be cut-off, or to prevent too large amounts of unuseful data using up storage space.
Further handling of the data is still problematic as neither the XSE nor the JSF data format can be read directly by our sidescan sonar and seismic (for the subbottom penetrator) processing software, which require NetCDF and SEG-Y formats, respectively. Major efforts to achieve data conversion into formats for use with either *PRISM* of *MB Systems* are still going on onshore and will soon allow proper processing of the sidescan sonar data.

4.8.2 Deployment and recovery procedures

Operations for deployment and recovery of the sidescan sonar are a bit demanding and require relatively calm sea for handling that is safe for both crew and instrument. During cruise M52/1 three seamen, the boatswain, the sidescan sonar technician and the responsible scientist were on deck for the operations. The sidescan sonar instrument should ideally be towed via the A-frame. With no speed made by the ship the kite tail is first thrown into the water and let to drift away. Then the sidescan towfish is heaved into the water (Fig. 4.8.3) and released with a special hook allowing to detach the crane cable. The sidescan fish then also drifts astern with minimal speed made by the ship. Meanwhile, the buoyant rope is secured. Then the depressor is put in place below the A-frame, the buoyant towing rope fitted to the end termination of the sea cable, and the umbilical cable connected to the sea cable. Any loose ends are securely tied up and the depressor, with the towfish attached to it, heaved into the water (Fig. 4.8.4).
During recovery, first the depressor is pulled in and secured on deck. Then the towfish is pulled close to the stern of the ship with the additional rope taped to the umbilical. This technique allows to recover the towfish with the air-pressure winches on the A-frame. This technique proved practical under good weather conditions, but for a short time during recovery, the sidescan sonar fish is only secured at one point and can turn freely along its long axis.

4.8.3 Settings used during the cruise

The sidescan sonar and streamer combination were deployed four times during cruise SO-162. As the focus of the cruise was mainly on testing the deep-towed seismic streamer, the sidescan sonar was not necessarily used in its best configuration and under ideal conditions. Nevertheless some useful tests have been performed with the sidescan sonar system and some data have been collected.

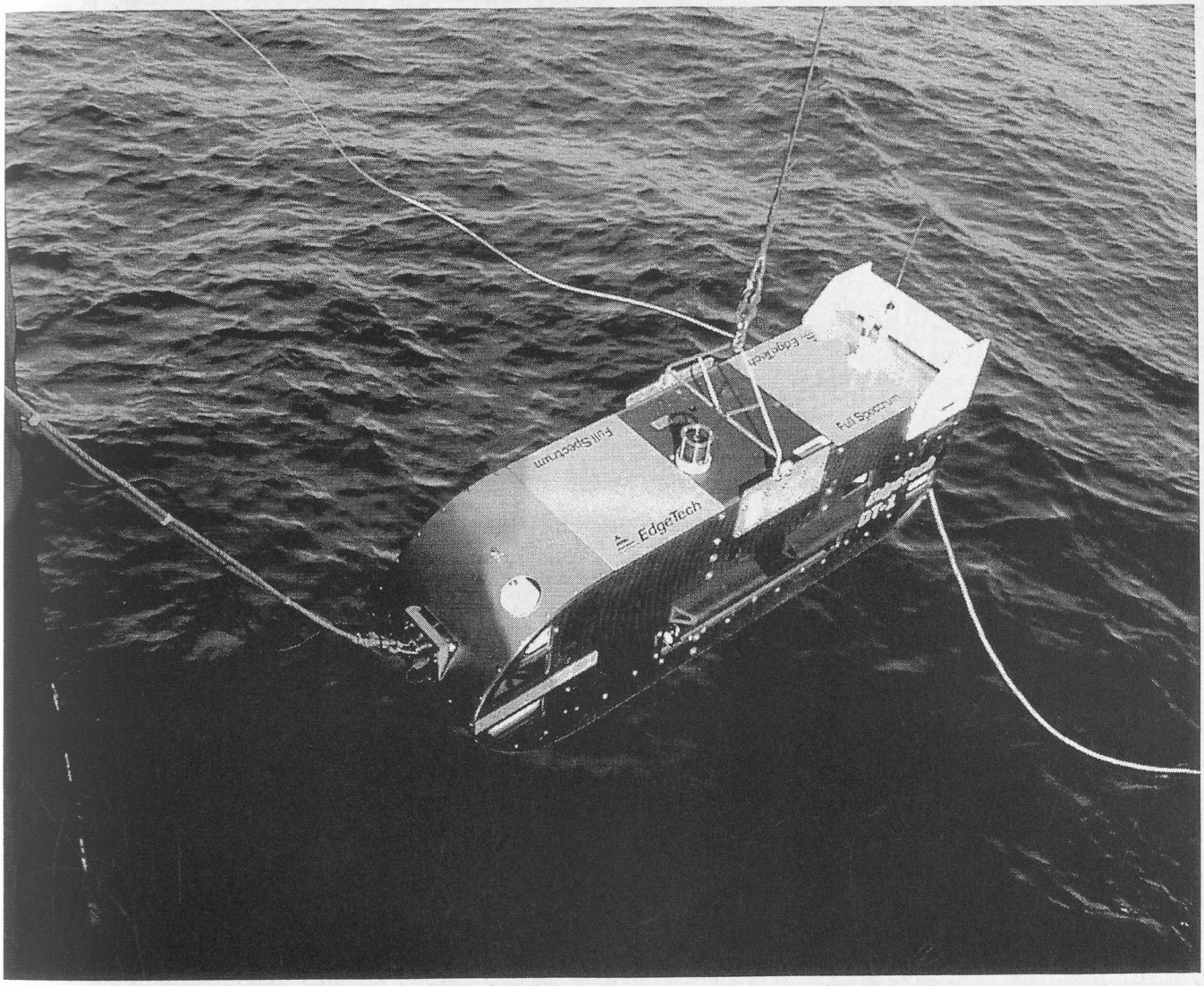

Figure 4.8.3: Deployment of the side-scan sled behind the ship. Thin white line goin up and to the left of the picture is connected to the release pin; thicker white line behind the sled connects to the deep-tow streamer.

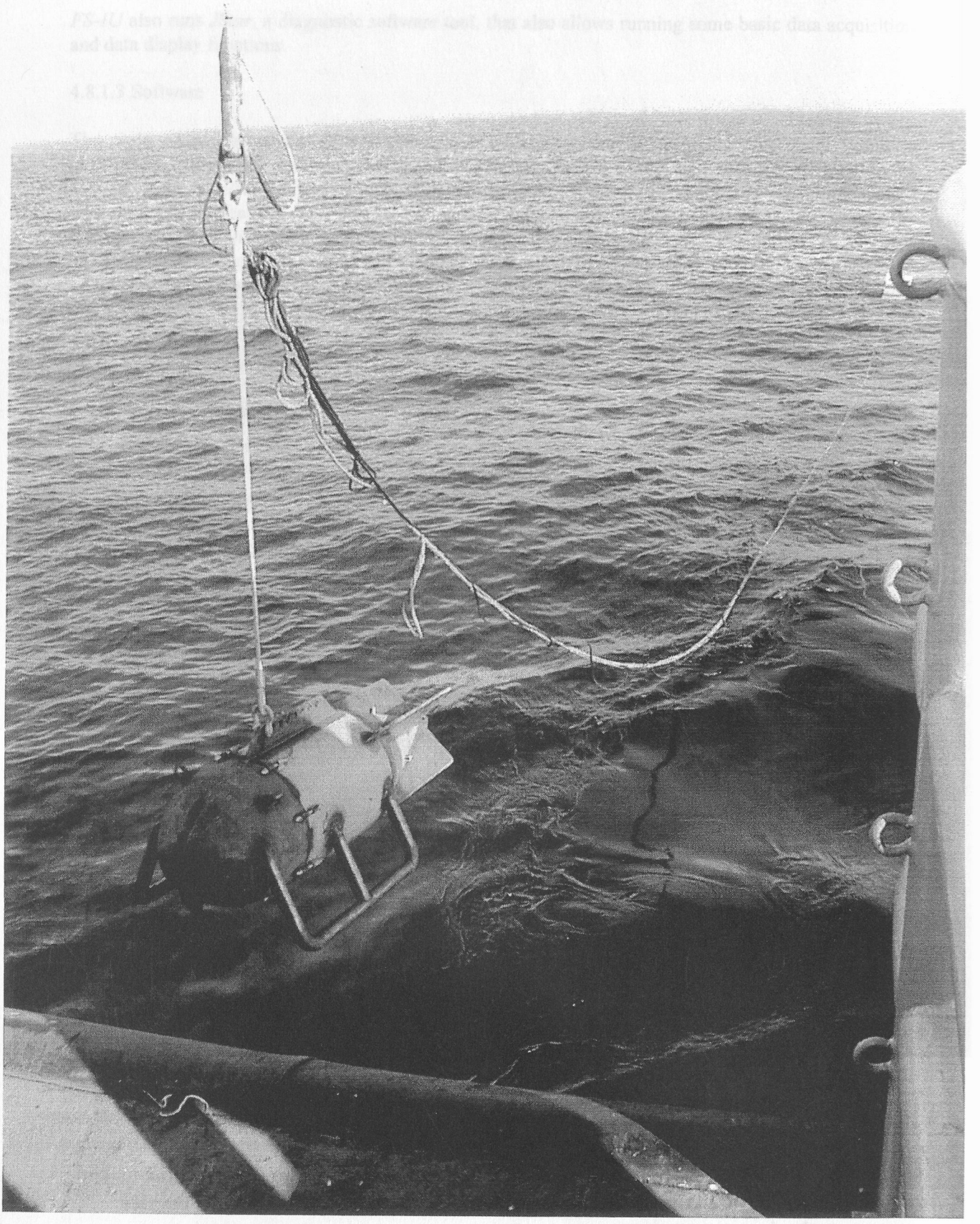

Figure 4.8.4: Deployment of depressor weight . The side-scan can just be seen (light "box" floating in the water well behind vessel)

Deployment 1

The fish deployment was carried out in order to test the new *Posidonia* transponder on the tow-fish. During this test the transponder received external power supply through the *DSC link telemetry*, which also provide a serial data link to operate the transponder in responder mode. *Posidonia* underwater navigation allowed for the first time to track the towfish while towed behind the ship. Unfortunately the *Posidonia* signal interferes with the operation of the low frequency side scan sonar and the subbottom profiler. During this test we also observed strong electrical interferences in the side scan sonar signal that we attributed in problems in shielding the power supply in the telemetry system and in particular the power supply to the *Posidonia* transponder.

Deployment 2

The second deployment was carried out in about 800 m water depth in the Yaquina basin offshore Peru. Here a 20 mile long profile was run a total of four times (Profiles 2-5). During the first three profiles the 75 kHz sidescan sonar (14 ms pulse) and the subbottom penetrator (2-10 kHz, 20 ms pulse) were used and tow speed was changed from 3.0 to 2.5 to 3.5 knots. The fourth profiles was run at 25 m distance above ground and data from the 75 kHz sidescan, the subbottom profiler and the 410 kHz sidescan sonar were gathered. During this deployment, the Posidonia system ran on batteries and the previously observed electrical noise fortunately disappeared. In turned out in a subsequent test that the noise was not connected to the power supply to the Posidonia system, but bad shielding of other components in the telemetry pressure housing. These problems with electrical noise are now under control, but not entirely solved. Another type of interferences appeared at shallow tow depths and during winch operation. The interferences seem to be generated by the ship, but at present it is not clear what actually causes them. In any case they disappeared in water depth below 1000 m.

Deployment 3

The third successful deployment of the sidescan sonar consisted of 9 parallel tracks of 3.5 miles length each and two short cross-profiles covering the area of the "Max, Moritz and Witwe Bolte" chemoherms. The parallel profiles are 100 m apart, resulting in large and multiple overlap of the sidescan sonar swaths. During this deployment 75 kHz and subbottom profiler data have been obtained (Figs. 4.8.5 and 4.8.6), but subbottom profiler data are sometimes truncated because the instrument was generally towed more than 140 m above ground. If the elevation of the sidescan above ground was even greater, 190 m of data registration window may not have been sufficient.

Deployment 4

The fourth deployment of the sidescan was to test the maximum reach of the Posidonia system in deep water. With only 7000 m of cable length available in 4000 m water depth we were not able to come within reach of the seafloor, except for a short moment while turning. During this deployment, the Posidonia system was again running on the external power supply, but this time without producing the same interference as before. Connection of the Posidonia system with the HydroStar Online proved to be difficult to obtain during this deployment. The Auto Search function in HydroStar Online did not find the proper connection although the serial connection between the two systems was established. In future it would be advantageous to be able to establish this serial link manually. No data were collected during this deployment.

Processing

No processing software was available during the cruise: we plan in future to convert the EdgeTech data (XSE format) to netcdf format (side-scan data) for processing with Southampton's PRISM software and SEGY (sub-bottom profiler data) for standard seismic processing. As a result only the raw data are shown in Figure 4.85 and 4.8.6.

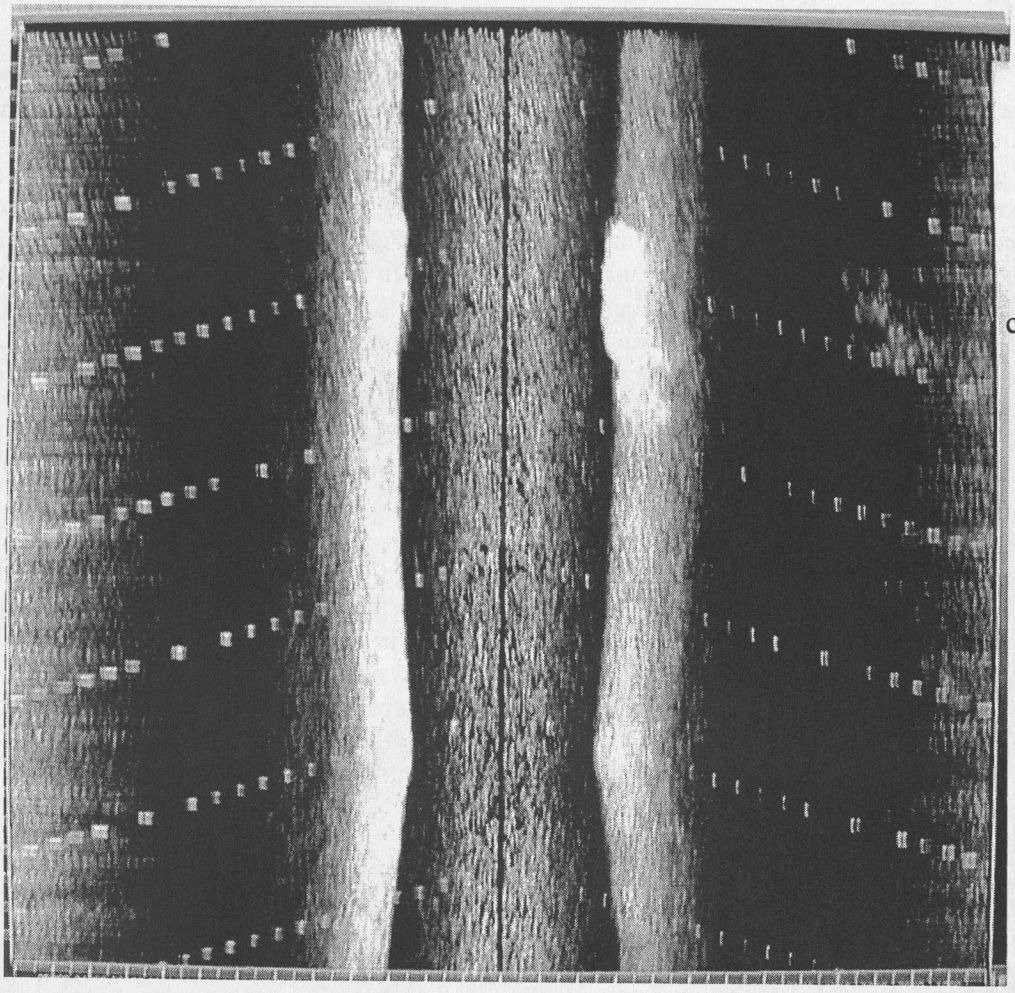

Figure 4.8.5 Photograph of the monitor displaying the raw side-scan sonar data. The image is of the "Witwe Bolte" chemoherm, and was made at the same time as Figure 4.8.6.

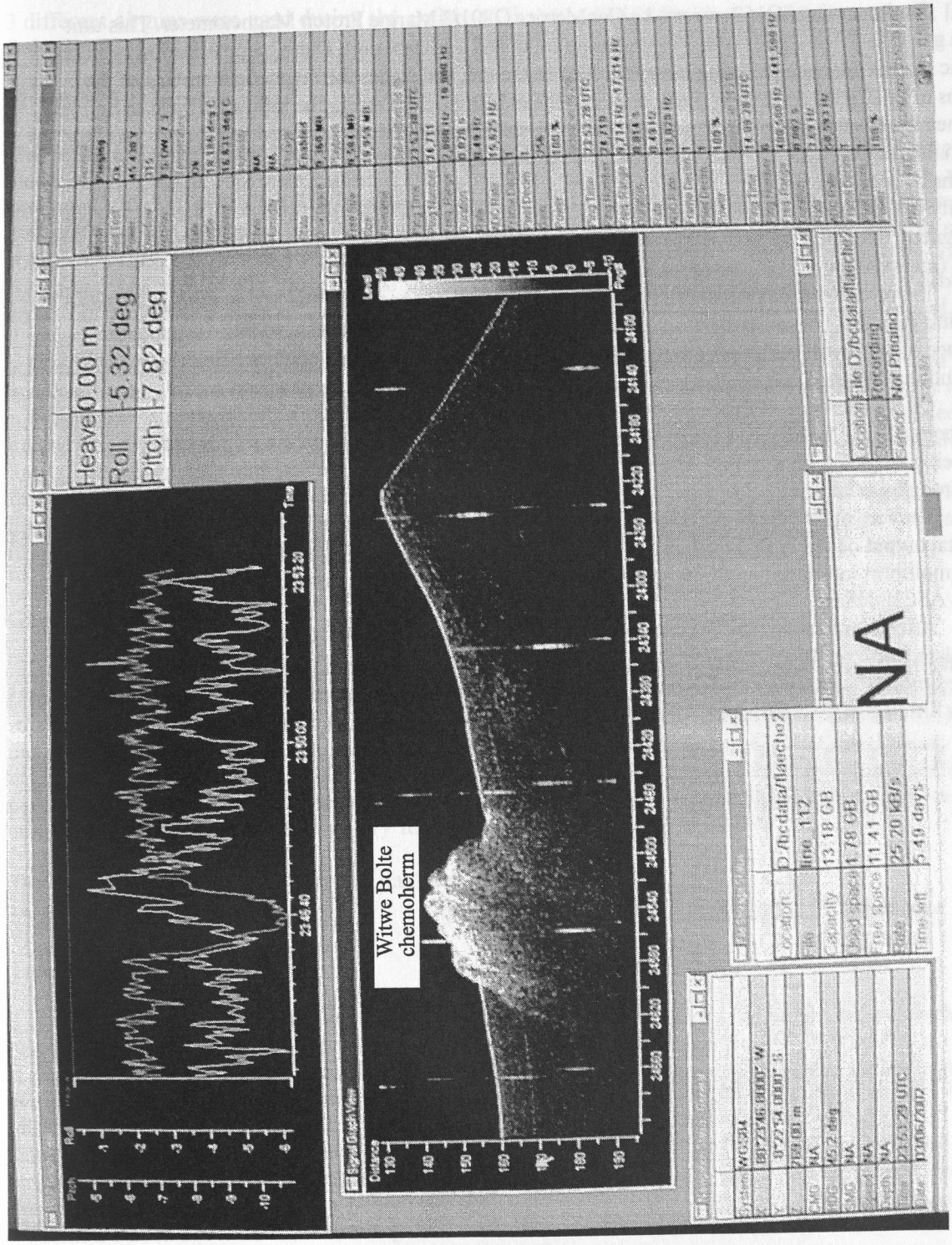

Figure 4.8.6 Photograph of the monitor displaying the raw data from the Sub-bottom profiler. The image shows the "Witwe Bolte" chemoherm. Note also the system data displayed in the other windows.

4.9 The Magnetometer

During cruise SO162 we used a GeoMetrics G801/3 Marine Proton Magnetometer. This unit uses a gasoline-filled sensor with 350 m marine cable and a control unit. During a polarisation cycle an electric current generates a strong magnetic field in the coil and forces the magnetic moments of the protons to be aligned for a short time parallel to the existing field. During the following measuring cycle, i.e. when the electric current is turned off, the previously excited field is removed and the protons "try" to realign themselves with the Earth's magnetic field. According to the moment preservation law, this happens by precession of the protons with a certain frequency, which is directly proportional to the intensity of the Earth's magnetic field. Basically, this frequency is measured as AC electric current created by magnetic induction in the coil, amplified, counted and transformed to the magnetic field intensity values (measuring unit: 10^{-9} Tesla = 1 nT), which are recorded.

In order to minimize the influence of the ship's hull, the sensor of the Magnetometer is towed 180 m behind the ship. This distance of the sensor from the ship was long enough, so that the magnetic influence of the vessel could not produce any disturbances in the recorded magnetic field, so we achieved a resolution of about 5 nT.

On board of RV SONNE, the winch was placed on the port back deck and the sensor was towed to the port side of the vessel. A boom leads the cable about 7 m to the side of the ship in order to prevent it from being tangled with the ship. After having some minor problems at the beginning, the system worked well throughout the trip.

The measured values of the total intensity magnetic field were displayed on a console and written as digital output coded in BCD values. The system was set to deliver one data value every 3 seconds via digital multiport interface to a PC, where a special software was used to store the data together with UTC-time in ASCII tables.

After data backup the files were transferred to a SUN workstation. GPS coordinates and time were taken from the ship's navigation system and assigned to each magnetic stamp on the basis of the recorded time. The magnetic and the navigation data were resampled to 10 s interval. After optional median filtering they were displayed using GMT plot routines (Wessel and Smith, 1995).

4.10 Airguns

3 different airguns were used during the cruise: a GI gun, a single Prakla-type airgun, and a 32 litre Bolt airgun.

32 l BOLT Airguns

The seismic signals of the lower frequency band were generated by a Model 800 CT *BOLT* airguns; a photo of the guns is shown in Figure 4.10.1. The gun has a volume of 32 liters (2000 $inch^3$), and generates a signal with a main frequency centered around 6 to 8 Hz and including higher harmonics. The gun was suspended on two floats with an additional float attached to the supply lines to prevent contact between the gun and the towing wire. As well as being deployed and towed from the assistant winch and beam normally used for the piston corer recovery, an elongation of the small starboard aft crane was available this time, as requested on previous cruises. The gun could be well operated with the use of this crane, allowing deployment well away from the cables towing the deep-towed equipment (Figure 4.10.2). However, it turned out that for safety reasons to protect crew and gear a small rail needs to be set up at the deployment point on starboard side of the vessel. Trigger cables and airhoses were deployed manually. The gun was towed 60 m behind the vessel and operated at 145 bar in 7 to 8 m depth. Due to good weather conditions the handling of the gun was smooth all the time.
During cruise SO162 the gun was used twice. The total operation time was about 10 hours, with more than 1500 shots being fired, either at a 20 s or a 15 s shot interval The ship's compressor system worked smoothly and caused no delays or interruptions.

GI-Gun

For SO162 INGGAS-Test cruise, the Geophysics Group from the Alfred Wegener Institute (AWI) provided a GI-Gun (Generator-Injector gun; manufactured by Sodera) for high-resolution surveys. Basically a GI-Gun consists of two airguns in one. The first gun, the generator, produces the primary pulse (Figure 4.10.1 and 4.10.2). Depending on the used chamber volume, which can be adjusted by volume reducers, the bubble can be significantly suppressed by triggering the second part of the gun, the injector, after a delay if the bubble collapses. Operation of this gun is very simple, especially as it is unnecessary to pressure it up prior to deployment.

The following GI-Gun configuration has been used:

Mode	Generator Volume (in^3)	Injector Volume (in^3)	Delay (ms)	Discharge Port
True GI	105	105	27	large

The GI-gun was operated through the LongShot seismic source controller where ports 7 and 8 were reconfigured for GI-gun mode. A special software layout, provided by RealTime through GEOMAR accounts, enabled the use of the Prakla gun array (see Reports on projects HYDGAS & GEOPECO) and the GI-gun without major reconfiguration of the control unit. The attached shot break hydrophone was used for automatic shot point adjustment. With the LongShot sensor display, the near field source wavelet was controlled and remained constant. A single gun hanger (provided by the Geophysics department of the University of Bremen) towed the GI-Gun approximately 10 m behind the ship's stern in a water depth of 1.5 m. Towing depth remained stable due to a fender on top of the gun hanger. Following the recommendation of the Sodera handbook, the gun was operated at a pressure of 140 , the nominal available pressure from the distribution station on board SONNE. For future use it is most advisable to increase the available pressure to 200 bar which is the nominal pressure for these modern gun types. Unfortunately the piston seemed to be damaged short before the end of the cruise. Due to the lack of replacement shooting was continued with a single Prakla type airgun of similar frequency range.

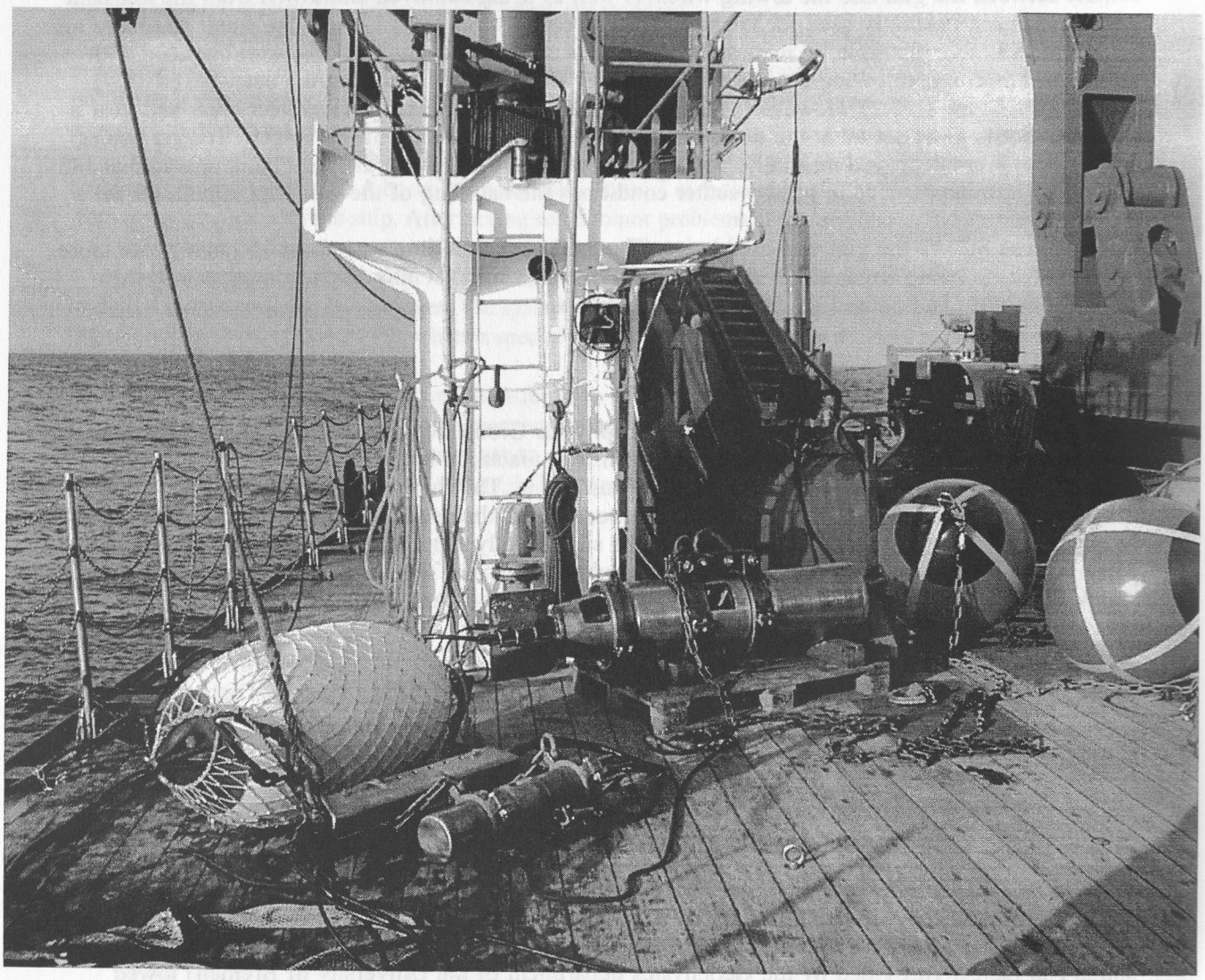

Figure 4.10.1 The 32 liter Bolt PAR 400 Airgun (large gun) and the GI gun (small gun attached to white buoy in the foreground) on deck between deployments.

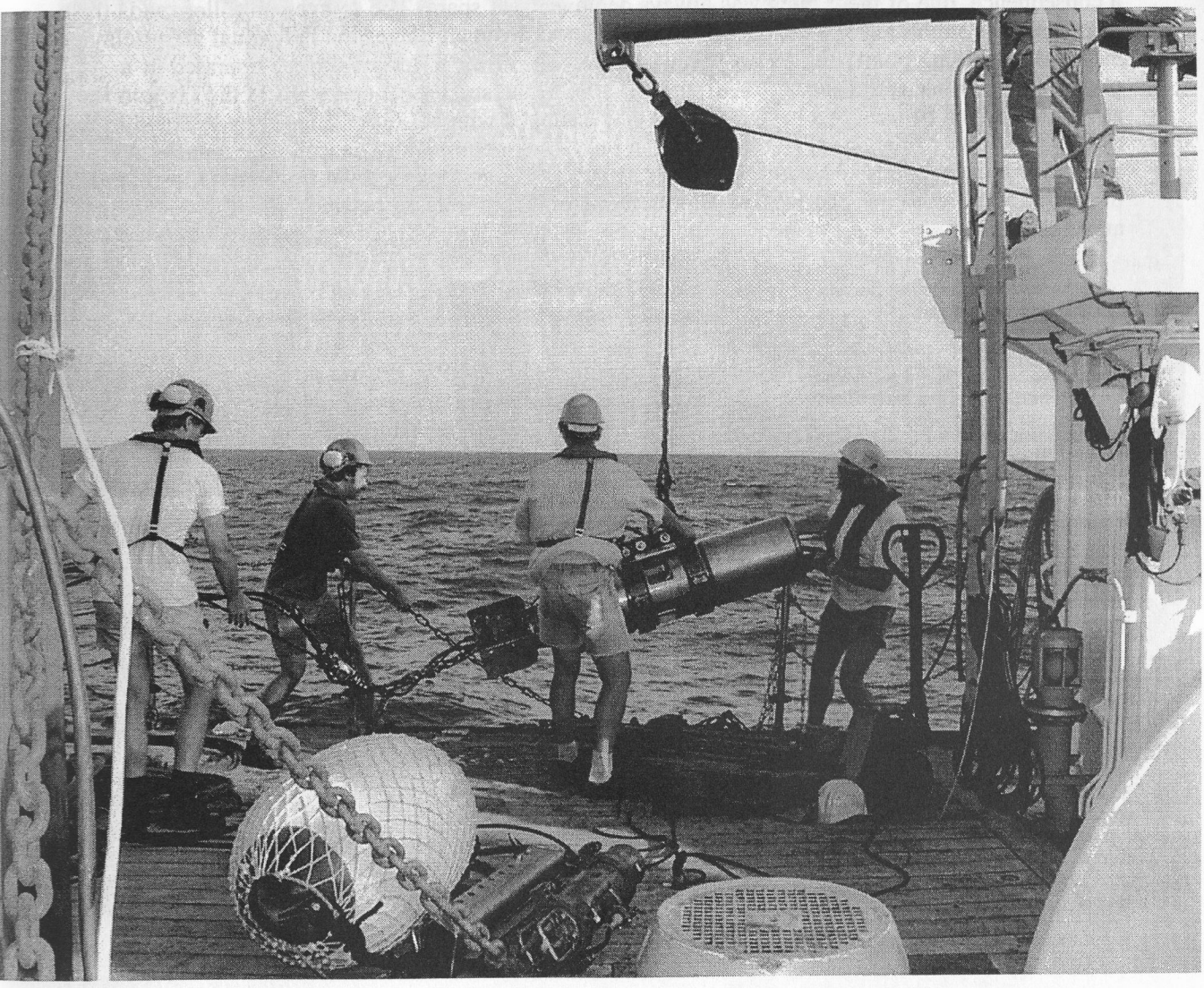

Figure 4.10.2 Bolt PAR 400 Airgun during deployment In the center the 32 l. Bolt airgun is shown during deployment operation. Handling and towing became more convenient by the modification of the port side assitant crane (at top border of picture). From this view the need of an additional rail in the area of deployment operation becomes immediately obvious. The rail will secure the seaman and the gun during pressure fill and release. In the foreground the Sodera GI gun can be seen attached to the buoy.

PRAKLA Airguns

In addition to the high and low frequency guns, a small airgun array was available to be used with the airgun slide at port aft of R/V Sonne. The array comprised of 7 Prakla VLA and VLF type guns, with volumes of 2.0 l, 1.6 l, 2 x 0.65 l, and 3 x 0.33l (Figure 4.10.3). Parts of the array were provided on loan from the Institut für Geowissenschaften, Abteilung Geophysik, Universität Kiel. Single gun volumes and separations had been tested during earlier cruises (e.g. PAGANINI, HYDGAS) with RV SONNE. Towing depth of the array was 2.5 m when three fenders were used as floatation buoys to carry the array. Shooting of the array was synchronized using a LongShot source controller with two FourShot power supplies. Two ports of the power supplies were reconfigured to operate the GI-gun, while the remaining 6 ports were used for the Prakla array. As a consequence, one of the 7 guns was always deployed as a spare. The source controller reads the sensor signals submitted from each gun at shot release. It synchronizes the individual shot delays to the same aiming point with an accuracy of 1 ms. The array is designed to be operated at a pressure of 140 bar and a shot interval of 10 s. Due to the successful operation of the GI gun the array need not to be used this time. A single gun equipped with a 1.6 l chamber was selected at the end of the cruise to replace the broken GI gun providing a comparable range of frequency. As expected the remaining bubble turned out to be stronger than those known from the GI gun and the entire array. Still the gun worked fine in terms of a compromise between quick replacement and signal quality.

External Trigger

The trigger signal was supplied from the ships *Ashtech* GG24 GPS/Glonass receiver, and was available in the Geology Lab and the Seismic Lab. The receiver can provide a one millisecond long 5 V-TTL pulse at intervals between 0.2 and 999 s. The impulse should be stable to within the accuracy of the GPS Time, which is 70 nanoseconds. The impulse was delivered to the *Longshot* trigger box, which can handle different guns (G-gun, GI-Gun, Bolt and Prakla guns). The shotbreaks, necessary for subsequent data processing and instrument location, were stored on a MBS recorder and displayed in real time to double check. For this process the same time basis was used that is used for the OBH (see chapter 4.4) and the trigger signal was converted into a 5 V TTL pulse of 250 ms length by a circuit provided from the ships technical support staff (WTD). Exact position calculation for the shot time should be done by later post-processing using shot time and UTC time values stored with DGPS coordinates in the ship's data base. As kwon from earlier cruises the coordinates stored within the data base were provided by the *Atlas ANP 2000* system, which does not copy the exact GPS time values but adds time stamps of its internal uncontrolled clock to the high precision coordinates of the DGPS system. Accuracy of the time values mainly depends on the operators skills by manually setting the ANP clock to GPS time. This is clearly a somewhat conservative method compared to the efforts of precise positioning. To enable the most accurate GPS related time stamps within the ANP system prior to each seismic survey the system operates were informed to reset the ANP.

Figure 4.10.3 The array of Prakla Airguns. One of these (volume 1.6 litre) was deployed in the Max-Moritz area when the GI-gun had broken down.

4.11 OBH/OBS Data Processing

The OBH/S data recorded in continuous mode on the MLS and MBS units have to be converted into standard trace-based SEG-Y format for further processing. The necessary program structure was mainly taken from the existing REFTEK routines and modified for the OBH requirements and GEOMAR´s hardware platforms.

The flow chart shown in Figure 4.11.1 illustrates the processing scheme applied to the raw data. A detailed description of the main programs follows below:

send2pas

For the PC-cards used with the MBS and MLS recorders, data expansion and format conversion into REFTEK data format is performed using a DOS/Windows based PC. The program send2pas reads data from the flashcards used during recording. To correct the filter delays during analog/digital conversion (up tp 44ms) the option tbc_ok in send2pas was used. Decompressed data are written onto the PC's hard disk using PASSCAL data format. Either 16 or 32 bit storage is available. After ftp transmission to a SUN workstation, ref2segy and all other software can be used to handle and process the data files and store them as SEG-Y traces.

While processing the MLS recordings many time slips of one sampling interval were detected by the send2pas software, typically at a rate of one time slip every 1-2 hours. The time slips are caused by mismatch of the actual sampling rate of the MLS recorder compared to the desired sampling rate. This mismatch arises because the clock rate of the crystal oscillator in the MLS recorder is temperature dependent (Klaus Schleisiek, SEND GmbH, pers. comm.). The temperature dependence is known and corrected for in the determination of the system time, but for performance reasons the sampling pulses are directly generated from the oscillator signal without any time correction. The send2pas routine detects when the accumulated inaccuracies of the sample rate cause an effective timing error of one sample, but only reports and does not correct the "time slip".

The resulting total time error was up to 200 ms for the wide-angle profiles, showing clearly the necessity of a special time slip correction for the MLS data. After careful analysis of the problem, we concluded that the best way to address the time slip timing error in the wide-angle data is to add the time slips reported in the send2pas logfile, and regard the time slip total as an extra skew contribution which later in the processing flow is corrected within the dat2segy program (see below, note that the sign of skew and time slips are opposite, i.e., a negative sum of time slips corresponds to a positive skew).

ref2segy

The ref2segy program converts the output of send2pas to a pseudo SEG-Y trace consisting of one header and a continuous data trace containing all samples, as used by the PASSCAL suite of seismic utility programs. For each channel (normally pressure, vertical velocity, and velocity along two mutually perpendicular horizontal directions for OBS; pressure for OBH) one file is created with the name derived from the start time, the serial number of the Methusalem system, and the channel number. The file size of the pseudo-SEGY file is directly related to the recording time. For instance, a recording time of one hour sampled at 200 Hz (16 Bit) will produce a file size of 1.44 MB per channel. A record with two channels and a recording time of two days will produce a total data volume of 70 MB.

merge

If an error occurs during the download process, the ref2segy program has to be restarted. This may lead to several data files with different start times. Merging these files into a single file is performed by the merge program. Gaps between the last sample and the first sample of the consecutive data traces are filled with zeros. Overlapping parts are cut out.

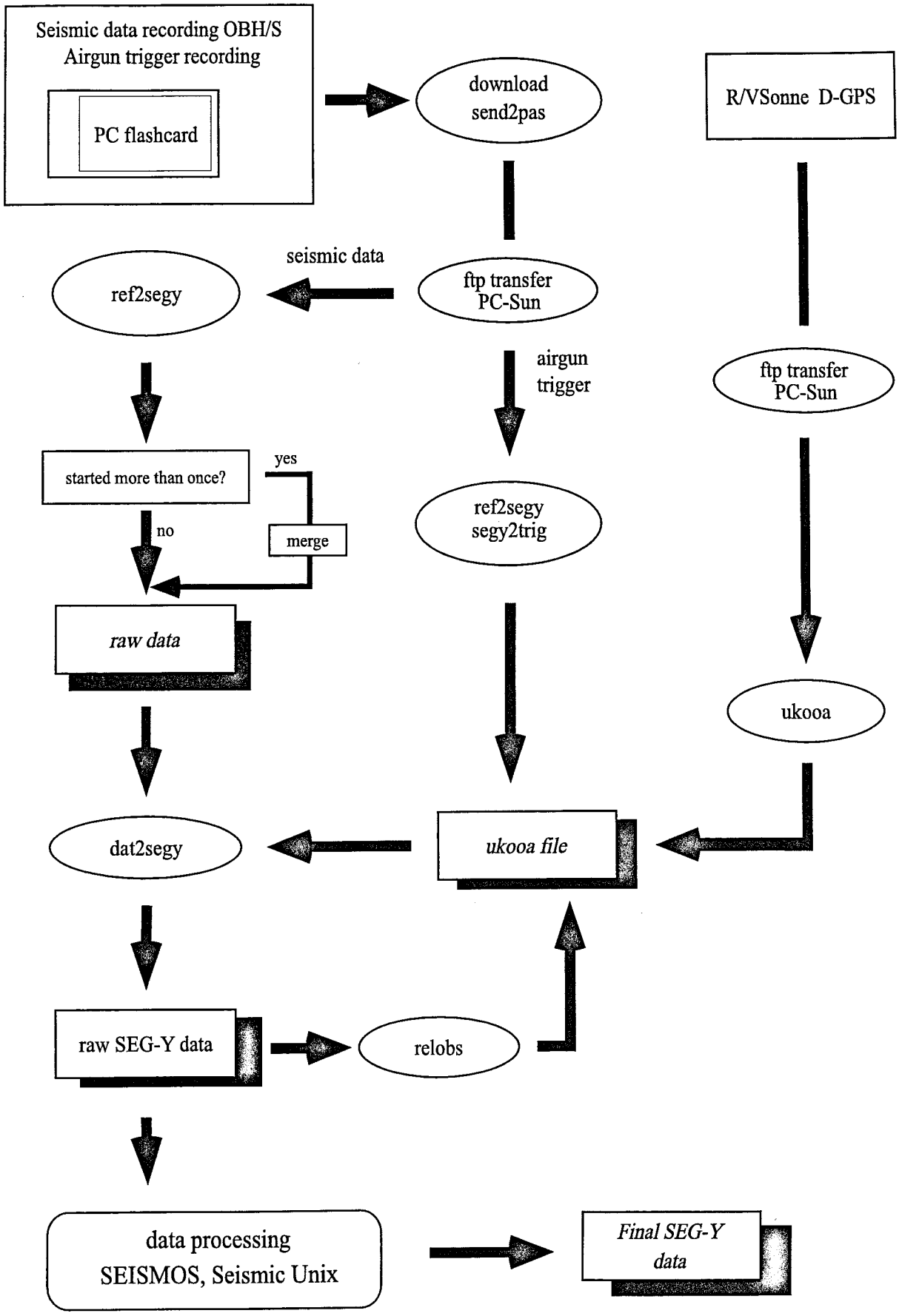

Figure 4.11.1: Processing flow of OBH/S data from raw data to SEG-Y records.

pql

pql (Passcal Quick Look) is a simple display program for continuous seismic data. Its interactive zooming capability allows a rapid inspection of data quality.

segy2trig

The trigger signal, provided by the airgun control system, is recorded on an additional MBS unit during the shooting period. The trigger data are treated similarly to regular seismic data and downloaded to the hard disk via the send2pas (including the tbc_ok option) and ref2segy programs. Then, the segy2trig program detects the shot times in the data stream by identifying the trigger signal through a given slope steepness, duration and threshold of the trigger pulse. The output is an ASCII table consisting of the shot number and the shot time. Accuracy of the shot time is one of the most crucial matters in seismic wide-angle work, and must be reproduced with a precision of a few ms. Due to this demand the shot times have to be corrected with the shift of the internal recorder clock. Additionally, the trigger file contains the profile number, the start/end time of the profile and the trigger recording. The shot times are part of the ukooa file, which links them with the coordinates of the source and the hydrophones.

ukooa

The ukooa program is used to establish the geometric database by calculating the positions of sources at any given shot time and offset from the ship. The source is placed on the ship track using simple degree/meter conversions and then written to a file in UKOOA-P84/1 format. Corrections for offsets between antenna and airguns as well as consistency checks are included. This file will be used when creating a SEG-Y section via the dat2segy program. The program requires the trigger file to contain the shot times, the ship's navigation, and a Parameter file containing information for the UKOOA file header as basic input information.

dat2segy

The dat2segy program produces standard SEG-Y records either in a 16 or 32 bit integer format by cutting the single SEG-Y trace (the ref2segy output) into traces with a defined time length based on the geometry and shooting time information in the ukooa file In addition, the user can set several parameters for controlling the output. These parameters are information about the profile and the receiver station, number of shots to be used, trace length, time offset of the trace and reduction velocity (to determine the time of the first sample within a record). Also the clock drift of the recorder (skew) is taken into account and corrected for. For the MLS data the total time error resulting from the observed time slips described above was subtracted from the clock drift value. The final SEG-Y format consists of the file header followed by the traces. Each trace is built up by a trace header followed by the data samples. The output of the dat2segy program can be used as input for further processing with GEOSYS, SEISMOS or Seismic Unix (SU).

relobs

Because of drifting of the OBH and OBS instruments during deployment and errors in the ship's GPS navigation system, the OBH positions may be mislocated by up to several 100 m. Since this error leads to asymmetry and incorrect traveltime information in the record section, it has to be corrected. This is accomplished with the program relobs.
For input, the assumed OBH location, shot locations and the picked traveltimes of the direct wave near to its apex are needed. To simplify the picking a static correction with a hyperbolic equation was performed to flatten the direct wave. This yields a much more coherent direct arrival which would normally suffer from strong spatial aliasing in the uncorrected section making it difficult to track. By shifting the OBH position, relobs minimizes the deviation between computed and real travel times using a least mean square fitting algorithm (assuming a constant water velocity).

Beside these main programs for the regular processing sometimes additional features are needed for special handling of the raw data:

divide

The program divide cuts the raw data stream into traces of a given length without offset and time information, storing the output in SEG-Y format. The routine is useful for a quick scan of the raw data or if a timing error has occurred.

segyhdr

The routine segyhdr prints all the header values of the raw data on the screen.

segyshift

Segyshift modifies the time of the first sample, allowing the whole raw data trace can be shifted by a given value. This is very useful when shifting the time base from Middle European Time to Greenwich Mean Time or any local time. Because of recording problems, the data sometimes show a constant time shift, which can be corrected as well with segyshift.

castout

The program castout allows the user to remove out a specified time window from the raw data stream. When the shooting window is much smaller than the recording time, one can reduce the data volume by cutting out only the useful information. This will reduce the demand on disk space.

OBH/OBS data examples

As data examples, four component (P, X1, X2 and Z) OBH/OBS recordings are shown for two different sources, a GI-gun (Figures 4.11.2-4.11.9) and a Bolt-gun (Figures 4.11.10-4.11.17) and for two different seismometer types, an Owen 4.5Hz (Figures 4.11.2-4.11.5 and 4.11.10-4.11.13) and an Owen 30Hz (Figures 4.11.6 - 4.11.9 and 4.11.14 - 4.11.17). On profile 1 the low frequent converted shear waves of the GI-gun signals are most significant on the an Owen 4.5Hz seismometers (compare Figure 4.11.5 and 4.11.9) whereas the primary high frequent compressional wave are most clearly on the Owen 30Hz seismometer. To record the low frequent signals from the Bolt-gun e.g. Profile 9 without losing the lower frequencies due to the seismometer characteristics, an Owen 4.5Hz seismometer would be adequate (compare Figure 4.11.13 and 4.11.17).

Probable S-wave arrivals are observed clearly on most of the horizontal channels (e.g. Figures 4.11.3, 4.11.7, 4.11.8, 4.11.11) of both geophone packages, indicating the suitability of the GEOMAR OBS for S-wave studies at a variety of frequencies (different sources).

Data archiving

Data recorded with the MBS/MLS recorder on flash discs were transferred via a PC to a SUN workstation. On the workstation they were transformed into a so-called PSEUDO-SEGY format. After navigation data had been merged and SEGY formatted traces with the appropriate header words had been created, the data were also archived.

Data exchange

For the exchange of the OBH/OBS data, the SEGY-format on disk with a Sun tar-format was chosen. The raw segy data is in Integer2 format with trailer bytes between the record structure of SEGY. For UTM transformation into Cartesian co-ordinates use: WGS84 spheroid, central meridian 76 0. 0. W, southern hemisphere.

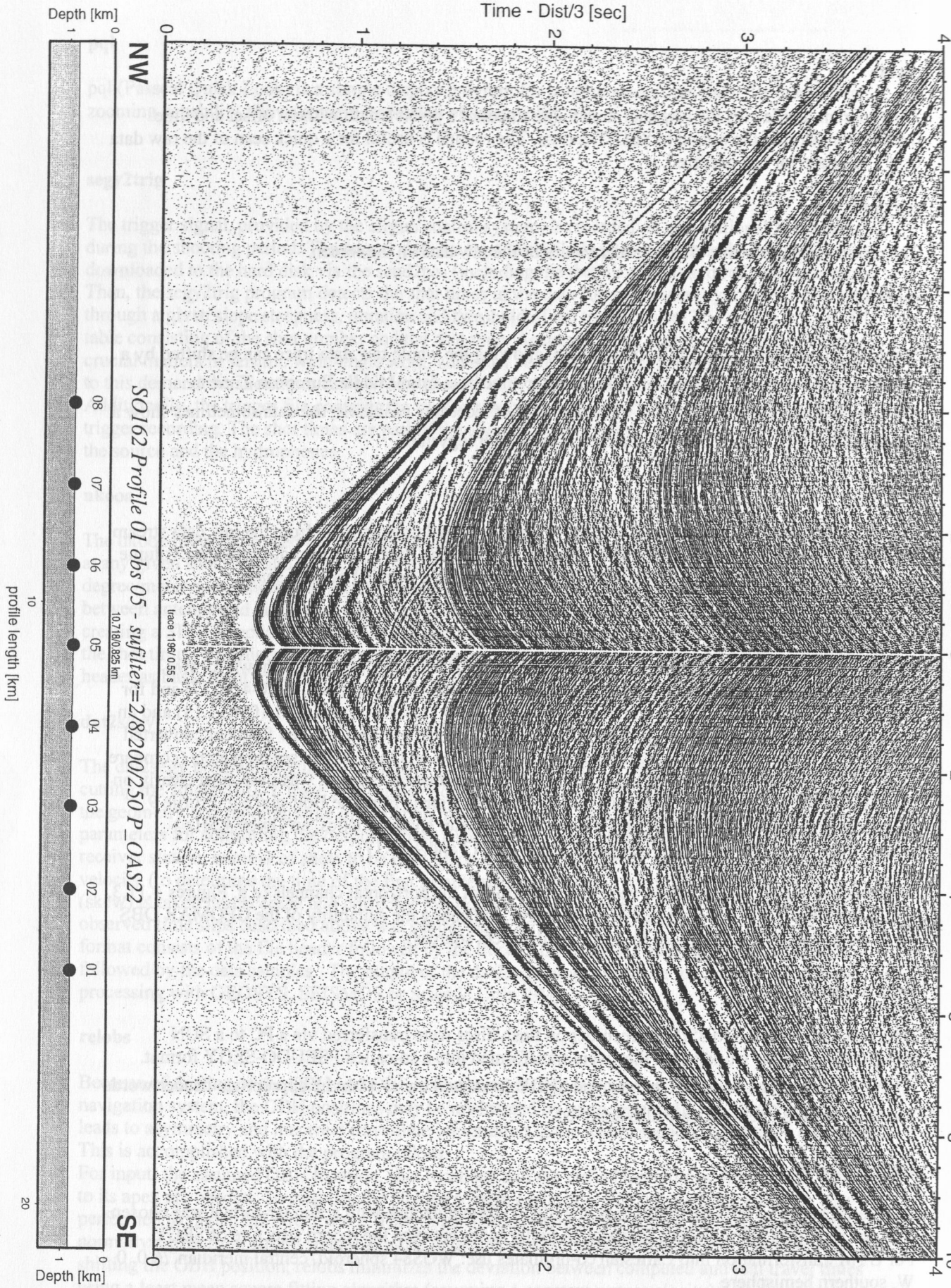

Figure 4.11.2 Record section from obs 05 P_OAS22, Profile 01 (GI-gun).

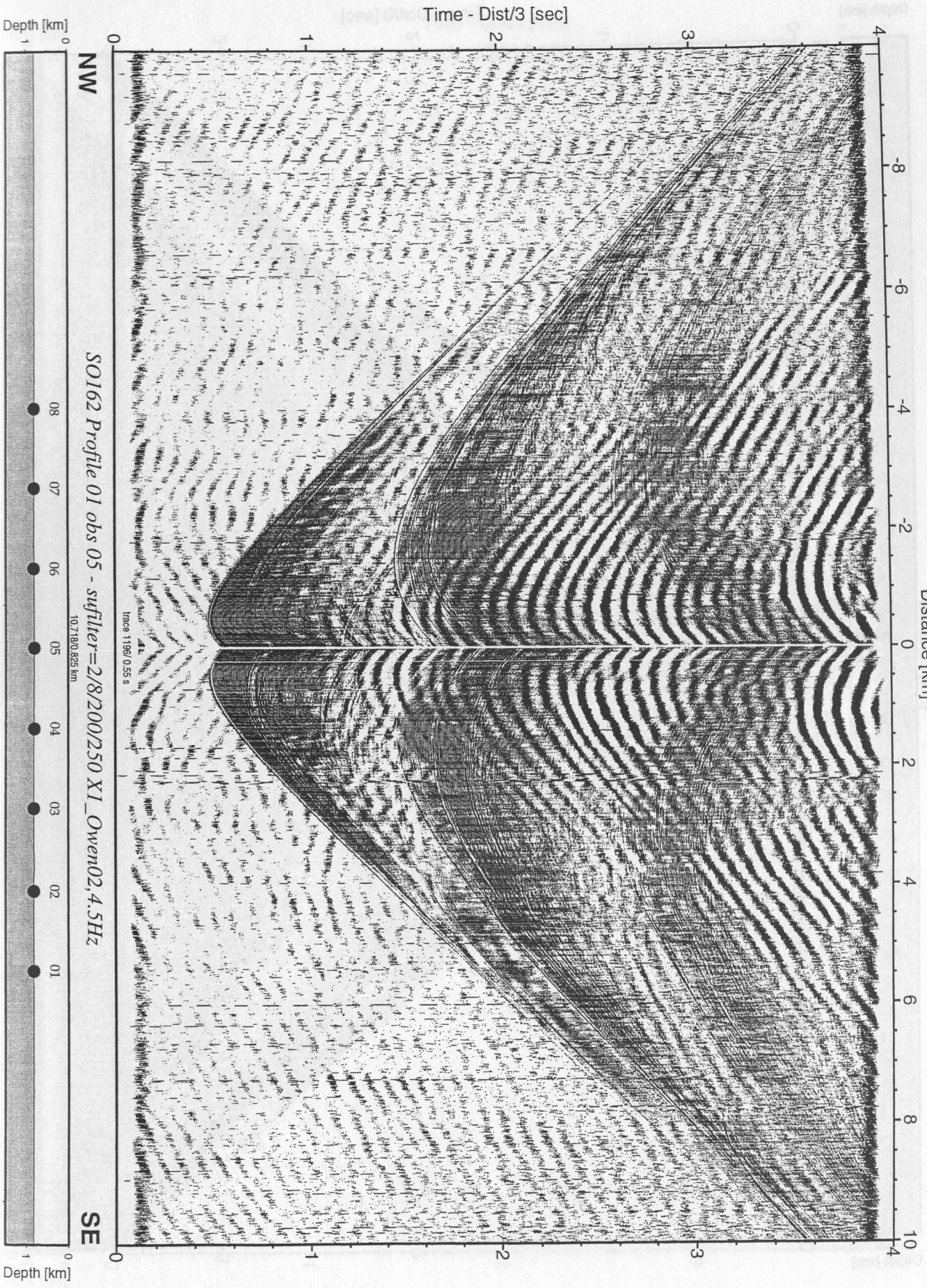

Figure 4.11.3 Record section from obs 05 X1_Owen02,4.5Hz, Profile 01 (GI-gun).

Figure 4.11.4 Record section from obs 05 X2_Owen02,4.5Hz, Profile 01 (GI-gun).

Figure 4.11.5 Record section from obs 05 Z_Owen02,4.5Hz, Profile 01 (GI-gun).

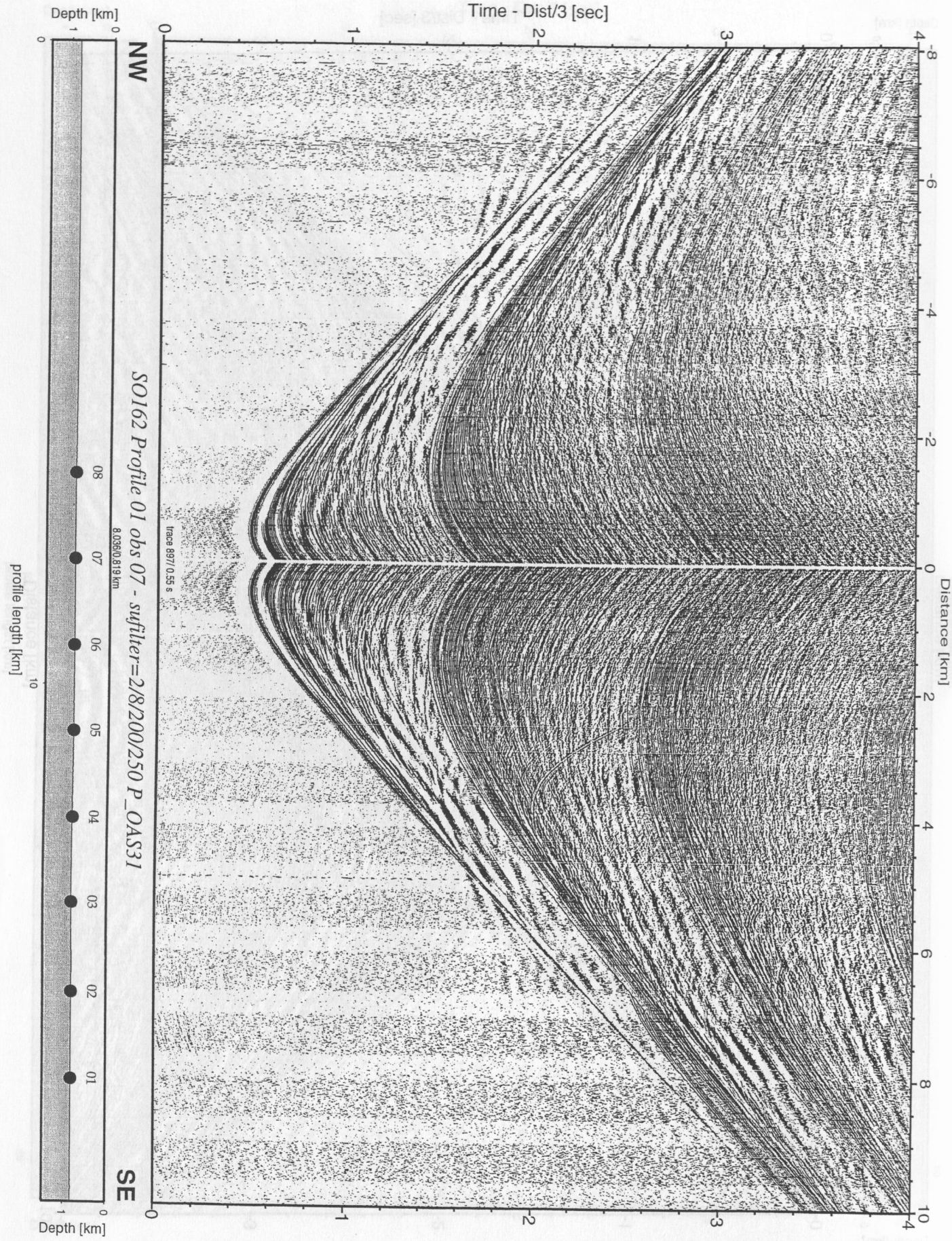

Figure 4.11.6 Record section from obs 07 P_OAS31, Profile 01 (GI-gun).

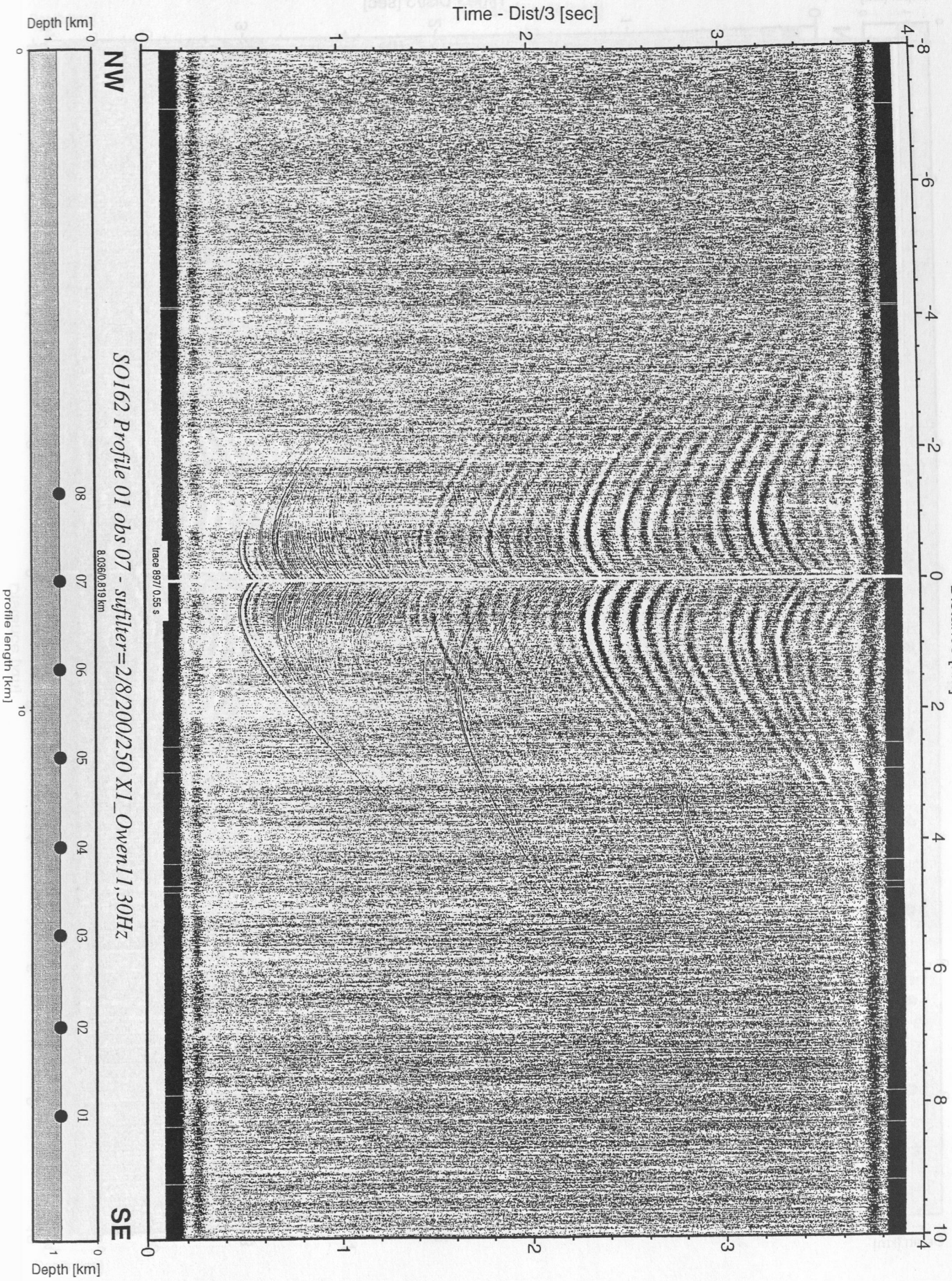

Figure 4.11.7 Record section from obs 07 X1_Owen11,30Hz, Profile 01 (GI-gun).

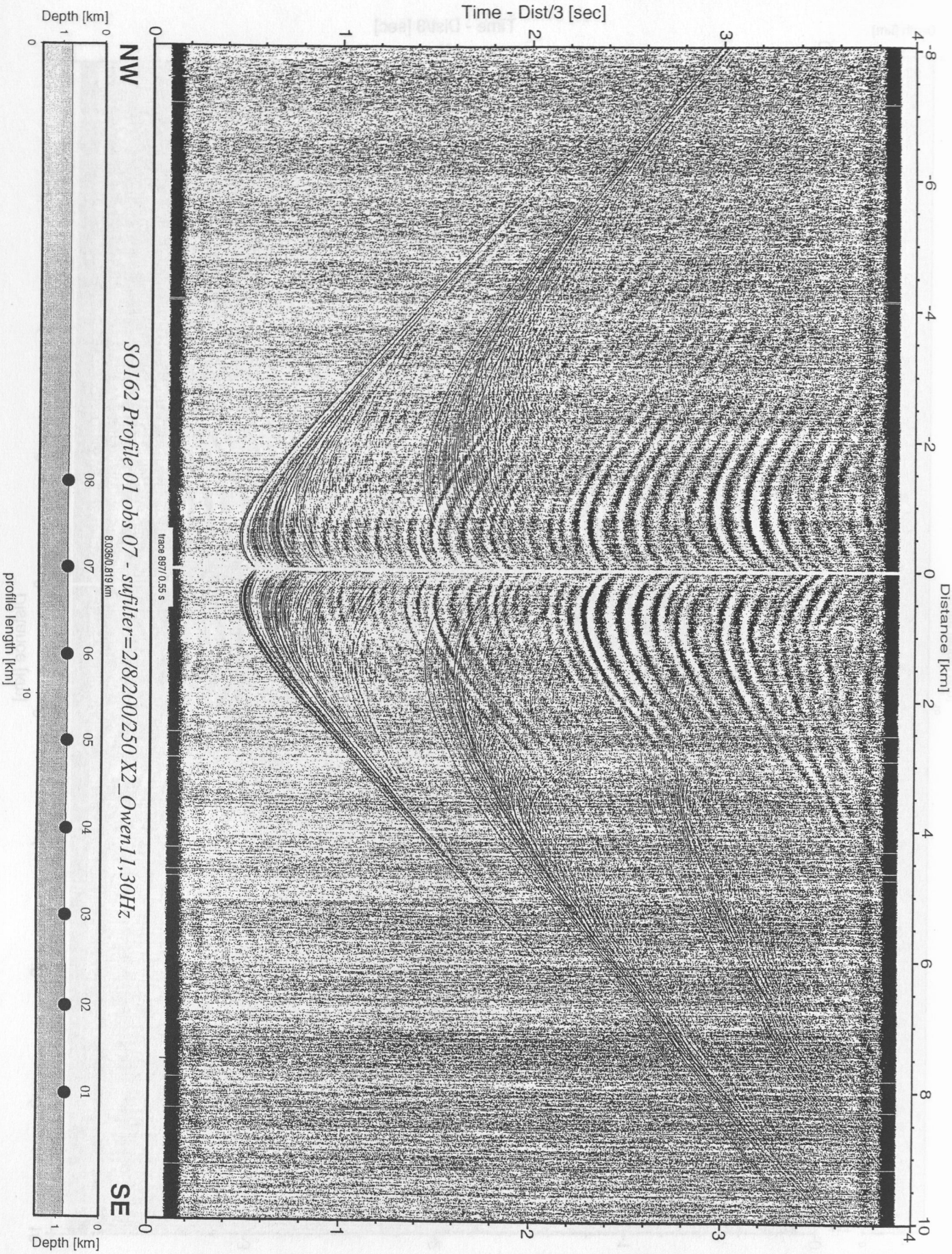

Figure 4.11.8 Record section from obs 07 X2_Owen11,30Hz, Profile 01 (GI-gun).

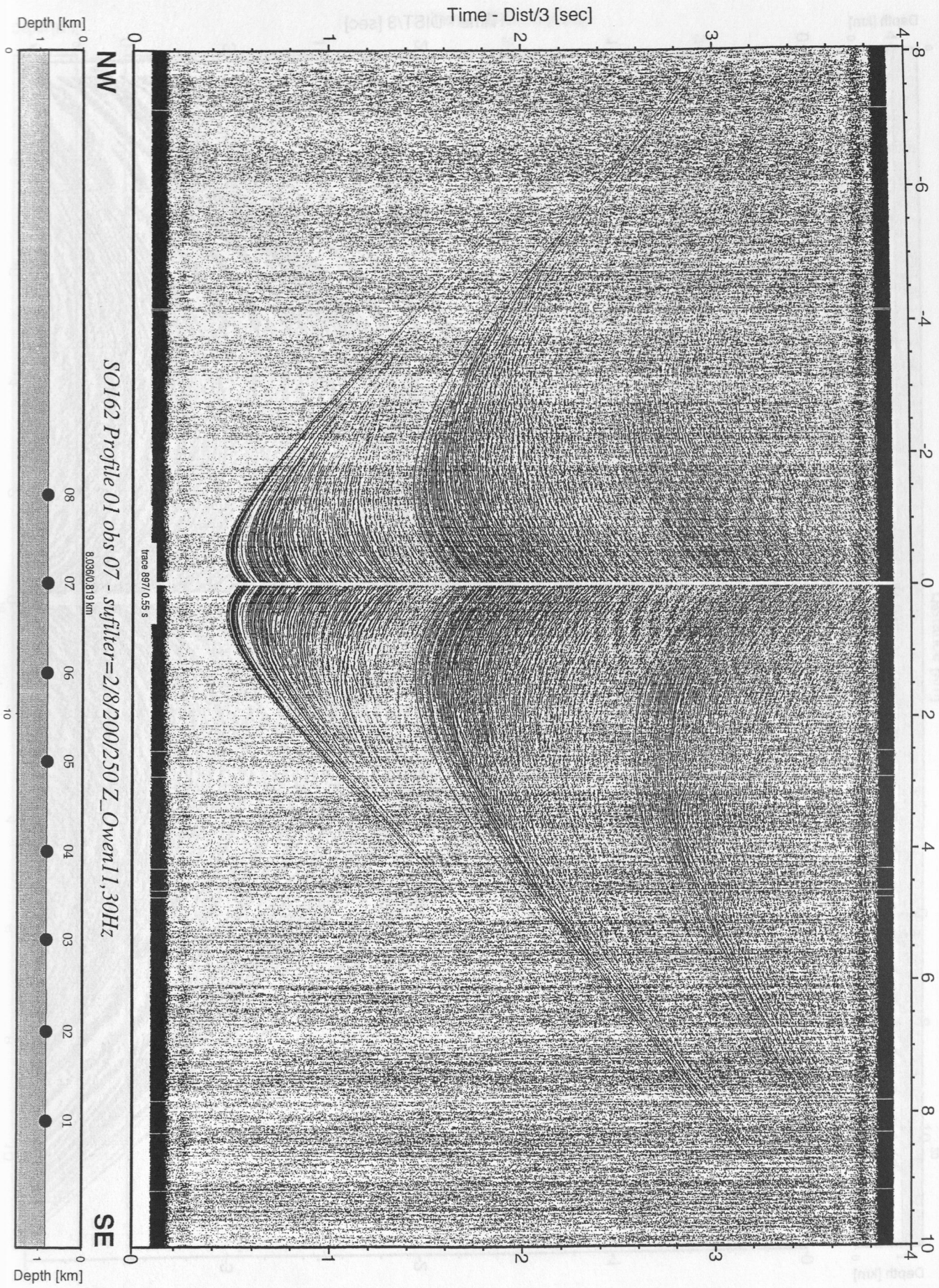

Figure 4.11.9 Record section from obs 07 Z_Owen11,30Hz, Profile 01 (GI-gun).

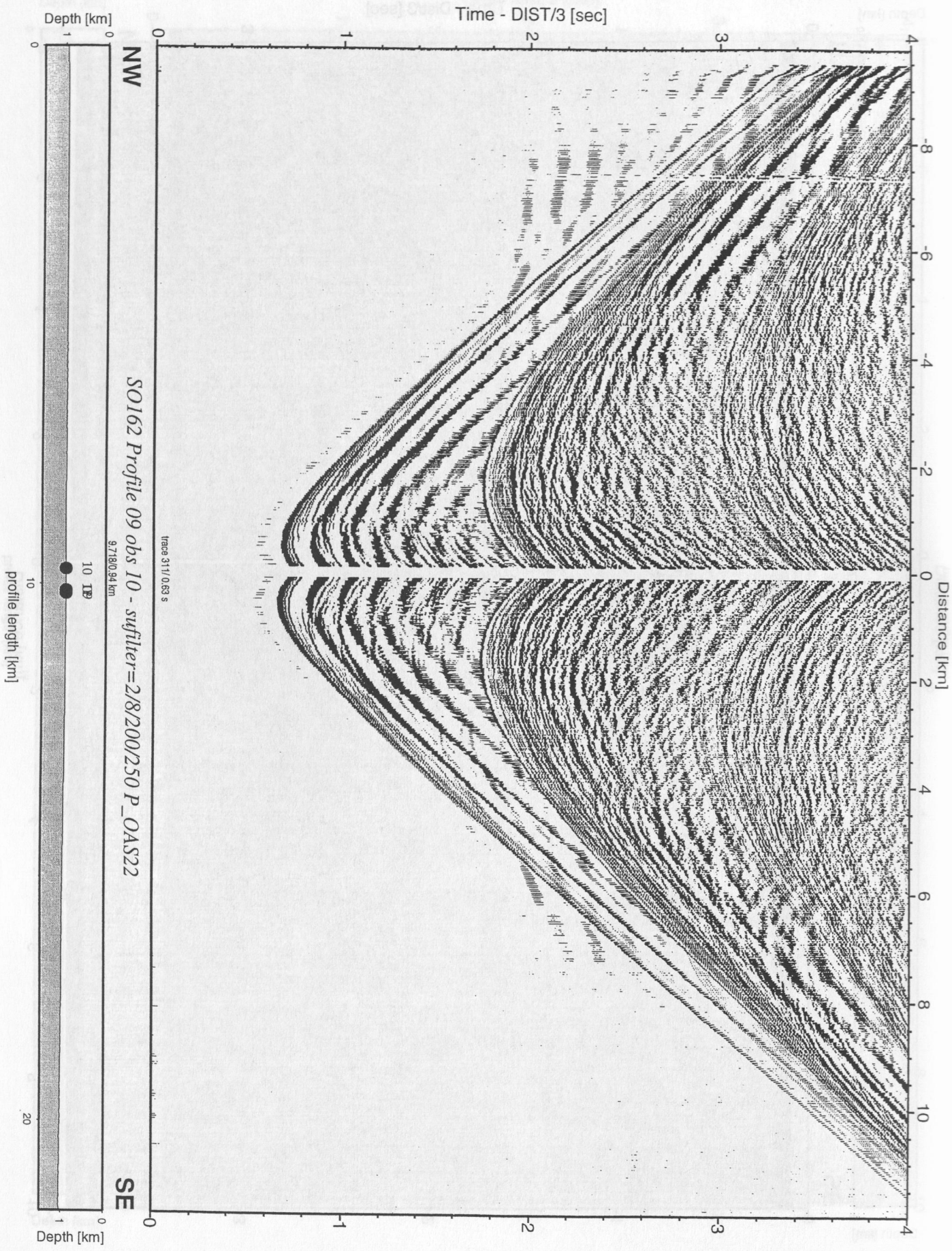

Figure 4.11.10 Record section from obs 10 P_OAS22, Profile 09 (32 l. Airgun).

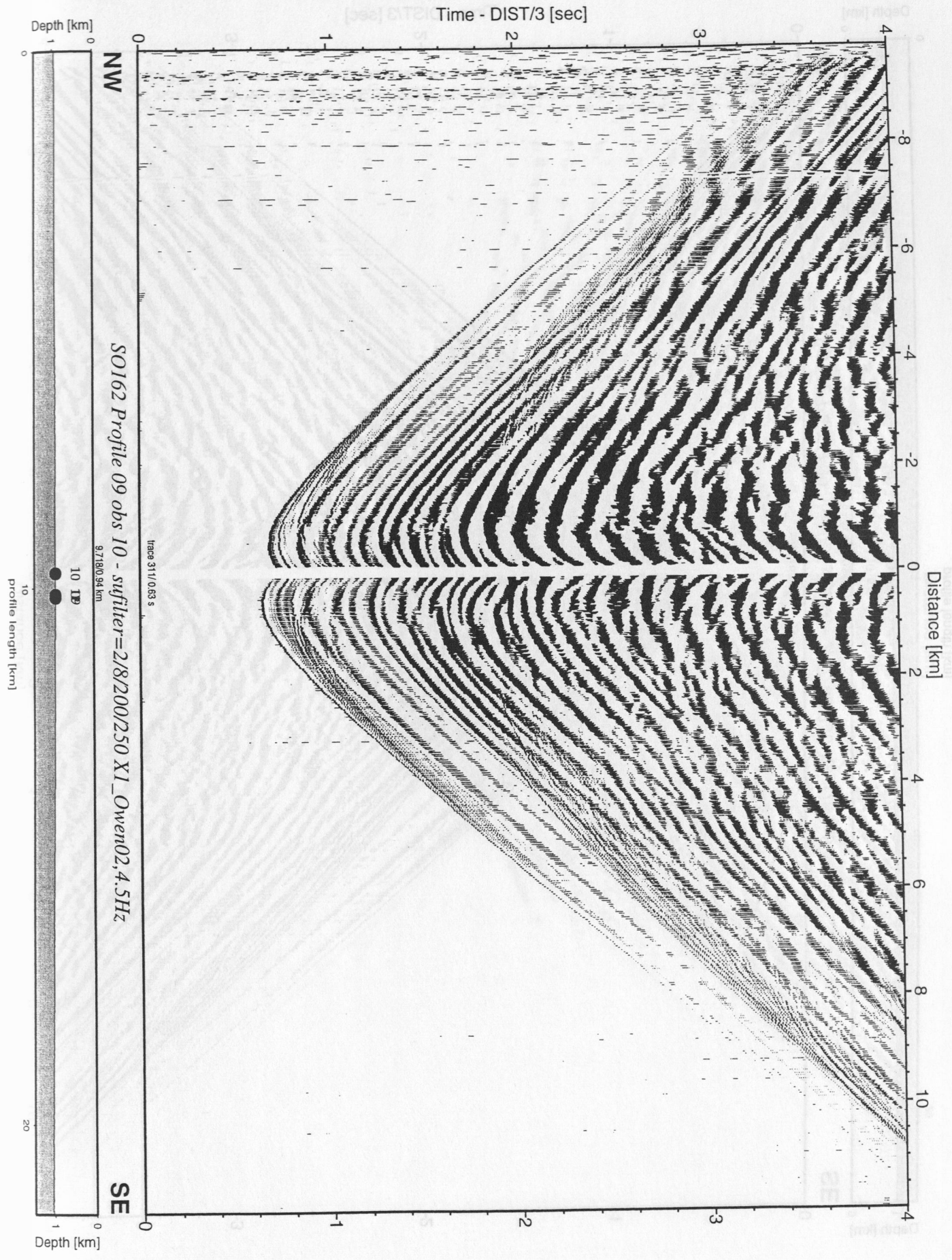

Figure 4.11.11 Record section from obs 10 X1_Owen02,4.5Hz, Profile 09 (32 l. Airgun)

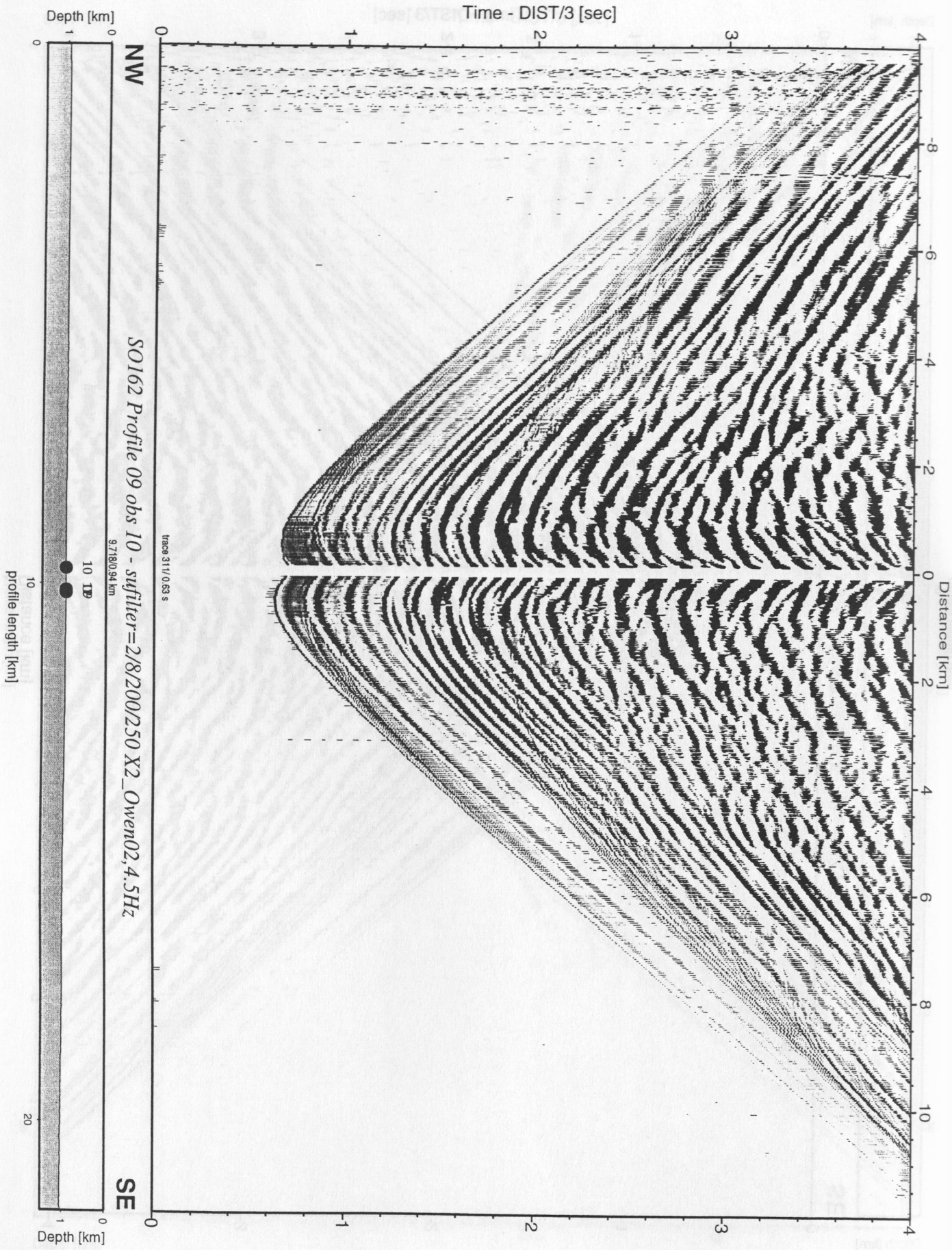

Figure 4.11.12 Record section from obs 10 X2_Owen02,4.5Hz, Profile 09 (32 l. Airgun)

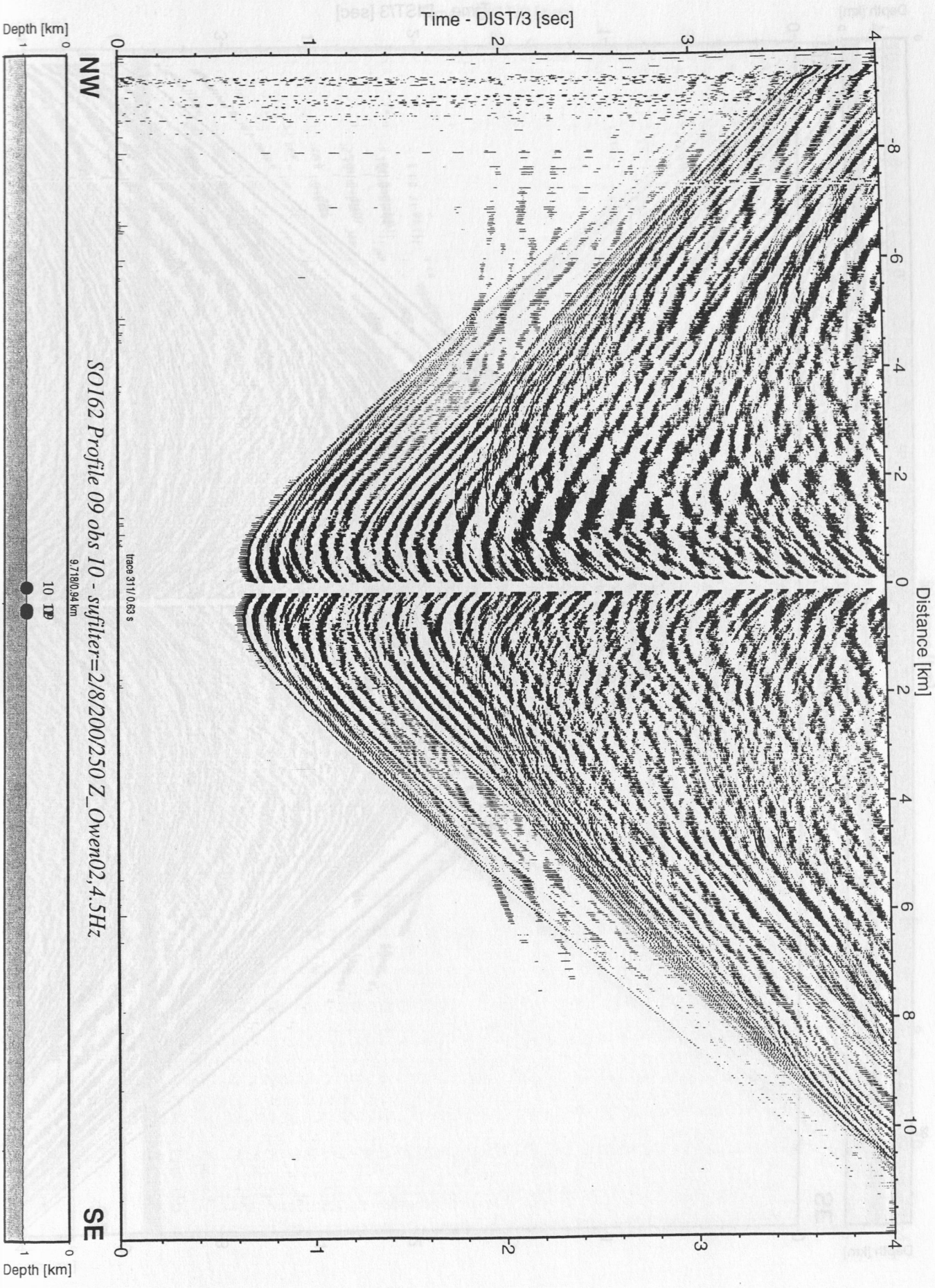

Figure 4.11.13 Record section from obs 10 Z_Owen02,4.5Hz, Profile 09 (32 l. Airgun).

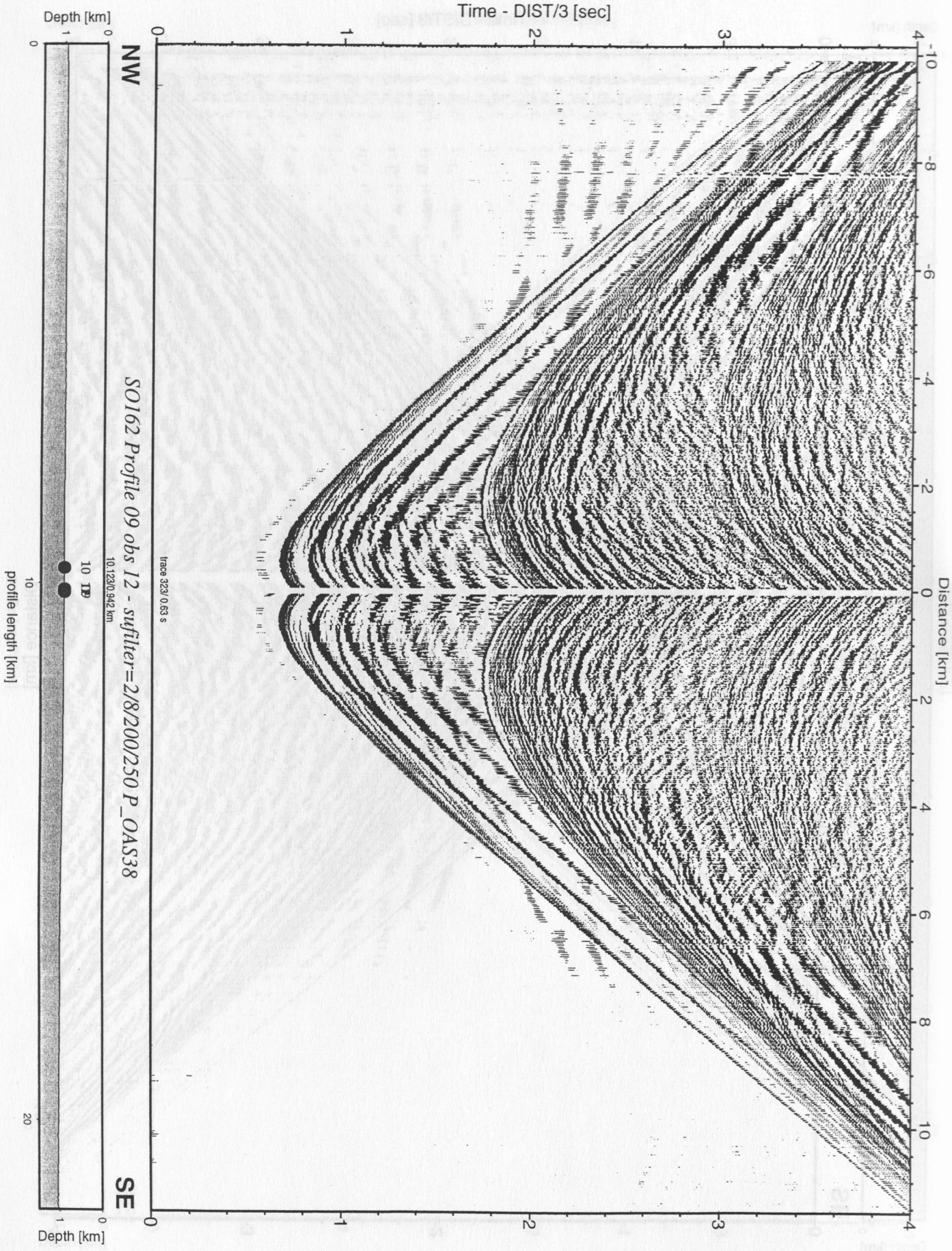

Figure 4.11.14 Record section from obs 12 P_OAS38, Profile 09 (32 l. Airgun).

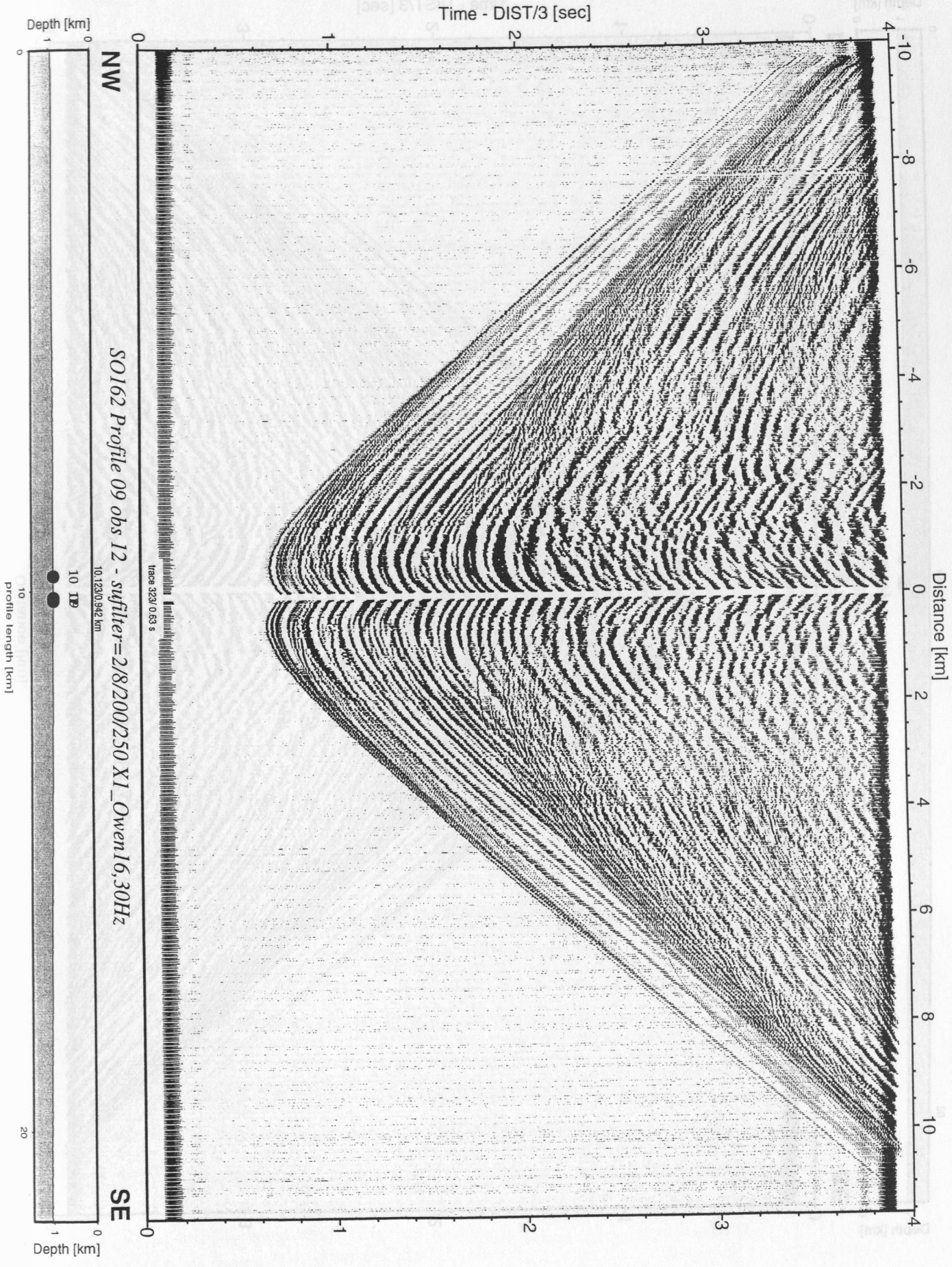

Figure 4.11.15 Record section from obs 12 X1_Owen16,30Hz, Profile 09 (32 l. Airgun).

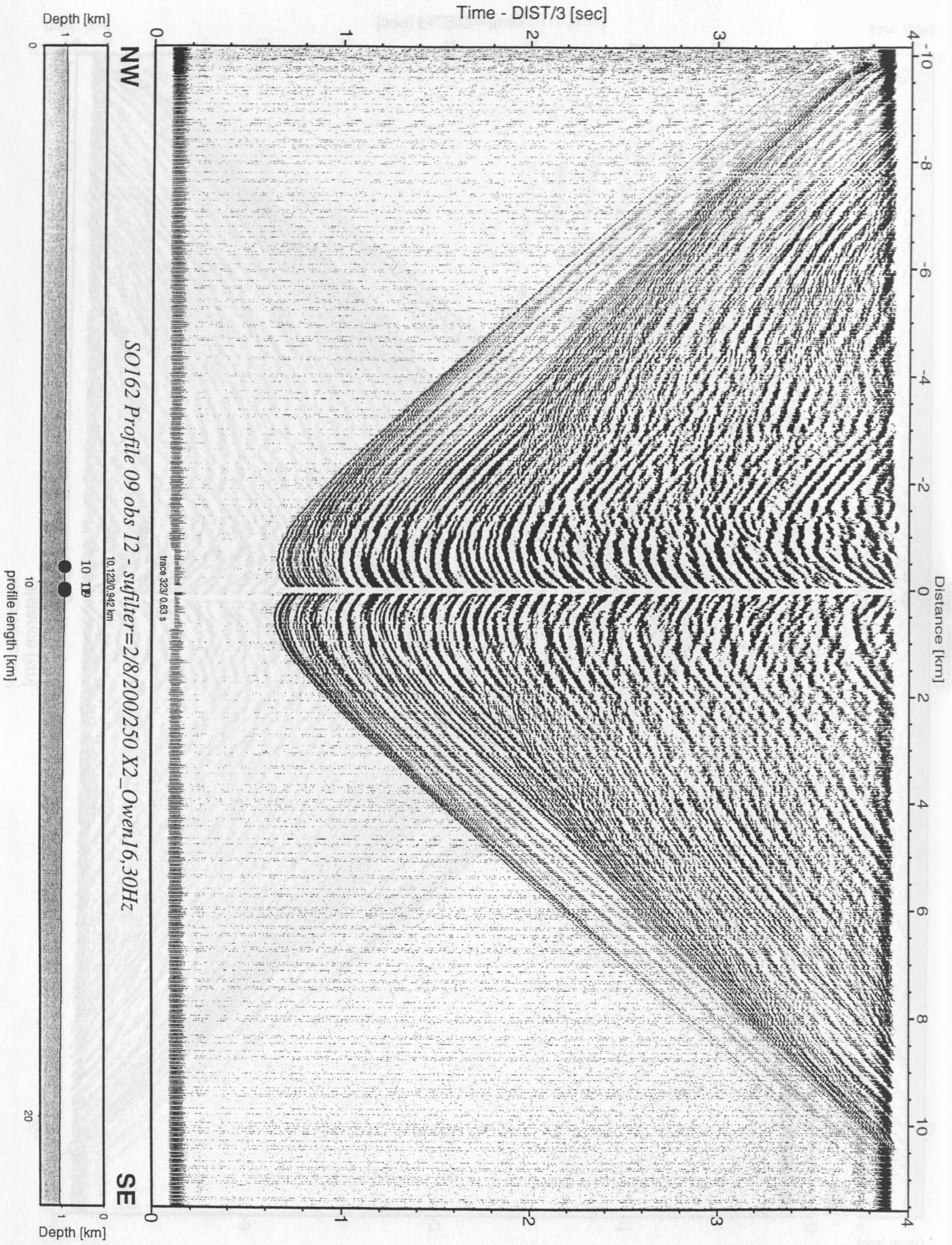

Figure 4.11.16 Record section from obs 12 X2_Owen16,30Hz, Profile 09 (32 l. Airgun).

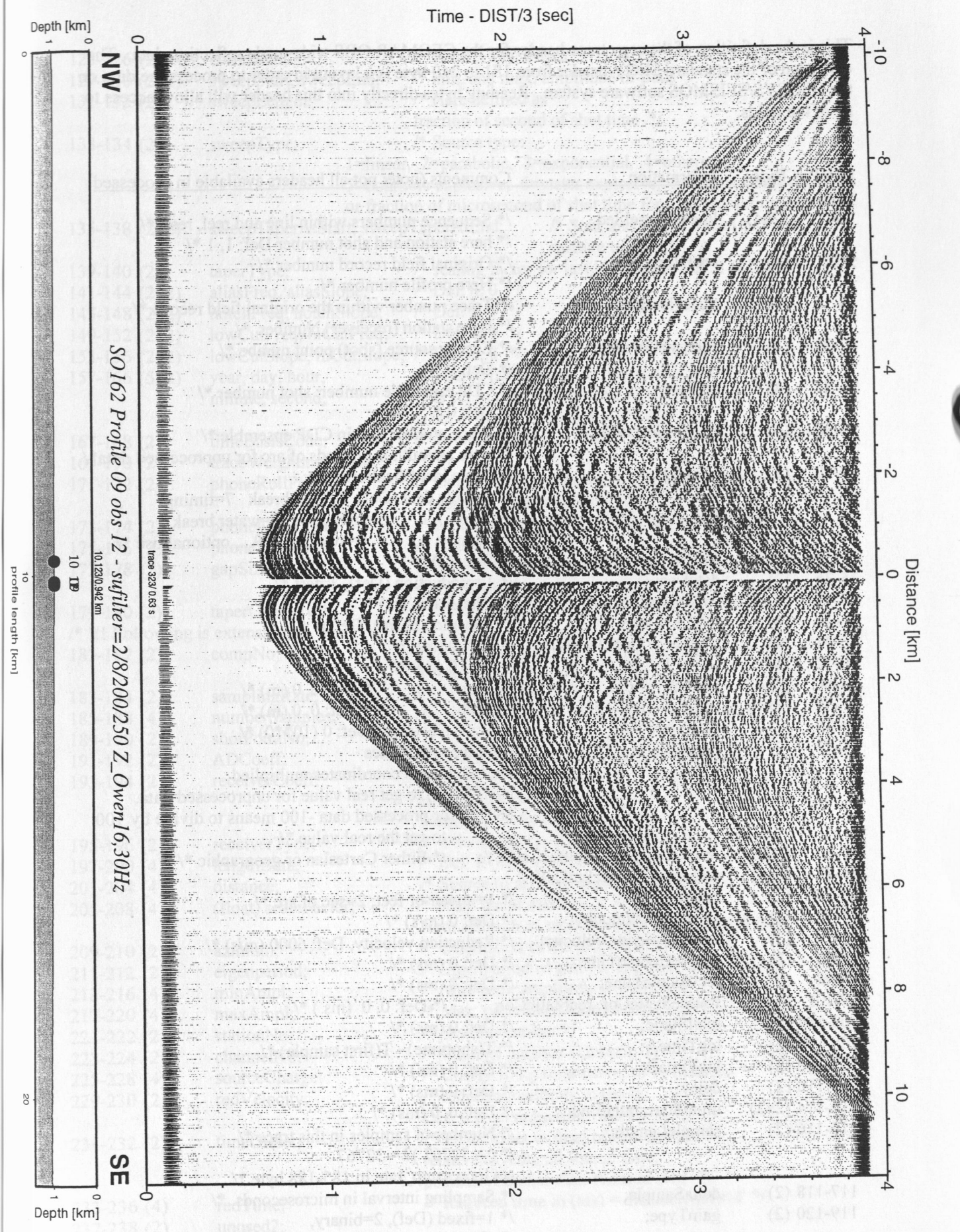

Figure 4.11.17 Record section from obs 12 Z_Owen16,30Hz, Profile 09 (32 l. Airgun).

This is the definition of the segy trace header for the GEOMAR OBS wide-angle reflection data. The extension of the standard SEGY header from 181 to 240 byte is a layout in order to process the data on the GEOSYS/SEISMOS software system. Reading bytes directly into this header will allow access to all of the fields.

BytePos	Bytes	Information	Comments (note: not all headers available in processed data)
1-8	(2x4)	lineSeq, reelSeq;	/* Sequence numbers within line and reel, resp.*/ /* here station and shot number Def: 1, 1 */
9-12	(4)	profNumber;	/* Original field record number */ /* Here profile number */
13-16	(4)	traceNumber;	/* Trace number within the original field record.*/ /* Here station (receiver) Number */
17-20	(4)	energySourcePt;	/* Energy source (shot) point numbe */ /* Def: 0 */
21-24	(4)	cdpEns;	/* CDP ensemble number: shot number */ /* Def: 0 */
25-28	(4)	traceInEnsemble;	/* Trace number within CDP ensemble */ /* Here azimuth in seconds of arc for unprocessed data*/
29-30	(2)	traceID;	/* Trace identification code: 1=seismic data (Def) 4=time break 7=timing 2=dead 5=uphole 8=water break 3=dummy 6=sweep 9..., optional use */
31-34	(2x2)	vertSum, horSum;	/* Def: 1, 1 */
35-36	(2)	dataUse;	/* 1=production (Def), 2=test */
37-40	(4)	sourceToRecDist;	/* Distance in (m) */
41-44	(4)	recElevation;	/* Elevation in (m), Def: 0 */
45-48	(4)	sourceSurfaceElevation;	/* Def: 0 (m) */
49-52	(4)	sourceDepth;	/* Def: 0 (m) */
53-60	(2x4)	datumElevRec, datumElemSource;	/* Def: 0, 0 (m) */
61-68	(2x4)	sourceWaterDepth, recWaterDepth;	/* Def: 0, 0 (m) */
69-70	(2)	elevationScale;	/* Scale elevations Def: 0 (10**0) */
71-72	(2)	coordScale;	/* Scale coordinates Def: -2, means coordinates multiplied by 10**(-2) to get real value for unprocessed data. NOTE: for processed data -100 means to divide by 100 to get the real value */
73-80	(2x4)	sourceLongOrX, sourceLatOrY;	/* Either Cartesian or geographic */
81-88	(2x4)	recLongOrX, recLatOrY;	
89-90	(2)	coordUnits;	/* 1= meter or feet; 2=sec of arc */
91-92	(2)	weatheringVelocity;	/* Def: 0 (m/s) */
93-94	(2)	subWeatheringVelocity;	/* Reduction velocity, Def: 6000 (m/s) */
95-96	(2)	sourceUpholeTime;	/* Def: 0 (ms) */
97-98	(2)	recUpholeTime;	/* Def: 0 (ms) */
99-102	(2x2)	sourceStaticCor, recStaticCor;	/* Def: 0, 0 (ms) */
103-104	(2)	totalStatic;	/* Def: 0 (ms) */
105-106	(2)	lagTimeA;	/* T(shottime) - T(first sample) */
107-108	(2)	lagTimeB;	/* Def: 0 (ms) */
109-110	(2)	delay;	/* Def: 0 (ms) */
111-114	(2x2)	muteStart, muteEnd;	/* Def: 0, 0 (ms) */
115-116	(2)	sampleLength;	/* Number of samples in this trace */ /* (> 32767)? = 32767 set long samp_rate in 185-188 byte */
117-118	(2)	deltaSample;	/* Sampling interval in microseconds. */
119-120	(2)	gainType;	/* 1=fixed (Def), 2=binary, 3=floating, 4... opt.*/
121-122	(2)	gainConst;	/* Gain of recording channel */
123-124	(2)	initialGain;	/* Gain of preamplifier in db */

```
125-126 (2)     correlated;                 /* 1=no (Def), 2=yes */
127-130 (2x2)   sweepStart, sweepEnd;       /* min. and max. amplitude of trace */
131-132 (2)     sweepLength;                /* Here defined as
                                            fraction of second of shot time  */
133-134 (29)    sweepType;                  /* Source type:
                                    1=linear, 2=parabolic, 3=exponential, 4=others
                                    5=bohrhole explosive, 6=water explosive, 7=airgun (Def)
                                    or fraction of microsecond of shot time for high resolution data */
135-138 (2x2)   sweepTaperAtStart, sweepTaperAtEnd;     /* Start and end of trace (ms)
                                                           relative to Tred(0) */
139-140 (2)     taperType;                  /* scaling factor for last two values Def: 1 (x10) */
141-144 (2x2)   aliasFreq, aliasSlope;      /* Def: 0, 0  */
145-148 (2x2)   notchFreq, notchSlope;      /* Def: 0, 0  */
149-152 (2x2)   lowCutFreq, hiCutFreq;      /* Def: 0, 0  */
153-156 (2x2)   lowCutSlope, hiCutSlope;    /* Def: 0, 0  */
157-166 (5x2)   year, day, hour,            /* Source (shot) time, the fraction of sec */
                minute, second;             /* is set in millisec between 131-132 byte
                                            is set in microsec between 133-134 */
167-168 (2)     timeBasisCode;              /* 1=local, 2=GMT, 3=MET (GMT + 1 hour) (Def) */
169-170 (2)     traceWeightingFactor;       /*  */
171-172 (2)     phoneRollPos1;              /* Component: 1=time code, 2=radial, 3=transverse
                                            4=vertical, 5=hydrophone (Def)  */
173-174 (2)     phoneFirstTrace;            /* Methusalem instrument number in YYNN */
175-176 (2)     phoneLastTrace;             /* Channel number */
177-178 (2)     gapSize;                    /* Source charge in cubic inches (airgun)
                                            or kg (explosives) */
179-180 (2)     taperOvertravel;            /* Def: 0=meaningless  1=up, 2=down    */
/* !!! Following is extension !!! */
181-182 (2)     compNo;                     /* 1=time code, 2=radial, 3=transverse
                                            4=vertical, 5=hydrophone (Def)  */
183-184 (2)     samplingRate;               /* samples/sec */
185-188 (4)     numberSamples;              /* ( <= 32767) ? sampleLength | ( > 32767) */
189-190 (2)     shotPointNo;
191-192 (2)     ADCoeff;                    /* Coefficient of A/D converter in mv/digit */
193-194 (2)     receiverCoeff;              /* Conversion coefficient of receiver,
                                            pascal/cm2 for hydrophone,
                                            velocity(m/s)/volt for geophone */
195-196 (2)     receiverType;               /* 1=hydrophone (Def), 2=geophone, 3...*/
197-200 (4)     lengthData;                 /* Def: 0 (ms), not used here */
201-204 (4)     distance;                   /* Source to receiver distance in (m)  */
205-208 (4)     (float) scaleFactor;        /* Scale factor same as in <segy.h>
                                            Here azimuth in second of arc for processed data */
209-210 (2)     azimuth;                    /* Orientation of the component in min */
211-212 (2)     eigenperiod;                /* Eigenperiod of geo- or hydrophone in (ms) */
213-216 (4)     minAmpl;                    /* Min. peak amplitude within trace     */
217-220 (4)     maxAmpl;                    /* Max. peak amplitude within trace */
221-222 (2)     stationNo;                  /* Station number */
223-224 (2)     channelNo;                  /* Channel number (Default: 1) */
225-228 (4)     sourceCharge;               /* Charge in kg (explosive) or cc (airgun) */
229-230 (2)     redVelocity;                /* reduction velocity in (m/s);
                                            Def: 0 if no reduction velocity se */
231-232 (2)     timeOffset;                 /* Time offset in (ms) of first sample
                                            relative to reduced source time:
                                            positive if earlier than reduced time  */
233-236 (4)     redTime;                    /* Reduced time in (ms) = distance/redVel  */
237-238 (2)     unused2;
239-240 (2)     instNo;                     /* Methusalem instrument number */
```

Acknowledgements

Cruises SO 162 was funded by the German Ministery of Education and Research (BMBF) under project No. 03G0162A to GEOMAR within the continued and generous most commendable support for marine sciences with an outstanding research vessel such as SONNE. The INGGAS Project, jointly carried out by GEOMAR and the universities in Bremen, Hamburg and Kiel is also supported by the German Ministery of Education and Research (BMBF) through the Geotechnologie programme under grant 03G0564A.

We warmly thank master H. Papenhagen and his crew for their excellent support in all work done and for the splendid working atmosphere throughout the entire, very flexible working program.

References

Ayres, A., Theilen, Fr.: Relationships Between P- and S-Wave Velocities and geological Properties of Near-Surface Sediments of the Continental Slope of the Barents Sea. Geophysical Prospecting, Vol. 47, No. 4, 1999.

Ballesteros, M.W., G.F. Moore, B. Taylor, and S. Ruppert, 1988: Seismic stratigraphic framework of the Lima and Yaquina forearc basins. In: E. Suess and R. von Huene, et al., Proc. ODP, Init. Repts., 112. College Station, TX (Ocean Drilling Program), 77-90.

Bialas, J., and E.R. Flüh, 1999: Ocean Bottom Seismometers; Sea Technology, 40, 4, 41-46.

Bialas, J. and Kukowski, N. 2000. Editors, FS Sonne: Fahrtbericht / Cruise Report SO 146 1&2: Geophysical Experiments at the Peruvian Continental Margin. Investigations of tectonics, mechanics, gas hydrates and fluid transport. GEOMAR Report 96, 490 pp.

Bohlen, T., Klein, G., Duveneck, E., Milkereit, B., Franke, D, 1999, Analysis of dispersive seismic surface waves in submarine permafrost , Presented at the EAGE 61th Conference and Technical Exhibition, Helsinki, Expanded Abstracts, talk 6-37.

Bangs, N., Sawyer, D., amd Golovchenko, X., 1993. Free gas at the base of the hydrate zone in the vicinity of the Chile triple junction. Geology, 21, 905-908.

Blondel, P., and B.J. Murton, 1997: Handbook of Seafloor Sonar Imagery, John Wiley and Sons, Chichester, 314.

Booth, J., Winters, W., and Dillon, W., 1984. Circumstantial evidence of gas hydrate and slope failure associations on the US Atlantic continental margin. Annals of the New York Academy of Sciences, 715, 487-489.

Booth, J., Winters, W.J., Dillon, W.P., Clennell, M.B., and Rowe, M.M., 1998. Mahor occurrences and reservoir concepts of marine clathrate hydrates: implications of filed evidence. , In: Henriet, J.P. and Mienert, J., (eds). Gas hydrates: Relevance to world margin stability and climate change. Geological Society Special Publication No. 137, 113-128.

Brown, K.M., Bangs, N.L., Froelich, P.N., and Kvenvolden, K.A, 1996. The nature, distribution and origin of gas hydrtae in the Chile triple junction region: Earth and Planetary Sci. Letts., 139, 471-483.

Clennell, M., Hovland, M., Lysen, D., and Booth, J., 1995. Role of Capillary forces, couple flows and sediment-water depletion in the habitat of gas hydrate. (abstract). EOS., 76, 164-165.

Delisle, G., Beiersdorf, H., and Neben, S., 1998. The geothermal filed of the North Sulawesi accretionary wedge and a model on BSR migraqtion in unstable depositional environments. , In: Henriet, J.P.

and Mienert, J., (eds). Gas hydrates: Relevance to world margin stability and climate change. Geological Society Special Publication No. 137, 267-274.
Ecker, C., 1998. Seismic characterisation of methane hydrate structures. Ph.D thesis, Stanford University.
Fink, C.R. and Spence, G.D., 1999, Hydrate distribution off Vancouver Island from multifrequency single-channel seismic reflection data. Journ. of Geophys. Res., Vol. 104, no. B2, 2909-2922
Flueh, E. R., and J. Bialas, 1996: A digital, high data capacity ocean bottom recorder for seismic investigations; Int. Underwater Sytems Design, 18(3), 18-20.
Flueh, E. R., Bialas, J. and Charvis, P., 2001. Editors, FS Sonne Fahrtbericht / Cruise Report SO159. SALIERI: South American Lithsopheric Transects across Volcanic Ridges. GEOMAR Report 101, 256 pp.
Gettrust, J.F., Ross, J.H., and Rowe. M.M., 1991. Development of a low-frequency deep-towed geoacoustic system. Sea Technology, 32, 23-32.
Gettrust, J.F., Wood, W., and Lindwall, D., 1999. New seismic study of deep sea gas hydrates results in greatly improved resolution. EOS,
Grevemeyer, I., Rosenberger, A., and Villinger, H., Natural gas hydrates on the continental slope off Pakistan: constraints from seismic techniques, Geophys. J. Int., 140, 295-310, 2000.
Henriet, J.P. and Mienert, J., (eds) 1998. Gas hydrates: Relevance to world margin stability and climate change. Geological Society, London, Special Publication No. 137, pp. 338.
Hobro, J.W., Minshull, T.A. and Singh, S., 1988, Tomographic seismic studies of the methane hydrate stability zone in the Cascadia margin, in: Henriet, J.-P. and Mienert, J. (eds) Gas Hydrates: Relevance to World Margin
Holbrook, W.S., Hoskins, H., Wood, W.T., Stephen, R.A., Lizzaralde, D. and Leg 164 Science party, 1996, Methane hydrate and free gas on the Blake Ridge from vertical seismic profiling; Science, 273, 1840-1843
Hyndman, R.D. and Davis, E.E., A mechanism for the formation of methane hydrate and seafloor bottom-simulating reflectors by vertical fluid expulsion. J. Geophys. Res., 97, 7025-7041, 1992.
Hyndman, R.D. and Spence, G.D., A seismic study of methan hydrtae seafloor bottom-simulating reflectors, J. Geophys. Res., 97, 6683-6698.
Knickmeyer, E.T., 1996: Hochgenaues Differential-GPS, Proc. 11th Annual Meeting of the German Hydrographic Society, Glücksburg, 3.-5.6.
Kosarev, G.L., Makeyeva, L.I., Vinnik, L.P., 1987, Inversion of teleseismic P-waves particle motions for crustal structure in Fennoscandia, Phys. Earth Planet. Inter., 47, 11-24.
Kosarev, G.L., Petersen, N.V., Vinnik, L.P., Roecker, S.W., 1993, Receiver function for the Tien Shan analog broadband network: contrast in the evolution of structure across the Talasso-Fargana fault. J. Geophys. Res. 98, 4437-4448.
Kvenholden, K.A., 1988. Methane hydrates - a major reserve of carbon in the shallow geopschere? Chemical Geology, 71, 41-51.
Kvenholden, K.A., 1993. Gas hydrates - geological perspective and global change. Reviews of Geophysics, 31, 173.
MacKay, M., Jarrad, R.D., Westbrook, G.K., Hyndman, R.D. and Shipboard Scientific Party, 1994. ODP Leg 146, Origin of BSRs: Geophysical evidence from the Cascadia accretionary prism. Geology, 22, 459-462.
Mienert J, Posewang J, Baumann M, 1998. Geophysical signature of gas hydrates along the north-eastern Atlantic Margins: Possible hydrate-bound margin instabilities and possible transfer of methane from oceanosphere to atmosphere. In: Henriet, J.P. and Mienert, J., (eds). Gas hydrates: Relevance to world margin stability and climate change. Geological Society Special Publication No. 137, 275-292.
Monastersky, R., 1998. Waves of Death. Science News, 154, 221-223.
Paull, C.K., Ussler, W. III, and Dillon, W.P., 1991. Is the extent of glaciation limited by marine gas-hydrates? Geophys. Res. Letts., 18, 432-434.

Paull, C.K., Ussler, W. III, and Borowski, W.., 1994. Sources of biogenic methane to form marine gas-hydrfates: In situ productionor upward migration? New York Academy of Sciene Annals., 715, 392-409.

Pecher, I., Minshull, T.A., Singh,S.C. and von Huene, R., 1996, Velocity structure of a Bottom Simulating Reflectoroffshore Peru: Results from full waveform inversion; Earth and Plant. Sci. Let., 139,459-469

Pecher, I., Ranero, C.R., von Huene, R., Minshull, T.A. and Singh, S.C., 1998, The nature and distribution of bottom simulating reflectors at the Costa Rica convergent margin; Geophys. J. Int., 133, p. 219-229

Rowe, M.M., and Gettrust, J.F., 1993. Fine structure of methane hydrate-bearing sediments on the Blake outer ridge as determined from multi-channel seismic data. J. Geophys. Res., 98, 463-473.

Sakai, A. 1999. Velocity analysis of vertical seismic profile (VSP) survey at JAPEX/JNOC/GSC Mallik 2L-38 gas hydrate research well, and related problems for estimating gas hydrate concentration. Geological Survey of Canada Bulletin 544, 323-340.

Seeber, G., 1996: Stand und Einsatzmöglichkeiten von GPS - ein Überblick, Proc. 11th Annual Meeting of the German Hydrographic Society, Glücksburg, 3.-5.6.

Sloan, E.D., 1990 Hydrate nucleation from ice. Proceedings of the 69th Annual Gas Proceedings Conference, Phoenix, AZ, 8.

Sloan,E.D., 1998. Physical/chemical properties of gas hydrates and applications to world margin stability and climatic change. In: Henriet, J.P. and Mienert, J., (eds). Gas hydrates: Relevance to world margin stability and climate change. Geological Society Special Publication No. 137, 31-50.

Stoll, R. and Bryan, G., 1979. Physical properties of sediments containing gas hydrates. J. Geophys. Res., 84, 1629.

Tappin, D., and 18 others, 1999. Sediment slump likely caused 1998 Papua New Guinea Tsunami. EOS, 30, 333-340.

Uchida, T., Dallinore, S.R., Mikami, J., and Noxon, F.M., 1999. Occurrences and X-ray computerised tomography (CT) observations of natural hydrate, JAPEX/JNOC/GSC Mallik 2L-38 gas hydrate research well. Geol. Survey. Canada, Bull 544, p. 197-228.

Vinnik, L.P., 1977, Detection of waves converted fron P to SV in the mantle, Phys. Earth Planet. Inter., 15, 39-45.

Walia, R., Mi, Y., Hyndman, R.D., and Sakai, A., 1999. Vertical seismic profile (VSP) in the JAPEX/JNOC/GSC Mallik 2L-38 gas hydrate research well. Geol. Survey. Canada, Bull 544, 341-355.

Wessel, P. and Smith, W., 1995. Free software helps map and display data. EOS, Transactions AGU, 72, 445-446.

Yuan, T., Hyndman, R., Spence, G. and Desmons, B., 1996, Seismic velocity increase and deep-sea gas hydrate concentration above a bottom-simulating reflector on the Northern Cascadia continetal slope; J. Geophys. Res., 101, 13655-13671

Yuan, T., Spence, G.D., Hyndman, R.D., Minshull, T.A., and Singh, S.C., 1999. Seismic velocity studies of a gas hydrate bottom-simultaing reflector on the northern Cascadia continental margin: ammplirude modelling and full waveform inversion. J. Geophys. Res., 104, 1179-1191.

APPENDIX 1

STATION / PROFILE LOG FROM THE BRIDGE

F.S. "S O N N E" Reise SO 162

Eingesetzte Geräte

OBH/ OBS	Ocean Bottom Hydrophones / Seismograph
Airgun	Luftkanone 1 , 7 und 32 Liter
SS	Sidescan Sonar
DTS	Deep-Tow-Streamer
O-S	Oberflächen-Streamer
BG	Beatgun / Hammerlot
SBS	SeeBodenSeismische (implodierende) Kugeln
PSD	POSIDONIO Transpondersystem zur Ortung des DTS
EM	SIMRAD-Fächerlot

Vermessen wurden :

0252 sml	seismisch
3300 sml	mit dem EM Fächerlot
0305 sml	mit EM-Lot und Magnetometer

Eingesetzte Winden :

Winde	*D/M*	*Typ*	*RF-Nr*	*SO 162 Einsatz*	*Gesamt Einsatz*	*SO 162 S`länge*	*Gesamt S`länge*	*Zust.*
W 1	18,2	LWL	812001	0000 h	0000 h	000000 m	0000000 m	1
W 2	18,2	LWL	810001	0085	0324	023402	0106086	3
W 4	11,0	NSW	819052	0000	0000	000000	0000000	1
W 5	11,0	NSW	817164	0013	0225	005200	0192353	4
W 6	18,2	DRAKO	814150	0159	2130	168465	1854693	3

Winde	*SO 162 gefierte max.Länge*	*jemals gefierte max.Länge*	
W 1	0000 m	0000 m	
W 2	7000	7000	
W 4	0000	0000	
W 5	1920	5200	
W 6	5000	7900	(SL aktuell = 6456 m)

Geräteverluste :

Keine

Abkürzungen im Stationsprotokoll:

z.W.	zu Wasser
a.D.	an Deck
Boko	Bodenkontakt
Bosi	Bodensicht
SL(max.)	(maximale)Seillänge
LT	Lottiefe nach Hydrosweep
W x	eingesetzte Winde
SM	Simrad- Multibeam-Lot
PS	Parasound
XPNDR	Transponder

Zeit : UTC – 03 Stunden

22.02.02

Teststation 1 W 5

1600	Beginn Station	LT = 1534 m	32 41,48 S 71 45,89 W
1601	POSIDONIO-Transpnder z.W.		
1611	SL = 200 m		
1636	Transp. A.D. / Ende Station		

23.02.02

Teststation 2 W 5

1306	Beginn Station	LT = 1500 m	28 27,97 S 72 01,22 W
1307	P-T z.W.		
1410	SL = 500 m		
1447	hieven		
1516	P-T a.D. Ende Station		

Zeit : UTC – 4 Stunden

24.02.02

Teststation 3 W 5

0804	Beginn Station		28 55,06 S 73 10,89 W
0808	P-T z.W.		
0912	SL = 750 m		
1055	P-T a.D./ Ende Station		

Teststation 4 W 5

1600	Beginn Station	LT = 3840 m	23 55,50 S 73 29,75 W
1603	P-T z.W.		
1608	SL = 200 m		
1704	P-T a.D.		
1705	Ende Station		

Zeit : UTC – 5 Stunden

25.02.02

Teststation 5 W 5

1032	Beginn Station		20 08,42 S 74 41,66 W
1035	P-T z.W.		
1141	SL = 500 m		
1150	hieven		
1205	P-T a.D./ Ende Station		

Teststation 6 W 5

1626	Beginn Station	LT = 4936 m	19 14,88 S 74 58,22 W
1627	P-T z.W.		
1635	SL = 150 m		
1735	hieven		
1747	P-T a.D./ Ende Station		

26.02.02

Teststation 7 W 5

0800	Beginn Station		16 15,88 S 75 54,11 W
0806	P-T z.W.		
0812	SL = 150 m		
0840	hieven		
0847	PT a.D. / Ende Station		

Teststation 8 W 2

1630	Beginn Station	LT = 3339 m	15 06,22 S 76 15,65 W
1636	Sidescan z.W.		
1810	Slmax = 2636 m	LT = 2852 m	
1816	Beginn hieven		
1953	Sidescan a.D.		
1955	Ende Station		

28.02.02

Teststation 9 W 5

1440	OBH-T z.W.	LT = 1114 m	08 31,75 S 80 16,11 W
1447	EM-Sonde z.E.		
1510	Slmax = 1050 m		
1540	EM-Sonde a.D. / Ende Station		
1614 – 1930	Kalibrierung POSIDONIA-System v = 2,5 kn		
1932	T-OBH ausgelöst		
1945	aufgetaucht		
1957	OBH a.D. / Ende Station		

Auslegung OBH/S 1 - 8

2129	OBS 1 z.W.	LT = 830 m	08 22,44 S 80 19,19 W
2148	OBH 2	LT = 827 m	08 21,93 S 80 19,68 W
2209	OBS 3	LT = 828 m	08 21,43 S 80 20,23 W
2224	OBH 4	LT = 826 m	08 20,90 S 80 20.75 W
2242	OBS 5	LT = 825 m	08 20,40 S 80 21,26 W
2256	OBH 6	LT = 828 m	08 19,89 S 80 21,79 W
2310	OBS 7	LT = 819 m	08 19,38 S 80 22,32 W
2323	OBH 8	LT = 819 m	08 18,88 S 80 22,83 W

01.03.02

WS-Profil 01

0032	GI-gun z.W.			
0034 – 0048	bringen streamer aus			
0051	Beginn Profil	08 14,87 S	80 26,96 W	
	Kurs = 134 Grad	v = 3,5 kn		
0646	Ende Profil	08 29,45 S	80 11,94 W	19 sml
0646 –0706	holen airgun und streamer ein			

Kalibrierung POSIDONIA

0753	OBH-T z.W.	LT = 1111 m	08 31,77 S 80 16,11 W
0813 – 0920	Kalibrierung v = 2,5 kn		
0921	OBH ausgelöst		
0932	aufgetaucht		
0944	OBH a.D.		08 32,00 S 80 16,01 W

Profil 02 W 2

1543	bringen Tiefseestreamer aus				
1550	Sidescan Sonar (SS) z.W.				
1600	Depressor z.W.				
1610	SL = 100 m Ausfall Kabel				
1616	hieven ein				
1624	Depressor a.D. / Steckerverbindung defekt				
1640 – 1739	Schleife und Reparatur				
1743	Depressor z.W.				
1800	Beginn Profil 02	08 30,1 S	80 11,3 W	Kurs = 314 Grad	v = 3,0 kn
2257	v = 3,3 kn				
2320	v = 3,0 kn				
2400	08 17,63 S 80 24,18 W				

02.03.02

0135	Beginn hieven Tiefssee-streamer	SL = 1070 m		
0140	Ende Profill	08 14,21 S	80 27,64 W	23 sml

Profil 03 W 2

0141 – 0218	drehen über Bb			
0200	SL = 500 m, hieven stop			
0218	Beginn fieren streamer			

0218	v = 2,5 kn	
0231	Beginn Profil	08 14,21 S 80 27,65 W
	Kurs = 134 Grad	v = 2,5 kn SL = 921 m
0528	v = 2,8 kn	
0536	v = 2,5 kn	
1108	Ende Profil	08 29,41 S 80 11,95 W 18 sml
	Beginn hieven	

Profil 04 W 2

1130	GI-gun vorgehievt; SL = 487 m	drehen über Stb
1206	Beginn Profil	08 29,44 S 80 11,97 W
	Kurs = 314 Grad	v = 2,5 kn
1217	SL = 902 m	
1220 – 1237	bringen Oberfächen-streamer aus	
1300	v = 2,0 kn	
1305 – 1308	hieven auf SL 864 m	
1324 – 1330	hieven auf 779 m	
1342	v = 2,5 kn	
1351 – 1359	fieren auf 872 m	
1405	v = 3,5 kn	
1406 – 1437	fieren auf 1266 m	
1900	Ende Profil	08 14,29 S 27 27,56 w 23 sml

Profil 05 W 2

1901	hieven SS-DTS	
1907	GI-gun a.D.	
1907 – 1933	Schleife über Stb	
1926	SL = 500 m	
1948	32-Liter-airgun z.W.	
1949	Beginn Profil	08 14,14 S 80 27,71 W
	Kurs = 134 Grad	v = 3,5 kn
ab 2030	fieren in verschiedenen Stufen SS-DTS	
2126	v = 3,0 kn	
2233 – 2258	wechseln Auftriebskörper der air-gun	
2400	Ende Profil	08 23,41 S 80 18,17 W 11 sml

03.03.02

Profil 06 W 2

0000 – 0007	hieven SS-DTS auf SL = 894 m	
0021	32-Liter-airgun a.D.	
0022 – 0040	drehen über Stb auf 236 Grad	
0032	GI-gun z.W.	
0108	Beginn Profil	08 25,64 S 80 19,17 W
	Kurs = 236 Grad	v = 3,0 kn
0110 – 1021	fieren SS-DTS entsprechend zunehmender Wassertiefe	
1021	Slmax = 7000 m	LT = 4179 m
1100	Ende Profil	08 41,75 S 80 44,50 W 34 sml
1100	Beginn hieven SS und DTS	
1225 – 1243	holen Ofl.-streamer ein	
1300- 1304	holen GI-gun ein	
1500	Depressor a.D.	
1513	SS und DTS a.D.	

Profil 07 EM/HS

1513	Beginn Profil	08 46,5 S 80 50,36 W Kurs = 50 Grad v = 12 kn
1820	reduzieren auf 3,0 kn	
1825 – 1836	bringen Ofl.-streamer aus	
1841	GI-gun z.W.	
1839	Ende Profil 07	08 22,21 S 80 21,04 W 38 sml

Profile 08 und 09 Seismik

1852	Beginn Profil 08	08 21,74 S 80 20,56 W	Kurs = 48 Grad v = 5,0 kn
1912	Ende Profil 08	08 26,65 S 80 19,50 W	2 sml
1940	Beginn Profil 09	08 19,69 S 80 20,52 W	Kurs=225 Grad v = 5,0 kn
2005	Ende Profil 09	08 21,15 S 80 22,03 W	2 sml

Aufnahme OBH/S 1-8 i.G. 08 21 S 80 22 W

2059	OBH 8	ausgelöst	2118	gesichtet	2119	a.D.	
2118	OBS 7		2127		2144		
2144	OBH 6		2155		2203		
2204	OBS 5		2212		2219		
2219	OBH 4		2230		2239		
2239	OBS 3		2249		2315		
2315	OBH 2		2330		2340		
2340	OBH 1		2357		0007		

04.03.02

Vermessung mit EM und PS v = 10,0 kn

0044	Beginn Profil	08 27,30 S 80 17,80 W	Kurs = 234 Grad
0155	ä.K. auf 286 Grad	08 34,25 S 80 27,0 W	12 sml
0250	ä.K. auf 358 Grad	08 31,60 S 80 36,33 w	09 sml
0336	ä.K. auf 336 Grad	08 23,82 S 80 36,60 W	08 sml
0548	ä.K. auf 339 Grad	08 03,50 S 80 45,60 W	22 sml
0609	ä.K. auf 057 Grad	08 00,31 S 80 46,85 W	03 sml
0625	ä.K. auf 152 Grad	07 58,78 S 80 44,57 W	03 sml
0648	ä.K. auf 155 Grad	08 02,11 S 80 42,76 W	04 sml
0739	ä.K. auf 138 Grad	08 09,91 S 80 39,15 W	09 sml
0858	Ende Vermessung	08 19,03 S 80 31,00 w	12 sml

Kalibrierung POSIDONIA-System

0902	OBH-T z.W.	08 19,04 S 80 30,99 W					
0921	Beginn Kalibrierung	div. Kurse (8) v = 2,5 kn					
1142	Ende Kalibrierung						
1153	OBH ausgelöst	1210	aufgetaucht	1218	a.D.	08 19,20 S	80 31,00 W

Auslegung OBH/S 9 - 13

1333	OBH 9	z.W.	LT = 942 m	08 23,52 S	80 24,01 W
1341	OBS 10		LT = 942 m	08 23,50 S	80 24,00 W
1348	OBH 11		LT = 941 m	08 23,48 S	80 23,98 W
1407	OBS 12		LT = 941 m	08 23,36 S	80 24,15 W
1410	OBH 9 und OBH 11		ausgelöst	1421	aufgetaucht
1430	OBH 11 a.D.				
1434	OBH 9 a.D.				
1447	OBH 9	z.W.	LT = 952 m	08 23,71 S	80 24,20 W
1501	OBH 11	z.W.	LT = 932 m	08 23,31 S	80 23,78 W

Teststation Beatgun W 2

1511	Beginn Station	LT = 950 m	08 23,85 S	80 23,69 W
1513	BG z.W.			
1537	Boko SL = 958 m	LT = 948 m	08 23,84 S	80 23,71 W
1539 – 1544	2 weitere Boko			
1546	hieven			
1613	BG a.D.			
1618	Ende Station			

SeeBoSeis

1647 – 1654	Auslage von 7 Stck SeeBoSeis-Kuglen im Abstand von 100 m Schnitt 08 23,64 S 80 23,88 W bis 08 23,87 S 80 23,68 W	

SIMRAD-Vermessung v = 7,8 kn

1859	Beginn	08 29,99 S 80 17,09 W	Kurs = 231 Grad
2155	ä.K. auf 154 Grad	08 43,41 S 80 22,92 W	21 sml
2309	ä.K. auf 038 Grad	08 51,81 S 80 30,02 W	09 sml
05.03.02			
0205	Ende Vermessung	08 40,85 S 80 21,19 W	22 sml

SS-DTS-Profil W 2

0420	Beginn Aussetzen	08 26,97 S 80 21,46 W
0425	SS z.W. v = 1,0 kn	
0432	DTS z.W. v = 3,0 kn	
	Beginn fieren W 2	
0444	SL = 396 m Ausfall Datenstrecke	
0525	hieven ein	
0545	Depressor a.D.	
0600	SS a.D.	
0606	streamer a.D.	

SIMRAD-Vermessung v = 7,8 kn

0702	Beginn Vermessung	08 18,00 S 80 21,99 W	Kurs = 60 Grad
0806	ä.K auf 329 Grad	08 15,09 S 80 15,09 W	08 sml
0828	ä.K. auf 245 Grad	08 11,48 S 80 16,54 W	03 sml
0954	Ende Vermessung	08 16,01 S 80 26,49 W	11 sml

Seismikprofile 7-9 v = 4,5 kn

1020	GI-gun z.W.		
1025	GI-gun a.D.		
1042		08 19,04 S 80 27,71 W	
1055	32-Liter-airgun z.W.	Beginn Profil 7	Kurs 139 Grad
1104	streamer z.W.		
1340	Ende Profil 7	08 28,29 S 80 19,93 W	12 sml
1401	Beginn Profil 8	08 28,29 S 80 19,93 W	Kurs = 291 Grad
1532	Profilwechsel 8/9	08 25,69 S 80 26,39 W	07 sml
1649	Ende Profil 9	08 21,87 S 80 22,16 W	06 sml

Station beatgun W 2

1815	Beginn Station	LT = 933 m	08 23,37 S	80 23,88 W
1817	BG z.W.			
1841	1. Boko	SL = 949 m LT = 939 m	08 23,45 S	80 23,88 W
1906	2. Boko	SL = 950 m LT = 945 m	08 23,55 S	80 23,81 W
1927	3. Boko	SL = 957 m LT = 943 m	08 23,65 S	80 23,76 W
1930	Beginn hieven			
2001	BG a.D. / Ende Station			

Aufnahme OBH/S 9-11

2010	OBH 09	ausgelöst	2023	gesichtet	2033	a.D.	08 23,75 S	80 24,22 W
2035	OBS 10		2046		2057		08 23,40 S	80 24,14 W
2102	OBS 12		2113		2124		08 23,61 S	80 24,00 W
2127	OBH 11		2139		2148		08 23,39 S	80 23,77 W

06.03.02

Teststation POSIDONIO / SIMRAD W 5

0018	Beginn Station	LT = 2153 m	08 27,50 S	80 38,01 W

0019 SIMRAD-Sonde z.W.
0056 SL = 1900 m
0105 hieven
0150 Sonde a.D./ Ende Station

SS und DTS-Seismik Profile 07 – 17 v = 3,0 Kn Kurse = 325 / 145 Grad

0404	Beginn Aussetzen			08 27,11 S 80 21,76 W
0407	DT-streamer z.W.			
0415	Depressor z.W. / fieren W 2			
0440	medium airgun z.W.			
0514	Beginn Profil 07	SL = 1145 m	LT = 940 m	08 24,58 S 80 23,33 W
0610	Ende Profil 07			08 22,24 S 80 24,94 W3 sml
0642	Beginn Profil 08	SL = 1048 m	LT = 928 m	08 22,47 S 80 24,33 W
0738	Ende Profil 08			08 24,79 S 80 22,77 W3 sml
0802	Beginn Profil 09	SL = 1075 m	LT = 964 m	08 24,64 S 80 23,42 W
0854	Ende Profil 09	SL = 1285 m	LT = 936 m	08 22,29 S 80 25,09 W3 sml
0922	Beginn Profil 10	SL = 1032 m	LT = 931 m	08 22,51 S 80 24,42 W
1019	Ende Profil 10			08 24,90 S 80 22,79 W3 sml
1028	Beginn Profil 11	SL = 1190 m	LT = 967 m	08 24,69 S 80 23,50 W
1156	Ende Profil 11			08 22,51 S 80 24,97 W3 sml
1230	Beginn Profil 12	SL = 1047 m	LT = 934 m	08 22,57 S 80 24,47 W
1327	Ende Profil 12	SL = 1060 m	LT = 967 m	08 24,97 S 80 22,82 W3 sml
1358	Beginn Profil 13	SL = 1152 m	LT = 960 m	08 24,72 S 80 23,58 W
1456	Ende Profil 13	SL = 1233 m	LT = 941 m	08 22,28 S 80 25,23 W3 sml
1521	Beginn Profil 14	SL = 1034 m	LT = 935 m	08 22,63 S 80 24,57 W
1616	Ende Profil 14	SL = 1222 m	LT = 968 m	08 24,94 S 80 22,97 W3 sml
1645	Beginn Profil 15	SL = 1014 m	LT = 971 m	08 24,78 S 80 23,63 W
1742	Ende Profil 15	SL = 1201 m	LT = 944 m	08 22,46 S 80 25,20 W3 sml
1820	Beginn Profil 16	SL = 1103 m	LT = 957 m	08 23,63 S 80 24,76 W
1856	Ende Profil 16	SL = 1216 m	LT = 909 m	08 22,56 S 80 23,21 W2 sml
1928	Beginn Profil 17	SL = 811 m	LT = 927 m	08 22,93 S 80 23,54 W
1937	Abbruch Profil 18 hieven ein			08 23,36 S 80 23,83 W1 sml
1949	airgun a.D			
2005	Depressor a.D.			
2020	Alles a.D. / Ende Station			

07.03.02

SIMRAD-Vermessung

2213 Beginn Vermessung 03 14,85 S 08 46,36 W
Kurs = 116 Grad v = 13,0 kn

08.03.02

0033	ä.K. auf 016 Grad	03 26,93 S 81 22,06 W	27 sml
0342	ä.K. auf 304 Grad	02 45,04 S 81 10,02 W	44 sml
0633	Ende Vermessung	02 24,94 S 81 38,98 W	35 sml

Kalibrierung POSIDONIA

0641	OBH-T z.W.	02 25,10 S 81 39,01 W
0736	OBH a, Grund	
0737	Beginn fahren einer 8 (acht) mit 2,5 kn um obige Position	
0907	Ende Kalibrierung	02 25,18 S 81 31,28 W
0909	OBH-T aus gelöst	
0935	OBH aufgetaucht	
0944	OBH a.D.	02 24,99 S 81 38,96 W

Profil SS-DIT 18 W 2

0959 Beginn aussetzen Tiefseestreamer
1008 Sidescan z.W.
1011 Depressor z.W.
1025 medium airgun z.W.

1025	Beginn Profil	02 24,09 S 81 37,70 W	
1210	reduzieren auf v = 2,8 kn		
1330	ä.K. auf 360 Grad	02 19,00 S 81 29,51 W	11 sml
	LT = 4077 m SL = 5441 m		
1418	Slmax = 7000 m LT = 4056 m	02 16,83 S 81 29,51 W	
1533	Beginn hieven SL = 7000 m LT = 3943 m	02 13,12 S 8129,52 W	
1527	Stop hieven SL = 5407 m LT = 3869 m	02 10,26 S 81 29,60 W	
1541	Fortsetzung hieven		
1934	SL = 100 m Winde stop	02 01,29 S 81 29,90 W	
1948	Ende Profil SL = 100 m	02 00,48 S 81 29,94 W	14 sml
1953	airgun a.D.		
1958	Depressor a.D.		
2006	sidescan a.D.		
2014	POSIDONIA-Transponder eingeholt		

09.03.02

EM- und Magnetik-Profile v = 11 kn

0815 – 0820	bringen Magnetometer aus		
0820	Beginn MG-Profil Kurs = 42 Grad	00 35,27 S 81 10,33 W	
1531	ä.K. auf 335 Grad	01 34,00 S 80 18,00 W	67 sml
1715	Ende Profil	01 50,01 N 80 25,38 W	14 sml

10.03.02

SS-DTS-Profil 19 W 2

0819	bringen DT-streamer aus		
825	Sidescan z.W.		
0832	Depressor z.W.		
0839	medium airgun z.W.		
0847	Beginn Profil SL = 0000 m LT = 3135 m	04 52,78 N 79 29,72 W	
	Kurs = 360 Grad v = 2,5 kn		
0849	Beginn fieren W 2		
1033	Slmax = 570 m hieven ein		
1052	Ende Profil	04 58,00 S 79 29,78 W	5 sml
1104	Depressor a.D.		
1111	Sidescan a.D.		
1117	Streamer a.D.		

EM-MAG-Vermessung v = 10,0 kn

1117 – 1122	bringen Magnetometer aus		
1127	Beginn MAG-Vermessung	05 59,02 N 79 29,73 W	
	Kurs = 360 Grad		
1411	ä.K. auf 291 Grad	05 25,93 N 79 29,57 W	22 sml
1520	ä.K. auf 045 Grad	05 30,01 N 79 40,02 W	11 sml
1656	ä.K. auf 090 Grad	05 41,98 N 79 28,03 W	17 sml
1657	v = 10,8 kn		
1800	ä.K. auf 356 Grad	05 42,00 N 79 16,07 W	29 sml

11.03.02

0805	Ende Vermessung	08 17,44 N 79 25,92 W	145 sml

Appendix II SO-162 INGGAS-Test Seismic Profiles collected

Profile	Start Latitude	Start Longitude	Start time UTC	End Latitude	End Longitude	End time UTC	Source	pop rate	Receivers
1 (DTS1)	08° 31,77 S	80°16,11 W	05:51 1.3.2	08°29,45 S	80°11,94 W	11:46 1.3.2	GI-gun	5	OBH/S 1-8; SIG
2 (DTS2)	08°30,1 S	80°11,3 W	23:00 1.3.2	08°14,21 S	80°27,64 W	06:40 2.3.2	GI-gun	5	OBH/S 1-8; DTS
3 (DTS3)	08°14,21 S	80°27,65 W	07:31 2.3.2	08°29,41 S	80°11,95 W	16:08 2.3.2	GI-gun	5	OBH/S 1-8; DTS
4 (DTS4)	08°29,44 S	80°11,97 W	17:06 2.3.2	08°14,29 S	80°27,56 W	24:00 2.3.2	GI-gun	5	OBH/S 1-8; DTS, SIG
5 (DTS5)	08°14,14 S	80°27,71 W	00:49 3.3.2	08°23,42 S	80°18,17 W	05:00 3.3.2	32 ltr gun	20	OBH/S 1-8; DTS, SIG
6 (DTS6)	08°25,64 S	80°19,17 W	06:08 3.3.2	08°41,75 S	80°44,50 W	16:00 3.3.2	GI-gun	9	OBH/S 1-8; DTS, SIG
7	08°46,5 S	80°50,36 W	20:13 3.3.2	08°22,21 S	80°21,04 W	23:39 3.3.2	SIMRAD	n/a	SIMRAD, Parasound
8	08°21,74 S	80°20,56 W	23:52 3.3.2	08°20,65	80°19,50 W	00:12 4.3.2	GI-gun	5	OBH/S 1-8, SIG
9	08°19,69 S	80°20,52 W	00:40 4.3.2	08°21,15 S	80°22,03 W	01:05 4.3.2	GI-gun	5	OBH/S 1-8; SIG
10	08°23,85 S	80°23,69 W	20:11 4.3.2	08°23,84 S	80°23,71 W	20:37 4.3.2	Beatgun I	n/a	OBH/S 9-12
11	08°23,64 S	80°23,88 W	22:39 4.3.2	08°23,87 S	80*23,68 W	22:45 4.3.2	SeeBoSeis	1 min	OBH/S 9-12
12 (7)	08°19,04 S	80°27,71 W	15:42 5.3.2	08°28,29 S	80°19,93 W	18:40 5.3.2	32 ltr gun	20	OBH/S 9-12
13 (8)	08°28,29 S	80°19,93 W	19:01 5.3.2	08°25,69 S	80°26,30 W	20:32 5.3.2	32 ltr gun	20	OBH/S 9-12
14 (9)	08°25,69 S	80°26,30 W	20:32 5.3.2	08°21,87 S	80°22,16 W	21:49 5.3.2	32 ltr gun	20	OBH/S 9-12
15	08°23,37 S	80°23,88 W	23:15 5.3.2	08°23,65 S	80°23,76 W	00:27 6.3.2	Beatgun 2	n/a	OBH/S 9-12
17 (DTS7)	08°24,58 S	80°23,33 W	10:14 6.3.2	08°22,24 S	80°24,94 W	11:10 6.3.2	1.6 ltr gun	5	DTS
18 (DTS8)	08°22,47 S	80°24,33 W	11:42 6.3.2	08°24,79 S	80°22,77 W	12:38 6.3.2	1.6 ltr gun	5	DTS
19 (DTS9)	08°24,64 S	80°23,42 W	13:02 6.3.2	08°22,29 S	80°25,09 W	13:54 6.3.2	1.6 ltr gun	5	DTS
20 -DTS10	08°22,51 S	80°24,42 W	14:22 6.3.2	08°24,90 S	80°22,79 W	15:19 6.3.2	1.6 ltr gun	5	DTS
21 -DTS11	08°24,69 S	80°23,50 W	15:58 6.3.2	08°22,51 S	80°24,97 W	16:56 6.3.2	1.6 ltr gun	5	DTS
22 -DTS12	08°22,57 S	80°24,47 W	17:30 6.3.2	08°24,97 S	80°22,82 W	18:27 6.3.2	1.6 ltr gun	5	DTS
23 -DTS13	08°24,72 S	80°23,58 W	18:58 6.3.2	08°22,28 S	80°25,23 W	19:56 6.3.2	1.6 ltr gun	5	DTS
24 -DTS14	08°22,63 S	80°24,57 W	20:21 6.3.2	08°24,94 S	80°22,97 W	21:16 6.3.2	1.6 ltr gun	5	DTS
25 -DTS15	08°24,78 S	80°23.63 W	21:45 6.3.2	08°22,46 S	80°25,20 W	22:42 6.3.2	1.6 ltr gun	5	DTS
26 -DTS16	08°23,63 S	80°24,76 W	23:20 6.3.2	08°22,56 S	80°23,21 W	23:56 6.3.2	1.6 ltr gun	5	DTS
27 -DTS17	08°22,93 S	80°23,54	00:28 7.3.2	08°23,36	80°23,83 W	00:37 7.3.2	1.6 ltr gun	5	DTS - interrupted
28 -DTS18	02:24,09 S	81°37,70 W	15:25 8.3.2	02°19,00 S	81°29,51 W	18:30 8.3.2	1.6 ltr gun	8	DTS
29 -DTS19	02°19,00 S	81°29,51 W	18:30 8.3.2	02°00,48 S	81°29,94 W	00:48 9.3.2	1.6 ltr gun	9	DTS
30 -DTS20	04°52,78 N	79°29,72 W	13:47 10.3.	04°58,00 N	79°29,78 W	15:52 10.3.	1.6 ltr gun	7	DTS

Profile	Start Latitude	Longitude	Date	Time (UTC)	End Latitude	Longitude	Date	Time (UTC)	Course	Number of shots	Length [nm]	Comment
DTS 2	08°30.07'S	80°11.36'W	01.03.2002	23:00	08°14.21'S	80°27.62'W	02.03.2002	6:40	314°	5173	23	along strike of continental margin
DTS 3	08°14.22'S	80°27.65'W	02.03.2002	7:32	08°29.39'S	80°11.98'W	02.03.2002	16:08	134°	6007	18	"
DTS 4	08°29.45'S	80°11.95'W	02.03.2002	17:06	08°14.31'S	80°27.54'W	03.03.2002	0:00	314°	5015	23	"
DTS 5	08°14.12'S	80°27.73'W	03.03.2002	0:48	08°23.55'S	80°18.02'W	03.03.2002	5:00	134°	627	11	Scholte wave experiment
DTS 6	08°25.62'S	80°19.13'W	03.03.2002	6:08	08°41.75'S	80°44.50'W	03.03.2002	16:00	236°	2721	34	Transect toward Trench
DTS 7	08°24.59'S	80°23.34'W	06.03.2002	10:14	08°22.25'S	80°24.93'W	06.03.2002	11:10	325°	666	3	Max & Moritz
DTS 8	08°22.47'S	80°24.34'W	06.03.2002	11:42	08°24.78'S	80°22.79'W	06.03.2002	12:38	145°	652	3	Max & Moritz
DTS 9	08°24.66'S	80°23.42'W	06.03.2002	13:02	08°22.29'S	80°25.02'W	06.03.2002	13:54	325°	568	3	Max & Moritz
DTS 10	08°22.51'S	80°24.42'W	06:03.2002	14:22	08°24.90'S	80°22.80'W	06.03.2002	15:20	145°	740	3	Max & Moritz
DTS 11	08°24.72'S	80°23.47'W	06.03.2002	15:58	08°22.34'S	80°25.07'W	06.03.2002	16:56	325°	694	3	Max & Moritz
DTS 12	08°22.59'S	80°24.47'W	06.03.2002	17:30	08°24.97'S	80°22.82'W	06:03.2002	18:28	145°	774	3	Max & Moritz
DTS 13	08°24.70'S	80°23.57'W	06.03.2002	18:58	08°22.28'S	80°25.23'W	06.03.2002	19:56	325°	461	3	Max & Moritz
DTS 14	08°22.67'S	80°24.53'W	06.03.2002	20:22	08°24.92'S	80°22.98'W	06.03.2002	21:16	145°	669	3	Max & Moritz
DTS 15	08°24.78'S	80°23.62'W	06.03.2002	21:46	08°22.45'S	80°25.20'W	06.03.2002	22:42	325°	669	3	Max & Moritz
DTS 16	08°23.63'S	80°24.76'W	06.03.2002	23:20	08°22.56'S	80°23.21'W	06.03.2002	23:56	55°	423	2	Max & Moritz
DTS 17	08°22.94'S	80°23.55'W	07.03.2002	0:28	08°23.29'S	80°23.78'W	07.03.2002	0:36	-	-	1	Max & Moritz
DTS 18/19	02°23.85'S	81°37.38'W	08.03.2002	15:24	02°00'48'S	81°29.94'W	09.03.2002	0:48	57°/360°	2130	25	Profile in Trench
DTS 20	04°52.78'N	79°29.72'W	10.03.2002	13:46	04°58.00'N	79°29.78'W	10.03.2002	15:52	360°	576	5	Final test
							Total without curves			28565	169	
							Total with curves			33235		

Appendix IV

SO-162 INGGAS TEST

OBH/S deployments

INST.	LAT (S)	LON (W)	DIST. TO	DEPTH	REL.	ANT.	REC.	SKEW	REMARKS	SENSOR	FIGURE
	D:M	D:M	NEXT (nm)	(m)	CODE	CH.	NO.	(ms)			
OBS01	08 22. 45	80 19. 19	0.72	830	3659	C	010405		cold	OAS30, PMD540	
OBH02	08 21. 94	80 19. 69	0.72	827	0386+0355	D	980401	-11		OAS34	
OBS03	08 21. 44	80 20. 24	0.72	831	3624	A	000616		cold	OAS38, Owen16, 30Hz	
OBH04	08 20. 90	80 20. 76	0.72	825	3669	C	980403	-1		OAS27	
OBS05	08 20. 40	80 21. 26	0.72	825	3664	C	000614	-10		OAS22, Owen02, 4.5 Hz	4.11.2-5
OBH06	08 19. 89	80 21. 79	0.72	828	6334	C	000612	+4		OAS18	
OBS07	08 19. 38	80 22. 32	0.72	819	3609	D	980901	+14		OAS31, Owen11, 30Hz	4.11.6-9
OBH08	08 18. 88	80 22. 84		819	039A+0355	D	000611	-5		OAS29	
OBH09	08 23. 713	80 24. 208	0.3	950	0398+0355	D	971202	-4		OAS27	
OHS10	08 23. 360	80 24. 162	0.3	943	3664	A	000614	-4		OAS22, Owen2, 4.5HZ	4.11.10-13
OBH11	08 23. 308	80 23. 775	0.2	941	0386+0355	D	980401	-4		OAS18	
OBS12	08 23. 511	80 24.00		941	039A+0355	C	980901	+7		OAS38, Owen16, 30Hz	4.11.14-17
											4.7.2, 4.7.3,
											4.6.4, 4.6.5
Trigger							000610	0			
Trigger							000610	0			
Trigger							000610	0			
Trigger							610	0			
Streamer							971202	0			
Streamer							971202	0			
Streamer							971202	0			
Streamer							971202	0			

GEOMAR REPORTS

1 GEOMAR FORSCHUNGSZENTRUM FÜR MARINE GEOWISSENSCHFTEN DER CHRISTIAN-ALBRECHTS-UNIVERSITÄT ZU KIEL. BERICHT FÜR DIE JAHRE 1987 UND 1988. 1989. 71 + 6 pp. In German

2 GEOMAR FORSCHUNGSZENTRUM FÜR MARINE GEOWISSENSCHAFTEN DER CHRISTIAN-ALBRECHTS-UNIVERSITÄT ZU KIEL. JAHRESBERICHT/ANNUAL REPORT 1989. 1990. 96 pp. In German and English

3 GEOMAR FORSCHUNGSZENTRUM FÜR MARINE GEOWISSENSCHAFTEN DER CHRISTIAN-ALBRECHTS-UNIVERSITÄT ZU KIEL. JAHRESBERICHT/ANNUAL REPORT 1990. 1991. 212 pp. In German and English

4 ROBERT F. SPIELHAGEN
DIE EISDRIFT IN DER FRAMSTRASSE WÄHREND DER LETZTEN 200.000 JAHRE. 1991. 133 pp.
In German with English summary

5 THOMAS C. W. WOLF
PALÄO-OZEANOGRAPHISCH-KLIMATISCHE ENTWICKLUNG DES NÖRDLICHEN NORDATLANTIKS SEIT DEM SPÄTEN NEOGEN (ODP LEGS 105 UND 104, DSDP LEG 81). 1991. 92 pp. In German with English summary

6 SEISMIC STUDIES OF LATERALLY HETEROGENOUS STRUCTURES – INTERPRETATION AND MODELLING OF SEISMIC DATA. Ed. by ERNST R. FLUEH
Commission on Controlled Source Seismology (CCSS), Proceedings of the 8th Workshop Meeting, held at Kiel – Fellhorst (Germany), August 27-31, 1990. 1991. 359 pp. In English

7 JENS MATTHIESSEN
DINOFLAGELLATEN-ZYSTEN IM SPÄQUARTÄR DES EUROPÄISCHEN NORDMEERES: PALÖKOLOGIE UND PALÄO-OZEANOGRAPHIE. 1991. 104 pp. In German with English summary. Out of print

8 DIRK NÜRNGERG
HAUPT- UND SPURENELEMENTE IN FORAMINIFERENGEHÄUSEN – HINWEISE AUF KLIMATISCHE UND OZEANOGRAPHISCHE ÄNDERUNGEN IM NÖRDLICHEN NORDATLANTIK WÄHREND DES SPÄTQUARTÄRS. 1991. 117 pp. In German with English summary. Out of print

9 KLAS S. LACKSCHEWITZ
SEDIMENTATIONSPROZESSE AM AKTIVEN MITTELOZEANISCHEN KOLBEINSEY RÜCKEN (NÖRDLICH VON ISLAND). 1991. 133 pp. In German with English summary. Out of print

10 UWE PAGELS
SEDIMENTOLOGISCHE UNTERSUCHUNGEN UND BESTIMMUNG DER KARBONATLÖSUNG IN SPÄTQUARTÄREN SEDIMENTEN DES ÖSTLICHEN ARKTISCHEN OZEANS. 1991. 106 pp.
In German with English summary

11 FS POSEIDON. EXPEDITION 175 (9.10.-1.11.1990)
175/1:OSTGRÖNLÄNDISCHER KONTINENTALRAND (65°N)
175/2: SEDIMENTATION AM KOLBEINSEYRÜCKEN (NÖRDLICH VON ISLAND).
Hrsg. von J. MIENERT und H.-J. WALLRABE-ADAMS. 1992. 56 pp. + app. In German with some English chapters

12 GEOMAR FORSCHUNGSZENTRUM FÜR MARINE GEOWISSENSCHAFTEN DER CHRISTIAN-ALBRECHTS-UNIVERSITÄT ZU KIEL. JAHRESBERICHT/ANNUAL REPORT 1991. 1992. 152 pp. In German and English.
Out of print

13 SABINE E. I. KÖHLER
SPÄTQUARTÄRE PALÄO-OZEANOGRAPHISCHE ENTWICKLUNG DES NORDPOLARMEERES UND EUROPÄISCHEN NORDMEERES ANHAND VON SAUERSTOFF- UND KOHLENSTOFF- ISOTOPENVERHÄLTNISSEN DER PLANKTISCHEN FORAMINIFERE *Neogloboquadrina pachyderma* (sin.).
1992. 104 pp. In German with English summary

14 FS SONNE. FAHRTBERICHT SO78 PERUVENT: BALBOA, PANAMA - BALBOA, PANAMA, 28.2.1992-16.4.1992
Hrsg. von ERWIN SUESS. 1992. 120 pp. In German with some English chapters. Out of print

15 FOURTH INTERNATIONAL CONFERENCE ON PALEOCEANOGRAPHY (ICP IV): SHORT- AND LONG-TERM GLOBAL CHANGE: RECORDS AND MODELLING. 21-25 SEPTEMBER 1992, KIEL/GERMANY.
PROGRAM & ABSTRACTS. 1992. 351 pp. In English

16 MICHAELA KUBISCH
DIE EISDRIFT IM ARKTISCHEN OZEAN WÄHREND DER LETZTEN 250.000 JAHRE. 1992. 100 pp.
In German with English summary

17 PERSISCHER GOLF: UMWELTGEFÄHRDUNG, SCHADENSERKENNUNG, SCHADENSBEWERTUNG AM BEISPIEL DES MEERRESBODENS; ERKENNEN EINER ÖKOSYSTEMVERÄNDERUNG NACH ÖLEINTRÄGEN. Schlußbericht zu den beiden BMFT-Forschungsvorhaben 03F0055 A + B. 1993. 108 pp. In German with English summary

18 TEKTONISCHE ENTWÄSSERUNG AN KONVERGENTEN PLATTENRÄNDERN / DEWATERING AT CONTINENTAL MARGINS. Hrsg. von/ed. by ERWIN SUESS. 1993. 196 + 32 + 68 + 16 + 22 + 38 + 4 + 19 pp.
Some chapters in English, some in German

19 THOMAS DICKMANN

DAS KONZEPT DER POLARISATIONSMETHODE UND SEINE ANWENDUNGEN AUF DAS SEIMISCHE VEKTORWELLENFELD IM WEITWINKELBEREICH. 1993. 121 pp. In German with English summary

20 GEOMAR FORSCHUNGSZENTRUM FÜR MARINE GEOWISSENSCHAFTEN DER CHRISTIAN-ALBRECHTS-UNIVERSITÄT ZU KIEL. JAHRESBERICHT/ANNUAL REPORT 1992. 1993. 139 pp. In German and English

21 KAI UWE SCHMIDT
PALYNOMORPHE IM NEOGENEN NORDATLANTIK - HINWEISE ZUR PALÄO-OZEANOGRAPHIE UND PALÄOKLIMATOLOGIE. 1993. 104 + 7 + 41 pp. In German with English summary

22 UWE JÜRGEN GRÜTZMACHER
DIE VERÄNDERUNGEN DER PALÄOGEOGRAPHISCHEN VERBREITUNG VON *Bolboforma* - EIN BEITRAG ZUR REKONSTRUKTION UND DEFINITION VON WASSERMASSEN IM TERTÄR. 1993. 104 pp.
In German with English summary

23 RV PROFESSOR LOGACHEV. Research Cruise 09 (August 30 - September 17, 1993): SEDIMENT DISTRIBUTION ON THE REYKJANES RIDGE NEAR 59°N. Ed. by H.-J. WALLRABE-ADAMS & K.S. LACKSCHEWITZ. 1993. 66 + 30 pp.
In English

24 ANDREAS DETTMER
DIATOMEEN-TAPHOZÖNOSEN ALS ANZEIGER PALÄO-OZEANOGRAPHISCHER ENTWICKLUNGEN IM PLIOZÄNEN UND QUARTÄREN NORDATLANTIK. 1993. 113 + 10 + 25 pp. In German with English summary

25 GEOMAR FORSCHUNGSZENTRUM FÜR MARINE GEOWISSENSCHAFTEN DER CHRISTIAN-ALBRECHTS-UNIVERSITÄT ZU KIEL. JAHRESBERICHT/ANNUAL REPORT 1993. 1994. 69 pp. In German and English

26 JÖRG BIALAS
SEISMISCHE MESSUNGEN UND WEITERE GEOPHYSIKALISCHE UNTERSUCHUNGEN AM SÜD-SHETLAND TRENCH UND IN DER BRANSFIELD STRASSE - ANTARKTISCHE HALBINSEL. 1994. 113 pp.
In German with English summary

27 JANET MARGARET SUMNER
THE TRANSPORT AND DEPOSITIONAL MECHANISM OF HIGH GRADE MIXED-MAGMA IGNIMBRITE TL, GRAN CANARIA: THE MORPHOLOGY OF A LAVA-LIKE FLOW. 1994. 224 pp. In English with German summary. Out of print

28 GEOMAR LITHOTHEK. Ed. by JÜRGEN MIENERT. 1994. 12 pp + app. In English. Out of print

29 FS SONNE. FAHRTBERICHT SO 97 KODIAK-VENT: KODIAK - DUTCH HARBOR - TOKYO - SINGAPUR, 27.7.- 19.9.1994. Hrsg. von ERWIN SUESS. 1994. Some chapters in English, some in German. Out of print

30 CRUISE REPORTS:
RV LIVONIA CRUISE 92, KIEL-KIEL, 21.8.-17.9.1992: GLORIA STUDIES OF THE EAST GREENLAND CONTINENTAL MARGIN BETWEEN 70°AND 80°N
RV POSEIDON PO200/10, LISBON-BREST-BREMERHAVEN, 7.-23.8.1993: EUROPEAN NORTH ATLANTIC MARGIN: SEDIMENT PATHWAYS, PROCESSES AND FLUXES
RV AKADEMIK ALEKSANDR KARPINSKIY, KIEL-TROMSÖ, 5.-25.7.1994: GAS HYDRATES ON THE NORTHERN EUROPEAN CONTINENTAL MARGIN
Edited by JÜRGEN MIENERT. 1994. 186 pp.
In English; report of RV AKADEMIK ALEKSANDR KARPINSKIY cruise in English and Russian

31 MARTIN WEINELT
BECKENENTWICKLUNG DES NÖRDLICHEN WIKING-GRABENS IM KÄNOZOIKUM - VERSENKUNGSGESCHICHTE, SEQUENZSTRATIGRAPHIE, SEDIMENTZUSAMMENSETZUNG. 1994. 85 pp.
In German with English summary

32 GEORG A. HEISS
CORAL REEFS IN THE RED SEA: GROWTH, PRODUCTION AND STABLE ISOTOPES. 1994. 141 pp.
In English with German summary

33 JENS A. HÖLEMANN
AKKUMULATION VON AUTOCHTHONEM UND ALLOCHTHONEM ORGANISCHEM MATERIAL IN DEN KÄNOZOISCHEN SEDIMENTEN DER NORWEGISCHEN SEE (ODP LEG 104). 1994. 78 pp.
In German with English summary

34 CHRISTIAN HASS
SEDIMENTOLOGISCHE UND MIKROPALÄONTOLOGISCHE UNTERSUCHUNGEN ZUR ENTWICKLUNG DES SKAGERRAKS (NE NORDSEE) IM SPÄTHOLOZÄN. 1994. 115 pp. In German with English summary

35 BRITTA JÜNGER
TIEFENWASSERERNEUERUNG IN DER GRÖNLANDSEE WÄHREND DER LETZTEN 340.000 JAHRE / DEEP WATER RENEWAL IN THE GREENLAND SEA DURING THE PAST 340,000 YEARS. 1994. 6 + 109 pp.
In German with English summary

36 JÖRG KUNERT
UNTERSUCHUJNGEN ZU MASSEN- UND FLUIDTRANSPORT ANHAND DER BEARBEITUNG REFLEXIONSSEISMISCHER DATEN AUS DER KODIAK-SUBDUKTIONSZONE, ALASKA. 1995. 129 pp.
In German with English summary

37 CHARLOTTE M. KRAWCZYK
DETACHMENT TECTONICS DURING CONTINENTAL RIFTING OFF THE WEST IBERIA MARGIN: SEISMIC REFLECTION AND DRILLING CONSTRAINTS.1995. 133 pp. In English with German summary

38 CHRISTINE CAROLINE NÜRNBERG

BARIUMFLUSS UND SEDIMENTATION IM SÜDLICHEN SÜDATLANTIK - HINWEISE AUF PRODUKTIVITÄTSÄNDERUNGEN IM QUARTÄR. 1995. 6 + 108 pp. In German with English summary

39 JÜRGEN FRÜHN
TEKTONIK UND ENTWÄSSERUNG DES AKTIVEN KONTINENTALRANDES SÜDÖSTLICH DER KENAI-HALBINSEL, ALASKA. 1995. 93 pp. In German with English summary

40 GEOMAR FORSCHUNGSZENTRUM FÜR MARINE GEOWISSENSCHAFTEN DER CHRISTIAN-ALBRECHTS-UNIVERSITÄT ZU KIEL. JAHRESBERICHT/ANNUAL REPORT 1994. 1995. 125 pp. In German and English.
Out of print

41 FS SONNE. FAHRTBERICHT / CRUISE REPORT SO 103 CONDOR 1 B: VALPARAISO-VALPARAISO, 2-21.7.1995. Hrsg. von ERNST R. FLUEH. 1995. 140 pp. Some chapters in German, some in English

42 RV PROFESSOR BOGOROV CRUISE 37: CRUISE REPORT "POSETIV": VLADIVOSTOK-VLADIVOSTOK, September 23 - October 22, 1994. Edited by CHRISTOPH GAEDICKE, BORIS BARANOV, and EVGENY LELIKOV. 1995. 49 + 33 pp.
In English

43 CHRISTOPH GAEDICKE
DEFORMATION VON SEDIMENTEN IM NANKAI-AKKRETIONSKEIL, JAPAN. BILANZIERUNG TEKTONISCHER VORGÄNGE ANHAND VON SEISMISCHEN PROFILEN UND ERGEBNISSEN DER ODP-BOHRUNG 808. II + 89 pp.
In German with English summary

44 MARTIN ANTONOW
SEDIMENTATIONSMUSTER UM DEN VESTERIS SEAMOUNT (ZENTRALE GRÖNLANDSEE) IN DEN LETZTEN 250.000 JAHREN. 1995. 121 pp. In German with English summary

45 INTERNATIONAL CONGRESS: CORING FOR GLOBAL CHANGE - ICGC '95. KIEL, 28 - 30 June, 1995.
Edited by JÜRGEN MIENERT and GEROLD WEFER. 1996. 83 pp. In English

46 JENS GRÜTZNER
ZUR PHYSIKALISCHEN ENTWICKLUNG VON DIAGENETISCHEN HORIZONTEN IN DEN SEDIMENTBECKEN DES ATLANTIKS. 1995. 96 pp. In German with English summary

47 INGO A. PECHER
SEISMIC STUDIES OF BOTTOM SIMULATING REFLECTORS AT THE CONVERGENT MARGINS OFFSHORE PERU AND COSTA RICA. 1996. 159 pp. In English with German summary

48 XIN SU
DEVELOPMENT OF LATE TERTIARY AND QUATERNARY COCCOLITH ASSEMBLAGES IN THE NORTHEAST ATLANTIC. 1996. 120 pp. +7 pl. In English with German summary

49 FS SONNE - FAHRTBERICHT/CRUISE REPORT SO108 ORWELL: SAN FRANCISCO - ASTORIA, 14.4. - 23.5.1996
Edited by ERNST R. FLUEH and MICHAEL A. FISHER. 1996. 252 pp. + app. In English with German summary

50 GEOMAR FORSCHUNGSZENTRUM FÜR MARINE GEOWISSENSCHAFTEN DER CHRISTIAN-ALBRECHTS-UNIVERSITÄT ZU KIEL. JAHRESBERICHT/ANNUAL REPORT 1995. 1996. 93 pp. In German and English

51 THOMAS FUNCK
STRUCTURE OF THE VOLCANIC APRON NORTH OF GRAN CANARIA DEDUCED FOM REFLECTION SEISMIC, BATHYMETRIC AND BOREHOLE DATA. 1996.VI, 144 pp. In English with German summary

52 PETER BRUNS
GEOCHEMISCHE UND SEDIMENTOLOGISCHE UNTERSUCHUNGEN ÜBER DAS SEDIMENTATIONSVERHALTEN IM BEREICH BIOSTRATIGRAPHISCHER DISKONTINUITÄTEN IM NEOGEN DES NORDATLANTIK, ODP LEG 104, SITES 642B UND 643A. 1996. V, 73 pp. In German with Engllish summary

53 CHRISTIANE C. WAGNER
COLD SEEPS AN KONVERGENTEN PLATTENRÄNDERN VOR OREGON UND PERU: BIOGEOCHEMISCHE BESTANDSAUFNAHME. 1996. 108, XXXVI pp. In German with English summary

54 FRAUKE KLINGELHÖFER
MODEL CALCULATIONS ON THE SPREADING OF SUBMARINE LAVA FLOWS. 1996. 98 pp.
In English with German summary

55 HANS-JÜRGEN HOFFMANN
OBJEKTORIENTIERTE ANALYSE UND MIGRATION DIFFRAKTIERTER WELLENFELDER UNTER VERWENDUNG DER STRAHLENMETHODE UND DER EDGE-WAVE-THEORIE. 1996. XXI, 153 pp. In German with English summary

56 DIRK KLÄSCHEN
STRAHLENSEISMISCHE MODELLIERUNG UNTER BERÜCKSICHTGUNG VON MEHRFACHDIFFRAKTIONEN MIT HILFE DER EDGE-WAVES: THEORIE UND ANWENDUNGSBEISPIELE 1996. X, 159 pp.
In German with English summary

57 NICOLE BIEBOW
DINOFLAGELLATENZYSTEN ALS INIKATOREN DER SPÄT- UND POSTGLAZIALEN ENTWICKLUNG DES AUFTRIEBSGESCHEHENS VOR PERU. 1996. IV, 100, 17, 14 (7 pl.) pp. In German with English summary

58 RV SONNE. CRUISE REPORT SO109: HYDROTRACE ASTORIA-VICTORIA-ASTORIA-VICTORIA. MAY 23 - JULY 8, 1996. Ed. by PETER HERZIG, ERWIN SUESS, and PETER LINKE. 1997. 249 pp. In English

59 RV SONNE. CRUISE REPORT SO110: SO - RO (SONNE - ROPOS). VICTORIA-KODIAK-VICTORIA. JULY 9 - AUGUST 19, 1996. Ed. by ERWIN SUESS and GERHARD BOHRMANN. 1997. 181 pp. In English

60 RV AKADEMIK M. A. LAVRENTYEV CRUISE 27. CRUISE REPORT: GREGORY. VLADIVOSTOK-PUSAN-OKHOTSK SEA-PUSAN-VLADIVOSTOK. SEPTEMBER 7 - OCTOBER 12, 1996.
Ed. by DIRK NÜRNBERG, BORIS BARANOV, and BORIS KARP.1997. 143 pp. In English

61 GEOMAR FORSCHUNGSZENTRUM FÜR MARINE GEOWISSENSCHAFTEN DER CHRISTIAN-ALBRECHTS-UNIVERSITÄT ZU KIEL. JAHRESBERICHT / ANNUAL REPORT 1996. 1997. 169 pp.
In German and English

62 FS SONNE. FAHRTBERICHT/CRUISE REPORT SO123: MAMUT (MAKRAN MURRAY TRAVERSE - GEOPHYSIK PLATTENTEKTONISCHER EXTREMFÄLLE). Maskat - Maskat, 07.09 - 03.10.1997. Ed. by ERNST R. FLUEH, NINA KUKOWSKI, and CHRISTIAN REICHERT. 1997. 292 pp. In English with German summary

63 RAINER ZAHN
NORTH ATLANTIC THERMOHALINE CIRCULATION DURING THE LAST GLACIAL PERIOD: EVIDENCE FOR COUPLING BETWEEN MELTWATER EVENTS AND CONVECTIVE INSTABILITY. 1997. 133 pp. In English

64 FS SONNE. FAHRTBERICHT/CRUISE REPORT SO112 HIRESBAT (HIGH RESOLUTION BATHYMETRY). Victoria, B.C., Canada - Apra Harbor, Guam. 17.09 - 08.10.1996. Hrsg. von WILHELM WEINREBE. 1997. 90 pp.
Some chapters in German, some in English

65 NIELS NØRGAARD-PEDERSEN
LATE QUATERNARY ARCTIC OCEAN SEDIMENT RECORDS: SURFACE OCEAN CONDITIONS AND PROVENANCE OF ICE-RAFTED DEBRIS. 1997. 115 pp. In English with German summary

66 THOMAS NÄHR
AUTHIGENER KLINOPTILOLITH IN MARINEN SEDIMENTEN - MINERALCHEMIE, GENESE UND MÖGLICHE ANWENDUNG ALS GEOTHERMOMETER. 1997. 119, 43 pp. In German with English summary

67 MATTIAS KREUTZ
STOFFTRANSPORT DURCH DIE BODENGRENZSCHICHT: REGIONALISIERUNG UND BILANZIERUNG FÜR DEN NORDATLANTIK UND DAS EUROPÄISCHE NORDMEER. 1998. IV, 166 pp. In German with English summary

68 AMIT GULATI
BENTHIC PRIMARY PRODUCTION IN TWO DIFFERENT SEDIMENT TYPES OF THE KIEL FJORD (WESTERN BALTIC SEA). 1998. 139 pp. In English with German summary

69 RÜDIGER SCHACHT
DIE SPÄT- UND POSTGLAZIALE ENTWICKLUNG DER WOOD- UND LIEFDEFJORDREGION NORDSPITZBERGENS. 1999. 123 pp. + app. In German with English summary

70 GEOMAR FORSCHUNGSZENTRUM FÜR MARINE GEOWISSENSCHAFTEN DER CHRISTIAN-ALBRECHTS-UNIVERSITÄT ZU KIEL. JAHRESBERICHT/ANNUAL REPORT 1997. 1998. 155 pp. In German and English

71 FS SONNE. FAHRTBERICHT/CRUISE REPORT SO118 BIGSET (BIOGEOCHEMICAL TRANSPORT OF MATTER AND ENERGY IN THE DEEP SEA). MUSCAT (OMAN) - MUSCAT (OMAN). 31.03.-11.05.1997. Ed. by OLAF PFANNKUCHE and CHRISTINE UTECHT. 1998. 188 pp. In English

72 FS SONNE. FAHRTBERICHT/CRUISE REPORT SO131 SINUS (SEISMIC INVESTIGATIONS AT THE NINETY EAST RIDGE OBSERVATORY USING SONNE AND JOIDES RESOLUTION DURING ODP LEG 179). KARACHI - SINGAPORE. 04.05-16.06.1998. Ed. by ERNST R. FLUEH and CHRISTIAN REICHERT. 1998. 337 pp. In English

73 THOMAS RICHTER
SEDIMENTARY FLUXES AT THE MID-ATLANTIC RIDGE: SEDIMENT SOURCES, ACCUMULATION RATES, AND GEOCHEMICAL CHARACTERISATION. 1998. IV, 173 + 29 pp. In English with German summary

74 BARBARA MARIA SPRINGER
MODIFIKATION DES BODENNAHEN STRÖMUNGSREGIMES UND DIE DEPOSITION VON SUSPENDIERTEM MATERIAL DURCH MAKROFAUNA. 1999. 112 pp. In German

75 SABINE JÄHMLICH
UNTERSUCHUNGEN ZUR PARTIKELDYNAMIK IN DER BODENGRENZSCHICHT DER MECKLENBURGER BUCHT. 1999. 139 pp. In German

76 WOLFRAM W. BRENNER
GRUNDLAGEN UND ANWENDUNGSMÖGLICHKEITEN DER MIKRO-ABSORPTIONSPHOTOMETRIE FÜR ORGANISCH-WANDIGE MIKROFOSSILIEN. 1999. 141 pp. In German with English summary

77 SUSAN KINSEY
TERTIARY BENTHIC FORAMINIFERAL BIOSTRATIGRAPHY AND PALAEOECOLOGY OF THE HALTEN TERRACE, NORWAY. 1999. VI, 145 pp. In English with German summary

78 HEIDI DOOSE
REKONSTRUKTION HYDROGRAPHISCHER VERHÄLTNISSE IM CALIFORNIENSTROM UND IM EUROPÄISCHEN MITTELMEER ZUR BILDUNGSZEIT ORGANISCH KOHLENSTOFFREICHER SEDIMENTE. 1999. IV, 111 pp. + app. In German with English summary

79 CLAUDIA WILLAMOWSKI
VERTEILUNGSMUSTER VON SPURENMETALLEN IM GLAZIALEN NORDATLANTIK: REKONSTRUKTION DER NÄHRSTOFFBILANZ ANHAND VON CADMIUMKONZENTRATIONEN IN KALKSCHALIGEN FORAMINIFEREN. 1999. 86, XXI pp. In German with English summary

80 FS SONNE. FAHRTBERICHT/CRUISE REPORT SO129. BIGSET (BIOGEOCHEMICAL TRANSPORT OF MATTER AND ENERGY IN THE DEEP SEA). PORT SULTAN QUABOOS - DUBAI. JANUARY 30 - MARCH 9, 1998.

Ed. by OLAF PFANNKUCHE and CHRISTINE UTECHT. 1999. 107 pp. In English

81 FS SONNE. FAHRTBERICHT/CRUISE REPORT SO138. GINCO-2 (GEOSCIENTIFIC INVESTIGATIONS ON THE ACTIVE CONVERGENCE ZONE BETWEEN THE EAST EURASIAN AND AUSTRALIAN PLATES ALONG INDONESIA). JAKARTA - JAKARTA. 29.12.1998 - 28.01.1999. Ed. by ERNST R. FLUEH, BERND SCHRECKENBERGER, and JÖRG BIALAS. 1999. 333 pp. In English

82 CRUISE REPORTS: KOMEX I and II (KURILE OKHOTSK SEA MARINE EXPERIMENT)
RV PROFESSOR GAGARINSKY CRUISE 22
RV AKADEMIK M. A. LAVRENTYEV CRUISE 28
VLADIVOSTOK - PUSAN - OKHOTSK SEA - PUSAN - VLADIVOSTOK. 7 JULY - 12 SEPTEMBER 1998.
Ed. by NICOLE BIEBOW and EDNA HÜTTEN. 1999. 188, 89 pp. In English

83 GREGOR REHDER
QUELLEN UND SENKEN MARINEN METHANS ZWISCHEN SCHELF UND OFFENEM OZEAN. REGIONALE VARIABILITÄT UND STEUERNDE PARAMETER DER METHANVERTEILUNG UND DER AUSTAUSCH MIT DER ATMOSPHÄRE. 1999. 161, 20 pp. In German with English summary

84 SVEN-OLIVER FRANZ
PLIOZÄNE ZEITREIHEN ZUR REKONSTRUKTION DER TIEFENWASSERZIRKULATION UND DER SILIZIKLASTISCHEN AMAZONASFRACHT IM ÄQUATORIALEN WESTATLANTIK
(CEARA SCHWELLE, ODP LEG 154). 1999. 183 pp. In German with English summary

85 SYLKE HLAWATSCH
Mn-Fe-AKKUMULATE ALS INDIKATOR FÜR SCHAD- UND NÄHRSTOFFFLÜSSE IN DER WESTLICHEN OSTSEE.
1999. 132 pp. In German with English summary

86 BETTINA GEHRKE
ZUSAMMENSETZUNG UND VERTEILUNG DER LITHOGENEN FEINFRAKTION IN SPÄTQUARTÄREN SEDIMENTEN DES MITTELATLANTISCHEN REYKJANES RÜCKENS (59°N) - TONMINERALE ALS INDIKATOREN FÜR LIEFERGEBIETE, TRANSPORTMECHANISMEN UND ABLAGERUNGSPROZESSE. 1999. 102 pp.
In German with English summary

87 JENS GREINERT
REZENTE SUBMARINE MINERALBILDUNGEN: ABBILD GEOCHEMISCHER PROZESSE AN AKTIVEN FLUIDAUSTRITTSSTELLEN IM ALEUTEN- UND CASCADIA-AKKRETIONSKOMPLEX. 1999. 196, XX pp.
In German with English summary

88 CRUISE REPORTS: KOMEX V and VI (KURILE OKHOTSK SEA MARINE EXPERIMENT)
RV PROFESSOR GAGARINSKY CRUISE 26
MV MARSHAL GELOVANY CRUISE 1
VLADIVOSTOK - PUSAN - OKHOTSK SEA - PUSAN - VLADIVOSTOK. 30 JULY - 5 SEPTEMBER, 1999.
Ed. by NICOLE BIEBOW, THOMAS LÜDMANN, BORIS KARP, and RUSLAN KULINICH. 2000. 296 pp. In English

89 FS SONNE. FAHRTBERICHT/CRUISE REPORT SO136. TASQWA (QUATERNARY VARIABILITY OF WATER MASSES IN THE SOUTHERN TASMAN SEA AND THE SOUTHERN OCEAN, SW PACIFIC SECTOR).
WELLINGTON - HOBART. OCTOBER 16 - NOVEMBER 12, 1998. Ed. by JÖRN THIEDE, STEFAN NEES et al. 1999.
78, 106 pp. In English

90 FS SONNE. FAHRTBERICHT/CRUISE REPORT SO142. HULA (INTERDISCIPLINARY INVESTIGATIONS ON THE TIMING OF THE HAWAII-EMPEROR BEND AND THE ORIGIN OF LITHOSPHERIC ANOMALIES ALONG THE MUSICIAN SEAMOUNT CHAIN. MIDWAY - HONOLULU. MAY 30 - JUNE 28, 1999. Ed. by ERNST R. FLUEH, JOHN O'CONNOR, JASON PHIPPS MORGAN, and JOCHEN WAGNER. 1999. 224 pp. In English

91 J. HAUSCHILD, T. GINDLER, D. RISTOW, A. BERHORST, C. BÖNNEMANN, K. HINZ
DFG-FORSCHUNGSPROJEKT *„KRUSTENSPLITTER"*. 3D-MAKRO-GESCHWINDIGKEITSBESTIMMUNGEN UND 3D-TIEFENMIGRATION DES SEISMISCHEN 3D-COSTA-RICA-DATENSATZES. 1999. 85 pp.
In German with English summary

92 FS AKADEMIK MSTISLAV KELDYSH. Fahrtbericht Reise Nr. 40: Norwegisch-Grönländische See, 27.6.-29.7.1998.
Hrsg. von J. MIENERT, A. OMLIN, T. GÖLZ, D. LUKAS, J. POSEWANG. 1999. 65, 7 pp. In German

93 FS SONNE. FAHRTBERICHT/CRUISE REPORT SO143 TECFLUX. Ed. by GERHARD BOHRMANN, PETER LINKE, ERWIN SUESS, and OLAF PFANNKUCHE. 2000. 243 pp. In English

94 FS SONNE. FAHRTBERICHT/CRUISE REPORT SO144-1&2. PAGANINI (PANAMA BASIN AND GALAPAGOS "PLUME" - NEW INVESTIGATIONS OF INTRAPLATE MAGMATISM). SAN DIEGO - CALDERA. SEPTEMBER 7 - NOVEMBER 7, 1999.
Ed. by JÖRG BIALAS, ERNST R. FLUEH, and GERHARD BOHRMANN. 1999. 437 pp. + app.
In English

95 CHRISTIAN MATTHIAS HÜLS
MILLENNIAL-SCALE SST VARIABILITY AS INFERRED FROM PLANKTONIC FORAMINIFERAL CENSUS COUNTS IN THE WESTERN SUBTROPICAL ATLANTIC. 2000. 81 pp. + app. In English with German summary

96 FS SONNE. FAHRTBERICHT/CRUISE REPORT SO146-1&2. GEOPECO (GEOPHYSICAL EXPERIMENTS AT THE PERUVIAN CONTINENTAL MARGIN - INVESTIGATIONS OF TECTONICS, MECHANICS, GASHYDRATES, AND FLUID TRANSPORT). ARICA - TALCAHUANO. MARCH 1 - MAY 4, 2000. Ed. by JÖRG BIALAS and NINA KUKOWSKI.
2000. 508 pp. In English

97 GEOMAR FORSCHUNGSZENTRUM FÜR MARINE GEOWISSENSCHAFTEN DER CHRISTIAN-ALBRECHTS-UNIVERSITÄT ZU KIEL. JAHRESBERICHT/ANNUAL REPORT 1998/1999. 2000. 261 pp. In German and English

98 RV SONNE. CRUISE REPORT SO148. TECFLUX-II-2000 (TECTONICALLY-INDUCED MATERIAL FLUXES.

VICTORIA - VICTORIA - VICTORIA. 20.07.-15.08.2000. Ed. by PETER LINKE and ERWIN SUESS. 122 pp. In English

99 GEOMAR FORSCHUNGSZENTRUM FÜR MARINE GEOWISSENSCHAFTEN DER CHRISTIAN-ALBRECHTS-UNIVERSITÄT ZU KIEL. JAHRESBERICHT/ANNUAL REPORT 2000. 2001. 180 pp. In German and English

100 FS POSEIDON. FAHRTBERICHT/CRUISE REPORT POS 260 BIGSET (BIOGEOCHEMICAL TRANSPORT OF MATTER AND ENERGY IN THE DEEP SEA). LEIXOES/OPORTO (PORTUGAL) - GALWAY (IRELAND) - CORK (IRELAND). 26.04.-23.06.2000. Ed. by OLAF PFANNKUCHE and CHRISTINE UTECHT. 2001. 67 pp. In English

101 FS SONNE. FAHRTBERICHT/CRUISE REPORT SO159. SALIERI (SOUTH AMERICAN LITHOSPHERIC TRANSECTS ACROSS VOLCANIC RIDGES). GUAYAQUIL - GUAYAQUIL. AUGUST 21 - SEPTEMBER 17, 2001. Ed. by ERNST R. FLÜH, JÖRG BIALAS, and PHILIPPE CHARVIS. 2001. 256 pp. In English

102 FS SONNE. FAHRTBERICHT/CRUISE REPORT SO161-1&4. SPOC (SUBDUCTION PROCESSES OFF CHILE). ANTOFAGASTA - VALPARAISO. OCTOBER 9 - OCTOBER 15, 2001 & VALPARAISO - VALPARAISO. NOVEMBER 30 - DECEMBER 23, 2001. Ed. by ERNST R. FLÜH, HEIDRUN KOPP, and BERND SCHRECKENBERGER. 2002. 383 pp. In English

103 FS SONNE. FAHRTBERICHT/CRUISE REPORT SO162. INGGAS TEST (INTEGRATED GEOPHYSICAL CHARACTERISATION AND QUANTIFICATION OF GAS HYDRATES - INSTRUMENT TEST CRUISE). VALPARAISO - BALBOA. FEBRUARY 21 - MARCH 12, 2002. Ed. by TIMOTHY JOHN RESTON and JÖRG BIALAS. 2002. In English